MODELING AND OPTIMIZATION FOR INTEGRATED PEOPLE-AND-GOODS TRANSPORTATION SYSTEMS

PENG SHOUGUO

PhD

The Hong Kong Polytechnic University

2025

The Hong Kong Polytechnic University

Department of Industrial and Systems Engineering

Modeling and Optimization for Integrated People-and-Goods Transportation Systems

Peng Shouguo

A thesis submitted in partial fulfillment of the requirements for the degree of Doctor of Philosophy

August 2024

CERTIFICATE OF ORIGINALITY

I hereby declare that this thesis is my own work and that, to the best of my knowledge and belief, it reproduces no material previously published or written, nor material that has been accepted for the award of any other degree or diploma, except where due acknowledgment has been made in the text.

Signature: ____________________________

Name of Student: Peng Shouguo

Abstract

Urban (goods) delivery and passenger transport are essential components of urban infrastructure. In recent years, an integrated people-and-goods transportation model that utilizes passenger transport vehicles for goods deliveries has been touted as one of the most promising alternatives to optimize both goods delivery and passenger transport. Nonetheless, several implementation challenges may hinder the viability of this service model. This thesis aims to address the core challenge of pricing optimization, along with a series of strategic- and operational-level problems for three specific forms of integrated people-and-goods transportation service.

Study I in Chapter 3 introduces an ordinary traveler-based crowd-shipping service, addressing a compensation and service routing (C&R) problem for a hybrid delivery system combining a dedicated delivery service and a crowd-shipping service by ordinary travelers. Two mixed integer programming models are formulated for the C&R problem under uniform and differentiated compensation modes. A customized hybrid algorithm, which employs a variable neighborhood search with a nested tabu search and an iterated local search, is developed to solve the problems.

Study II in Chapter 4 extends the investigation in Chapter 3 by examining a collaborative alliance, allocation of delivery orders, compensation, and route joint optimization (CACR) problem for a collaborative hybrid delivery system involving multiple retailers. A bi-objective optimization model is formulated to minimize total operational costs and carbon emissions. A decomposition-based iterative optimization method is developed to find Pareto-optimal solutions by solving a series of decomposed sub-problems with the updated collaboration strategy and compensation rate. Each sub-problem is solved by using a cluster-first route-second approach with a customized spatiotemporal clustering technique and a non-dominated sorting genetic algorithm-II enhanced with a Clarke and Wright saving method.

Study III in Chapter 5 investigates a public transit-based co-modal transportation service price (CSP) problem considering the collaborative interaction between the logistics service provider (LSP) and public transit operator (PTO). A bilevel path-based programming model is formulated based on the interactive dynamics between LSP and PTO, where a lower-level bus trip scheduling problem is proposed for optimizing the PTO's decision while an upper-level vehicle routing problem with pricing is designed for optimizing the LSP's decision. A tailored iterated three-stage hybrid method, combining two granular tabu search algorithms and an artificial bee colony algorithm, is developed to solve the problem.

Study IV in Chapter 6 examines an outsourcing service price (OSP) problem for co-modal

delivery service based on on-demand mobility services. A lower-level co-modality delivery service problem with ridesharing is formulated to determine the OMP's optimal decision under the outsourcing service price offered by PSP, while an upper-level multi-depot pickup and delivery problem with pricing is formulated to determine the PSP's optimal decision, including the service price. A customized iterative hybrid algorithm, integrating two granular tabu search algorithms and a genetic algorithm, is developed to solve the problem.

These mathematical models and solution methodologies formulated in the four studies are tested on adapted benchmark instances, randomly generated instances, and real-life cases, and offer managerial insights for the urban delivery service providers.

Publications Arising from the Thesis

Journal Publications and Conference Proceedings

1. **Shouguo Peng**, WooYong Park, Abdelrahman E. E. Eltoukhy, Min Xu. (2024). Outsourcing service price for crowd-shipping based on on-demand mobility services. *Transportation Research Part E: Logistics and Transportation Review*, 183, 103451.
2. **Shouguo Peng**, Hoiching Kwok, Min Xu. (2023). Public attitudes towards carpooling services in Hong Kong: perceptions, acceptance, and feasibility. *Proceedings of the 27th International Conference of Hong Kong Society for Transportation Studies.* Hong Kong, China.
3. **Shouguo Peng**, Min Xu. (2022). Personnel scheduling for vehicle restoration problem in one-way electric carsharing services. *Proceedings of the 101st Annual Meeting of Transportation Research Board.* Washington DC, USA.
4. Tszting Li, **Shouguo Peng**, Min Xu. (2022). Impact analysis of COVID-19 on travel behavior and mode preferences of Hong Kong residents. *Proceedings of the 24th COTA International Conference of Transportation Professionals.* Changsha, Hunan, China.

Working Papers

1. **Shouguo Peng**, Min Xu. (2024). Compensation and service route optimization for hybrid delivery systems with crowd-shipping.
2. **Shouguo Peng**, Min Xu. (2024). Optimizing service price for a new public transit-based co-modality transportation service.
3. **Shouguo Peng**, Min Xu. (2024). Collaborative crowd-shipping as a sustainable urban delivery service for shared customers.

Conference Presentation

1. **Shouguo Peng**, Min Xu. (2023). Outsourcing service price for crowd-shipping based on on-demand mobility services. *Presentation at the 5th International Symposium on Multimodal Transportation.* Dalian, China.

Acknowledgements

I wish to convey my profound appreciation to my chief-supervisor, Associate Professor Xu Min, for her systematic training, help, and guidance during my Ph.D. journey. Her insightful thinking, global view, incisive comments, and logical academic writing have significantly shaped my research mindset and enhanced my academic writing skills. Indeed, pursuing a Ph.D. under her supervision has been a challenging yet immensely rewarding journey. I am also thankful to my co-supervisor, Professor Fu Xiaowen, for his generous recommendations and support, particularly during my tenure as his teaching assistant. I also extend my gratitude to the members of the Ph.D. committee—Professor Chung Sai Ho (Nick), Professor Qi Mingyao, and Professor Chow Ho Fai (Andy)—for their review and invaluable feedback on my dissertation.

I am thankful for the financial support provided by The Hong Kong Polytechnic University for my doctoral studies, and I appreciate the assistance and support from the university staff throughout my academic journey. I am deeply grateful to my friends and research colleagues for their encouragement and help: Dr. Lei Da, Dr. Xiao Haohan, Dr. Zhang Lin, Dr. Zhang Wenwei, Dr. Zheng Yuan, Dr. Li Wu, Dr. Li Tongfei, Dr. Wang Li, Dr. Wu Ting, Dr. Yan Xiaoyuan, Dr. Shao Shuai, Mr. Song Yang, Dr. Shi Tao, Ms. Chu Kathy, Mr. Yousaf Ayub. I express my sincere thanks to my fellow Ph.D. candidates and teammates for their support and assistance: Ms. Huang Jiangyan, Mr. Yang Lu, Mr. Wang Yilun, Mr. Ren Qiaoqiao, Mr. Ran Tanghong, Ms. Chen Xiaohua, Ms Ji Rumei, Ms Su Hang, Ms. Tu Lin, and Mr. Xiong Ya.

I am deeply appreciative of my family's understanding and support over the years. My heartfelt gratitude goes to my beloved girlfriend, Yuan, for her unwavering trust over the past eight years and for her encouragement and support, especially during those struggling times.

Table of Contents

List of Figures

List of Tables

Glossary of Abbreviations

ABC	Artificial bee colony
ALNS	Adaptive large neighborhood search
BO-MVCRP-C	Bi-objective multi-depot vehicle and crowd routing problem with compensation optimization
BTS	Bus trip scheduling
C&R	Compensation and service routing
C&R-D	Compensation and service routing problem under the differentiated mode
C&R-U	Compensation and service routing problem under the uniform compensation mode
CACR	Collaboration alliance, allocation of delivery orders, compensation, and route joint optimization
CDA	Crowding-distance calculation algorithm
CDC	Consolidation and distribution center
CE	Carbon emission
COM	Co-modal delivery service based on on-demand mobility services
CM	Co-modal
CS	Crowd-shipping
CSP	Co-modal delivery service price
CSP-R	Co-modal delivery service problem with ridesharing
CW	Clarke and Wright
DDS	Dedicated delivery services
DIO	Decomposition-based iterative optimization
EBT	Extended bus trip network
ETP	Expect-to-be-paid
FCU	Frequency-based compensation updating
FNDS	Fast non-dominated sorting
FRPT	Fixed-route public transport
GA	Genetic algorithm
GTS	Granular tabu search
HDS	Hybrid delivery system
IH	Iterative hybrid
IPG	Integrated people-and-goods
ILS	Iterated local search

ITH	Iterated three-stage hybrid
LSP	Logistics service provider
MILP	Mixed-integer linear programming
MINLP	Mixed-integer nonlinear programming
MIP	Mixed-integer programming
MOPSO	Multi-objective particle swarm optimization
MPDP-P	Multi-depot pickup and delivery problem with pricing
NSGA-II	Non-dominated sorting genetic algorithm-II
O2O	Online-to-Offline
OMP	On-demand mobility service provider
OMS	On-demand mobility service
OSP	Outsourcing service price
OT	Ordinary traveler
PSP	Parcel delivery service provider
PT	Public transit
PTO	Public transit operator
PTS	Passenger transport service
RDS	Regional delivery station
SARP	Share-a-ride problem
SCC-VRP	Shared customer collaboration vehicle routing problem
STC	Spatiotemporal clustering
TC	Total cost
TS	Tabu search
TS-C	Cost-oriented granular tabu search
TS-P	Profit-oriented granular tabu search
UDS	Urban delivery service
UPR	Unserved parcel request network
VNS	Variable neighborhood search
VRPOD	Vehicle routing problem with occasional drivers
VRP-P	Vehicle routing problem with pricing
VRPTW	Vehicle routing problem with time windows

Chapter 1 Introduction

1.1 Background

This section first offers an introduction of urban delivery and passenger transport. Subsequently, it examines various emerging delivery models and their practical applications. Finally, it discusses the potential benefits and challenges associated with these emerging models.

1.1.1 Urban delivery and passenger transport

With the advent of electronic payment systems and online shopping platforms, the last few years have witnessed the continuous growth of global e-commerce sales from 1.336 trillion dollars in 2014 to 5.311 trillion dollars in 2022, with an average annual growth rate of over 20% (Statista, 2024b), as illustrated in Figure 1.1. Notably, online-to-offline (O2O) commerce, which allows customers to order products online and then receive them offline, has witnessed a significant surge in demand, particularly during the COVID-19 pandemic (Zhao et al., 2021).

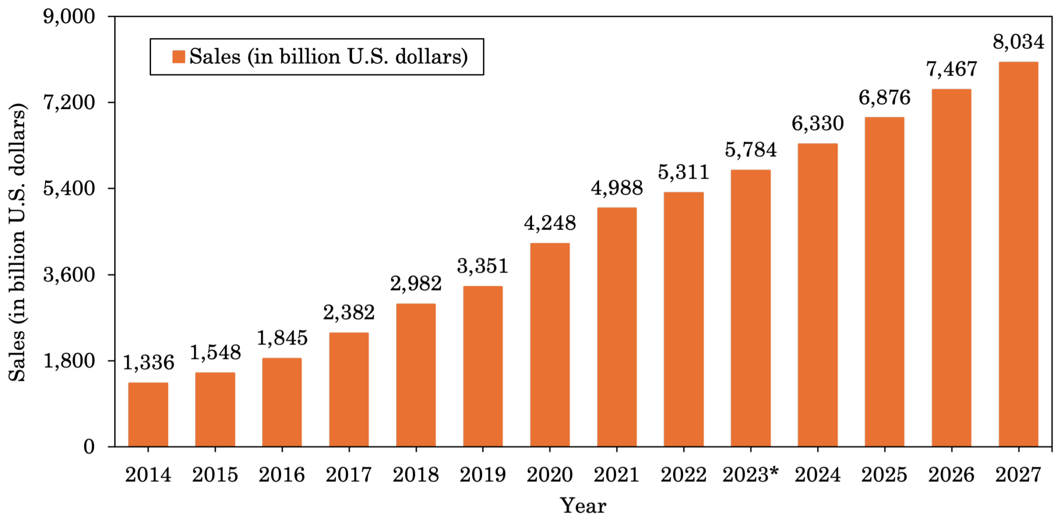

Figure 1.1. Global retail e-commerce sales from the years 2014 to 2027 (Statista, 2024b)

For example, Yonghui Superstores, a major supermarket chain in China, reported an annual growth rate of over 20% in O2O orders in 2022 (He, 2023). Additionally, the demand for last-mile delivery services, which are crucial for transporting goods to customers, has also surged, with the market growing from \$108.1 billion in 2020 to over \$128 billion in 2022 and projected to exceed \$200 billion by 2027 (Placek, 2023). Urban delivery, which facilitates the distribution of goods within city areas, is thus under increasing pressure to meet these rising demands as a result of the swift growth in e-commerce activities. Traditionally, urban delivery service (UDS) providers, e.g., logistics companies and retailers offering delivery services, have relied on the (self-operating) dedicated vehicle fleets with professional drivers. This model, however, is becoming increasingly unsustainable and less competitive due to rising operational costs and environmental impacts, particularly the escalating expenses associated with acquiring additional delivery vehicles and recruiting dedicated drivers (Castillo et al., 2018; Han, 2021). UDS providers are striving to develop high-efficient, cost-effective, and environmentally-friendly delivery models to alleviate their delivery pressure and improve operational competitiveness in the era of e-commerce.

Passenger transport, which facilitates the mobility of passengers, is generally managed by various passenger transport service (PTS) providers such as public transit operators (e.g., bus companies) and on-demand mobility service providers (e.g., ride-hailing companies). However, these systems face chronic inefficiencies, particularly in terms of vehicle utilization: vehicles are often overloaded during peak hours, while they are largely underused during off-peak hours (Elbert and Rentschler, 2022; Yu et al., 2019). This inefficiency is exemplified by the fluctuating 24-hour passenger flow in Nanjing's metro system during weekdays, as presented in Figure 1.2.

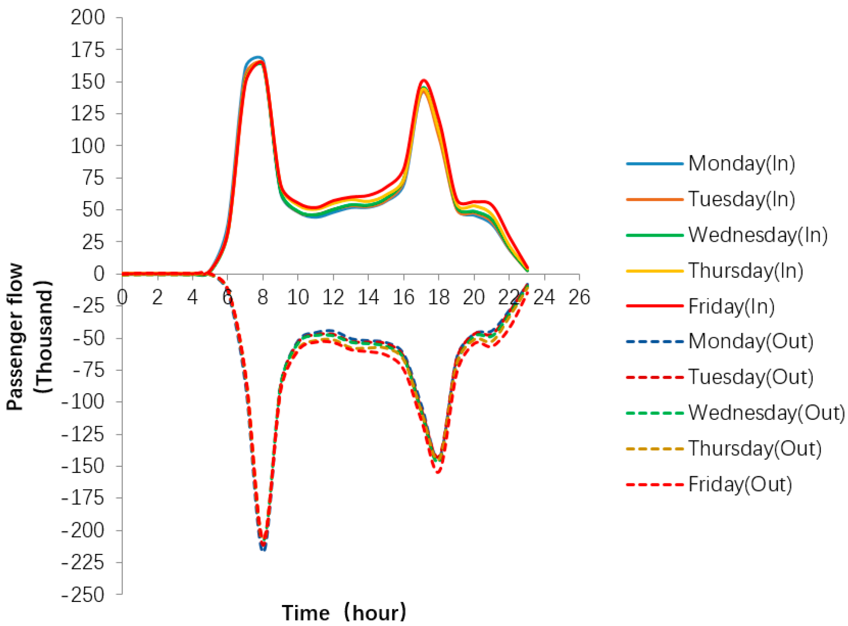

Figure 1.2. Fluctuation of 24-hour passenger flow over a five-day workweek (Yu et al., 2019)

For public transit operators, their public transit buses often exhibit substantial unused space and experience prolonged dwell times at bus terminals during off-peak hours (Kumar et al., 2019), with instances of up to 40 $\sim$ 60 minutes, resulting in significant underutilization of capacity. Similarly, for on-demand mobility service providers, their low-occupancy vehicles are frequently free-floating in the city in search of passengers during non-peak hours, resulting in reduced revenue and heightened environmental costs. Additionally, some passenger transport is carried out by ordinary travelers themselves using their private cars. The significant increase in privately owned vehicles in recent years, exemplified by the rise in China from 45.75 million vehicles in

2009 to 277.92 million vehicles in 2022 (Statista, 2024a), further complicates the urban passenger transport inefficiency and exacerbated the negative impacts on the urban environment. These challenges highlight the need for innovative solutions that optimize both goods delivery and passenger transport efficiently, in an era of rapid urbanization and technological advancement.

1.1.2 Emerging delivery services and their practices

Facilitated by the progression of smartphones and communication technologies, an integrated people-and-goods (IPG) transportation system has emerged recently as a promising solution for both UDS providers and PTS providers. This system aims to leverage the spare capacity of passenger transport vehicles to carry out goods deliveries, alongside their primary function of transporting passengers. *Crowd-shipping(CS)* and *co-modal (CM) transportation* are two most representative concept of the IPG transportation systems. Based on different passenger transport modes, there are broadly three forms of IPG transportation service:

(1) CS service based on ordinary travelers (OTs)

The CS service model aims to employ some ordinary travelers, e.g., in-store customers and commuter with private cars, as crowd-couriers to deliver goods or parcels (a package containing multiple items) during their personal itineraries, and offers them monetary compensation upon successful delivery completion (Arslan et al., 2019). A practical demonstration of this CS model is the MyWays platform implemented by DHL Express in Stockholm, as presented in Figure 1.3.

Figure 1.3. MyWays platform

This platform enhances last-mile delivery services by engaging local residents. Through a customized mobile application, the system pairs users seeking flexible delivery options with those willing to transport parcels along their regular commutes in exchange for monetary payment (Bonn, 2013). Other pilot projects have also explored this model, including Hitch and Roadie in the United States, and Nimber in London, Athens, and Oslo (Alnaggar et al., 2021). These initiatives demonstrate the potential of leveraging ordinary travelers to improve the efficiency and flexibility of urban delivery.

(2) CM transportation service based on fixed-route public transport (FRPT)

The FRPT-based CM transportation service model seeks to integrate the goods deliveries into existing fixed-route public transportation systems, e.g., tram lines, bus networks, and metro systems (Li et al., 2021). An example for this CM transportation model is the Cargo-Tram (also named by E-Tram) program in Zürich, Switzerland, as illustrated in Figure 1.4, which uses trams to transport large or bulky items for urban dwellers without vehicle access (de Kemmeter, 2021).

Figure 1.4. Zurich's cargo tram (de Kemmeter, 2021)

The program's success has led to its expansion to include the collection of discarded or malfunctioning electronics. In addition, various other pilot projects have been implemented using different types of FRPT vehicles. Examples include Bussgods business in Sweden, the Matkahuolto initiative in Finland, the Greyhound Freight service in Australia, the Greyhound Package Express in the United States, and a shared city logistics system based on subway system in Japan (Cheng et al., 2023; Alnaggar et al., 2021). These projects indicate the benefits of integrating urban logistics into public transportation systems to enhance efficiency and sustainability.

(3) CM delivery service based on on-demand mobility services (OMS)

The OMS-based CM delivery service model aims to employ on-demand mobility vehicles, such as taxis, ride-hailing services, and potentially autonomous vehicles in the future, to fulfill goods/parcel delivery requests (Li et al., 2014). A notable example is Walmart's pilot program for same-day grocery delivery, which utilizes Uber and Lyft vehicles (see Figure 1.5) (Wahba, 2016) to delivery parcels to customers. This initiative facilitates the rapid delivery of groceries to customers who shop online, representing a significant shift towards integrating e-commerce with contemporary transportation solutions. This model capitalizes on the existing infrastructure of ride-hailing services to enhance delivery efficiency and flexibility.

Figure 1.5. Walmart grocery delivery by Uber vehicle (Springer, 2017)

In summary, the implementation of the above three forms of IPG transportation service may bring a range of potential benefits across various sectors:

(1) Demand-side

UDS providers, such as logistics service providers and retailers (e.g., Walmart) can take advantage of the underused capacities in passenger transport vehicles, such as private cars, buses, and taxis. This, firstly, enhances operational efficiency by reducing the reliance on dedicated delivery vehicles and professional drivers. Furthermore, these UDS provider can lower delivery pressures and cut costs, particularly those related to the payment for employing professional driver and the acquisition and maintenance of delivery vehicle fleets.

(2) Supply-side

The supply-side may includes various participants of different IPG transportation models. For OTs who provide CS service during their personal travels, they can get additional income from this part-time 'hitch-hiking' delivery service, thereby potentially offsetting some of their travel costs. For PTS providers, e.g., FRPT operators and OMS providers who integrate goods delivery into their regular operations, they can enhance the profitability and operational efficiency by allowing for more productive utilization of their vehicles for goods deliveries, particularly during periods of low passenger demand.

(3) Customer-side

The IPG transportation model may offer customers enhanced convenience and the potential for faster delivery times. By integrating goods deliveries within existing travel routes, this model can expedite services, overcoming the typical route and scheduling limitations associated with traditional delivery methods. Moreover, the flexibility of this approach, including the possibility of after-hours deliveries, can significantly improve customer satisfaction.

(4) Environment-side

From an environmental standpoint, the IPG transportation model could offer the advantage of reduced emissions and decreased traffic congestion. By maximizing the use of existing vehicle capacities, it limits the necessity for additional delivery trips, thus minimizing the overall environmental footprint. Such efficient utilization of transportation resources supports broader sustainability objectives, including the reduction of carbon emissions and the promotion of environmentally-friendly urban logistics practices.

1.1.3 Challenges of implementing emerging IPG transportation services

Despite the foreseeable great benefits for various stakeholders, implementing these emerging IPG transportation models presents numerous challenges.

(1) Challenges of implementing CS service based on OTs

One significant challenge is to determine the compensation rate for employing ordinary travelers, who may have varying expectations for compensation. This rate must attract ordinary travelers without imposing excessive compensation cost burden to UDS providers. Additionally, UDS providers may also operate the traditional dedicated delivery service in addition to employing CS service, resulting in a hybrid delivery system. Unlike dedicated delivery vehicles that are homogeneous and centrally coordinated, ordinary travelers may have diverse itineraries, carrying capacities, available service time periods, and compensation expectations. Allocating delivery tasks between ordinary travelers and dedicated delivery vehicles, and optimizing their service routes, is challenged while considering these heterogeneous service requirements. Furthermore, for the scenario that multiple UDS providers may collaboratively serve the parcel delivery demands, how to determine collaboration strategies and task allocation among them is also crucial. Meanwhile, beyond cost minimization, employing CS services to reduce environmental impact is also important. Addressing these challenges is essential for the effective implementation and sustainability of this innovative business model.

(2) Challenges of implementing CM transportation service based on FRPT

Using FRPT vehicles for parcel deliveries offers potential benefits for both UDS provider and FRPT operator; however, these vehicles, e.g., public transit buses, normally operate on strict timetables dedicated to passenger transport and have limited and distinct capacities for goods during different time periods. A primary challenge is how to coordinate and schedule these vehicles to fulfill additional parcel delivery requests while adhering to the fixed timetable for passenger transport. More importantly, this form of business model requires collaboration between UDS provider and FRPT operator. In this context, how to designing an attractive collaborative mechanism, e.g., a well-designed service price for parcel delivery that benefits both parties, is crucial for the viability of this delivery model.

(3) Challenges of implementing CM delivery service based on OMS

The OMS-based CM delivery service necessitate close collaboration between UDS provider and OMS provider. Without an attractive mechanism for the two potential participants, this business model may not be viable. In this context, how to determine a service price that benefits both participants considering the interaction between UDS provider and OMS providers is fundamentally significant. Particularly, OMS providers providing a more flexible passenger transportation service primarily for passengers' pickup and delivery requests, which come with specific requirements for ride duration and experience. How to optimize the service routes of on-demand mobility vehicles to accommodate additional goods delivery requests while ensuring passenger satisfaction presents a significant challenge. Addressing this challenges is necessary for implementing this form of CM delivery service.

1.2 Research Objectives

To tackle these distinguished challenges, this study will formulate mathematical programming models and develop various solution techniques to address a series of decision-making problems for three forms of IPG transportation models, and conducts numerical experiments on benchmark instances and customized case studies for evaluation. The primary objective is to optimize the service price or compensation rate for these IPG transportation services, alongside a series of strategical-level and operational-level decision optimization such as collaboration alliance determination, delivery order allocations, and service route optimization for dedicated vehicles and ordinary travelers. The research topics addressed in this study are outlined in Figure 1.6. The detailed objectives are set out below:

- To determine compensation rate of employing ordinary travelers for the UDS provider, i.e., retailer in Figure 1.6, considering their heterogeneous service requirements, such as expects-to-be-paid, carrying capacity, and available service time period, and optimize delivery order allocation between ordinary travelers and dedicated vehicles as well as their service routes. These objectives will be addressed by conducting study I in Chapter 3;

- To determine compensation rate of employing ordinary travelers, considering the collaboration among UDS providers, i.e., multiple retailers in Figure 1.6, with their own ordinary travelers, evaluate the benefits of collaboration, and optimize the order allocation among ordinary travelers and dedicated vehicles as well as their service routes. These objectives will be addressed by conducting study II in Chapter 4;

- To optimize service price for a new public transit-based CM transportation service considering the gameplay between UDS provider, i.e., logistics service provider (LSP) in Figure 1.6, and PTS operator, i.e., public transit operator (PTO) in Figure 1.6, and design the public transit bus's working schedules of parcel delivery service for PTO and dedicated vehicle service routes for LSP. These objectives will be achieved by conducting study III in Chapter 5;

- To determine the optimal outsourcing service price for the CM delivery service based on OMS, taking into account the interactive dynamics between between UDS provider, i.e., parcel delivery service provider (PSP) in Figure 1.6, and PTS operator, i.e., on-demand mobility service provider (OMP) in Figure 1.6, and optimize the service routes of dedicated vehicles for PSP and on-demand mobility vehicles for OMP. These objectives will be achieved by conducting study IV in Chapter 6.

1.3 Thesis Organization

The thesis includes seven chapters, each addressing different aspects of the emerging IPG transportation services. with four core chapters presenting four studies for the three forms of IPG transportation services. Specifically, three forms of IPG transportation models are designed for different types of urban delivery demands, e.g., O2O orders and last-mile delivery demand, based on the characteristics of each type of IPG transportation models.

Chapter 1 introduces the background and issues of urban delivery as well as passenger transport and introduces three forms of emerging IPG transportation model. This chapter then identifies the primary challenges associated with these models and outlines the research objectives of this study aiming at addressing these identified challenges.

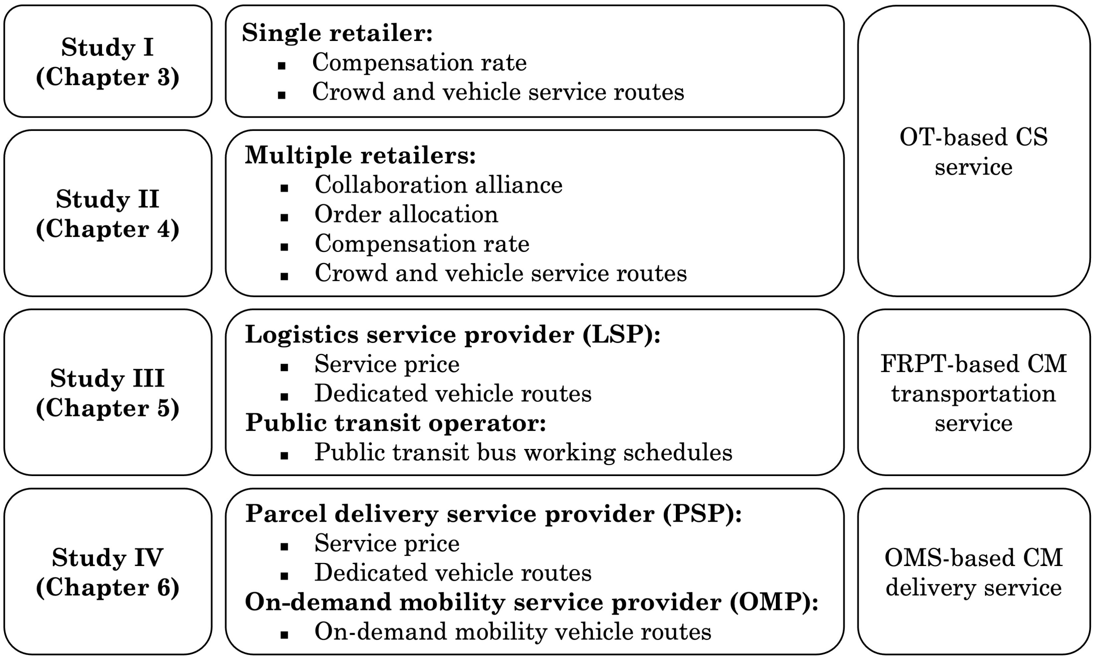

Figure 1.6. Four studies explored by this thesis

Chapter 2 extensively reviews the most relevant studies pertaining to the three IPG transportation models, identifies existing research gaps, and emphasizes the significance of this study.

Chapter 3 explores the CS service using ordinary travelers as crowd-couriers to serve door-to-door O2O orders. This chapter studies the joint optimization of compensation rate and service routes for a hybrid delivery system with traditional dedicated delivery fleets and crowd-couriers considering the heterogeneous crowd-couriers. Two mathematical programming models are established for two studied problems under different compensation schemes, and a hybrid solution approach that combines an iterated local search (ILS) and a variable neighborhood search (VNS) with a nested tabu search (TS) is proposed to find good-quality solution. Numerical experiments on several adapted benchmark instances are employed to assess the efficacy of the suggested methodologies and OT-based CS service.

Chapter 4 builds upon the research presented in Chapter 3, and considers various collaboration alliances among multiple retailers with shared customers. This chapter investigates the joint optimization of collaboration alliance, compensation rate, order allocation, and service routes for a collaborative delivery system with OT-based CS service and examines the collaboration strategies for optimizing costs and reducing carbon emissions. A bi-objective programming model and a decomposition-based iterative optimization method are developed. Numerical experiments on adapted benchmark instances and a simulated case are utilized to validate the efficacy of our developed solution methods and collaborative delivery system.

Chapter 5 introduces a new public transit-based CM transportation service, which leverages the spare capacity of existing bus fixed-scheduled trips to carry out parcel backbone transportation. This chapter optimizes the service price and bus working schedule for the public transit-based CM transportation service considering the collaborative gameplay between LSP and PTO. A bilevel path-based programming model is formulated based on the interactive dynamics between the two participants, and a tailored iterated three-stage hybrid method combining two granular TS algorithms and an artificial bee colony (ABC) algorithm is designed to tackle the studied problem. Numerical experiments are carried out on randomly generated instances and simulated cases assess our proposed solution method and benefits of incorporating public transit-based CM transportation service.

Chapter 6 introduces the OMS-based CM delivery service, which leverages the spare space of on-demand mobility resources (such as taxis and ride-hailing vehicles) for multiple parcel pickup and delivery demand. This chapter explores a pricing strategy for outsourced services within the collaborative CM service framework, taking into account the interactions between two service providers (PSP and OMP). A bilevel arc-based programming model is developed, and a novel iterative hybrid algorithm that combines two tabu search algorithms with targeted granularity and a genetic algorithm is designed to generate good-quality solutions. Numerical experiments are performed on randomly generated scenarios and a case study simulated in Hong Kong, China. This chapter has been published by Transportation Research Part E: Logistics and Transportation Review (Peng et al., 2024).

Chapter 7 provides the overview and research contributions by this thesis and recommendations for future studies.

Chapter 2 Literature Review

Over the past decade, many scholars have investigated various decision-making and optimization problems for the IPG transportation service. This chapter will commence by examining the most pertinent research related to the three IPG transportation models: (i) CS based on ordinary travelers (OTs), (ii) CM transportation service based on fixed-route public transport (FRPT), and (iii) CM delviery service based on on-demand mobility services (OMS). Furthermore, since collaborative delivery strategy is considered in the first CS service, this chapter will also review the studies related to collaborative delivery service with shared customers.

2.1 CS Service based on OTs

Archetti et al. (2016) initiated investigations into OT-based CS services by utilizing occasional drivers as crowd-sourced couriers. They introduced a vehicle routing problem with occasional drivers (VRPOD) in a hybrid delivery system with dedicated delivery vehicles and occasional drivers as crowd-couriers. In their study, it was assumed that each participating crowd-courier would deliver no more than one parcel with a pre-specified compensation rate for employed crowd-couriers. An integer programming model was formulated and a multi-start heuristic method integrating TS and VNS was developed to tackle the problem. The numerical experiments were conducted on adapted Solomon instances with 100 parcel delivery requests and 100 crowd-couriers. Later on, a range of extensions and problem variants have been explored. For example, Macrina et al. (2017) extended the VRPOD to a more general scenario, wherein each crowd-courier can undertake multiple deliveries while considering the time windows of the parcel demands. Different from Archetti et al. (2016), they compensated the crowd-couriers based on a fixed compensation rate and additional travel cost. Tao et al. (2021) explored the VRPOD with in-house, full-time, and part-time couriers with different salary/compensation modes, i.e., fixed salary for in-house drivers and fixed rate-based compensation for full-time and part-time couriers. They formulated a mixed-integer linear programming (MILP) model and proposed TS method to determine the order assignment and routing solution. Macrina et al. (2020) expanded the VRPOD to a flexible scenario where each parcel delivery order can be served by multiple crowd-couriers with transshipment at pre-specified locations. A VNS method was employed to find the optimal service routes. Sampaio et al. (2020) tackled a similar problem to Macrina et al. (2020) by adaptive large neighborhood search (ALNS) algorithm. Vincent et al. (2022) also investigated a similar problem but additionally considered different delivery options of customers. They proposed a mixed-integer nonlinear programming (MINLP) model and developed ALNS to find the solution. Ghaderi et al. (2022) examined the last-mile delivery by crowd-couriers with parcel lockers as transshipment locations. They designed a two-phase approach to find the optimal placement of parcel lockers and tasks assignment to the crowd-couriers.

2.2 CM Transportation Service based on FRPT

Ghilas et al. (2013) conducted a pioneering study on the FRPT-based CM transportation service for parcel transportation. They proposed a parcel transportation system that utilized FRPT lines as a backbone transportation from one "station hub" to another, e.g., a bus line from one bus terminal to another. The study assumed that FRPT lines could transport parcels with a specified cost coefficient based on the number of parcels. They formulated an mixed-integer programming (MIP) model and employ commercial solver CPLEX to find the optimal service routes. They later proposed an ALNS heuristic to solve the larger-scale instances (Ghilas et al., 2016b) and address the scenario with stochastic demand (Ghilas et al., 2016a), and developed a branch-and-price method to get exact solution (Ghilas et al., 2018). Masson et al. (2017) explored a similar scenario to Ghilas et al. (2013) but expanded the station hubs to multiple stops along an FRPT line for enhanced delivery efficiency, utilizing an MIP model and the ALNS method for route optimization. Behiri et al. (2018) extended the study by Masson et al. (2017), focusing on parcel delivery along a single rail line while considering rail station storage capacity. They developed customized heuristics for optimal parcel allocation to each stop that can minimize the total waiting time of all demands. More recently, Delle Donne et al. (2023) investigated an FRPT-based CM transportation network design problem to determine the selected FRPT lines that can maximize the covered parcel delivery demands. They built an MIP model and devised a heuristic method with column generation to determine the selected FRPT lines as well as constructed CM service network.

2.3 CM Delivery Service based on OMS

The pioneering study on CM delivery service based on OMS was conducted by Li et al. (2014). They introduced a share-a-ride problem (SARP) that aimed to optimize the taxis' routes for fulfilling additional parcel delivery requests subject to the maximum ride time of on-board passengers. The problem was formulated as an MILP, which could be solved directly by commercial solvers. An ALNS algorithm was then developed by Li et al. (2016a) to handle large-scale cases for the SARP. Later on, various extensions and problem variants considering realistic constraints, emerging vehicle technologies, or other decisions have been investigated. For example, Li et al. (2016b) investigated two SARP stochastic variants considering the stochastic travel times and delivery locations. They formulated the two variants as two-stage stochastic programming models with recourse and proposed a solution approach that integrated ALNS and sampling strategies. Ren et al. (2021) studied a special SARP that used an online car-hailing service to carry out last-mile delivery while considering the request dynamics. They formulated the problem as an MILP model and developed an improved genetic algorithm to obtain the optimal service routes that can minimize the total cost of drivers, passengers, and car-hailing company. Yu et al. (2018) later explored a general SARP that allowed a taxi to serve multiple passenger ride requests simultaneously and relaxed the restriction on passenger's maximum ride time. A simulated annealing algorithm was developed to obtain the optimal service routes. It was found that solutions of the general SARP increase the operator's total profit compared with that of SARP. Based on the general setting, Beirigo et al. (2018) further studied the shared transportation of passengers and parcels using autonomous vehicles with different compartments. The heterogeneity of vehicle's compartments for carrying parcels and passenger were considered to better accommodate passenger and parcel requests. The problem was formulated as an MILP model, which was solved by commercial solvers. More recently, Lu et al. (2022) extended the problem by considering a mixed fleet of gasoline vehicles and electric vehicles to provide shared transportation for passengers and parcels. They incorporated different operational characteristics of gasoline vehicles and electric vehicles, e.g., energy consumption, speed, and charging requirement, into the model formulation and developed a network partitioning-based heuristic to solve large-scale cases in the real world. Chen et al. (2016) investigated a CM delivery service that exploited taxi relays to deliver parcels. Based on the offline historical trajectory data of taxis, they developed an online adaptive taxi scheduling algorithm to determine the taxi delivery routes for satisfying the real-time passenger ride and parcel delivery requests. Chen et al. (2017) later tested the viability of this CM delivery model for the citywide returned goods collection, which used the spare space of taxis to collect returned goods from a collection point to a distribution center. Zhan et al. (2023) examined a ride-hailing sharing problem in that passengers and parcels can be transported by ride-hailing vehicles and electric motorcycles. They incorporated the parcel size and urgency, characteristics of ride-hailing vehicles and electric motorcycles, e.g., speed and unit travel costs, into the task assignment and routing optimization. They formulated a lexicographic multi-objective model to maximize the total profit for ride-hailing platform and minimize the total driving cost of ride-hailing vehicles and electric motorcycles and developed a modified artificial bee colony algorithm to solve the problem.

2.4 Collaborative Delivery with Shared Customers

For the studies on collaborative delivery service with shared customers, Fernández et al. (2018) were first to introduce the shared customer collaboration vehicle routing problem (SCC-VRP), where multiple carriers may form a collaborative delivery alliance and share customers, allowing any carrier within the alliance to serve shared customers. They formulated two MIP models for SCC-VRPs, and developed branch-and-cut methods. This collaborative delivery model has since been adapted to various other scenarios. For example, Guajardo et al. (2018) expanded SCC-VRP by allowing carriers to participate in multiple service alliances and proposed MILP models, which they solved with commercial solvers. Mancini et al. (2021) further refined SCC-VRP by incorporating considerations for time window and service consistency, along with considerations for balancing workload. They established an MIP model and proposed a matheuristic alongside an ILS approach to find service plans. Paul et al. (2019) investigated store inventory replenishment and supplying pick-up points optimization problem considering shared customers. They devised branch-and-cut and heuristic approaches to obtain routing plans. Wang et al. (2021) applied the shared customer concept to logistics network design while considering the sharing of customers and facilities. They devised a multi-stage hybrid heuristic to construct the optimal emergency logistics network. More recently, Amiri and Farvaresh (2023) examined a collaborative last-mile delivery problem considering the collaboration among multiple carriers. They constructed dual multi-objective frameworks under collaborative and non-collaborative contexts with the goals of maximizing profitability and improving customer reach. To identify Pareto-optimal solutions, they devised a heuristic and implemented a complete enumeration technique.

2.5 Research Gap Summary

This section will summarize the previous studies and identify specific research gaps identified for three forms of IPG models.

2.5.1 Research gap of OT-based CS

Although fruitful results have been achieved for OT-based CS service, most studies focused the assignment of tasks to couriers (Archetti et al., 2016; Macrina et al., 2017), optimization of service routes (Tao et al., 2021; Macrina et al., 2020; Sampaio et al., 2020; Vincent et al., 2022), and transshipment location problem (Ghaderi et al., 2022), under a predefined compensation rate. Nonetheless, different compensations may lead to varying levels of willingness and availability of crowd-couriers, as they may have distinct expected payments when they are engaged in the CS service (Punel and Stathopoulos, 2017). A lower compensation may diminish the willingness of these available individuals to provide delivery services, while a high compensation level reduces the cost savings of CS service. Therefore, it is significant to determine the compensation rate in the context of OT-based CS service model. However, to our knowledge, only Le et al. (2021) and Hou et al. (2022) have considered compensation optimization for OT-based CS service. Le et al. (2021) assumed that each crowd-courier would declare an expect-to-be-paid for per kilometer and would like to provide the delivery service only if the compensation rate was larger than their expectations. The aim was to identify the most advantageous compensation rate and matching strategy in order to maximize overall profits. An MIP model was established, and CPLEX was used to solve the cases with up to 20 parcel delivery requests and 30 crowd-couriers. Hou et al. (2022) assumed that the crowd-couriers would decline the assigned parcel delivery task with a certain probability dependent on compensation amount. However, both the above relevant studies considered a stand-alone OT-based CS service, instead of a hybrid delivery system with dedicated vehicles, and in their studies, a crowd-courier can serve one delivery request. To our knowledge, there has been no research investigating the joint compensation and vehicle and crowd-courier service routing problem for a hybrid delivery system with dedicated delivery vehicles and crowd-couriers.

In addition, despite the considerable body of research on the OT-based CS service and collaborative delivery models, there exists a notable research gap where these two approaches have not been effectively integrated into an integrated collaborative delivery system with OT-based CS service. Specifically, the joint optimization of collaboration strategy, order allocation, compensation design, and service routes has not been adequately addressed in previous studies. Moreover, most previous studies has concentrated on minimizing total costs while overlooking the environmental implications associated with the implementation of this new service, particularly the environmental impact resulting from compensation optimization. Table 2.1 presents a detailed comparison of problem characteristics, objective, decision, and solution techniques between the studies in Chapters 3 and 4 and representative studies on OT-based CS service.

2.5.2 Research gap of FRPT-based CM transportation

While previous studies have made significant progress in aspects for the FRPT-based CM transportation model, such as parcel allocation and service route optimization (Ghilas et al., 2013, 2016b,a; Masson et al., 2017; Behiri et al., 2018), FRPT-based CM transportation network design (Cheng et al., 2018; Delle Donne et al., 2023), and location selection of parcel loading/unloading (Zhao et al., 2018; Ji et al., 2020), most have concentrated on parcel delivery using a single line without parcel transshipment among multiple lines. Kızıl and Yıldız (2023) recently proposed a new FRPT-based CM transportation service, allowing for parcel transshipment among multiple FRPT lines; however, they assumed that parcel delivery could be facilitated through FRPT network interconnectivity without the consideration of detailed coordination among multiple FRPT vehicles under timetable constraints. Furthermore, all prior studies assumed that the FRPT operator will provide a CM transportation service, given a pre-defined

Table 2.1. A detailed comparison between studies I and II and studies on crowd-shipping based on ordinary travelers

Reference	Problem characteristics	Objective	Model decision			Solution method
			Dedicate vehicle routes	Crowd-courier routes	Compensation optimization	
Archetti et al. (2016)	VRPOD	Minimize UDS* provider's costs	✓	×	×	Multi-start heuristics
Macrina et al. (2017)	VRPOD with time windows and multiple deliveries by a crowd-courier	Minimize UDS provider's costs	✓	✓	×	CPLEX
Tao et al. (2021)	VRPOD with hybrid couriers	Maximize UDS provider's profits	✓	✓	×	Tabu search
Macrina et al. (2020)	VRPOD considering the transshipment of parcels	Minimize UDS provider's costs	✓	✓	×	VNS
Sampaio et al. (2020)	VRPOD with time windows and transshipment node	Minimize UDS provider's costs	✓	✓	×	ALNS
Vincent et al. (2022)	VRPOD with time windows, transshipment node, and delivery options	Minimize UDS provider's costs	✓	✓	×	ALNS
Ghaderi et al. (2022)	VRPOD with parcel lockers	Maximize number of serviced orders	×	×	×	A two-phase algorithm
Le et al. (2021)	Compensation optimization for OT-based CS service	Maximize UDS provider's profits	×	×	✓	CPLEX
Hou et al. (2022)	Compensation optimization for OT-based CS service considering acceptance uncertainty	Minimize UDS provider's costs	×	×	✓	GUROBI
Chapter 3 (Study I)	Compensation and service route optimization for OT-based CS service	Minimize UDS provider's costs	✓	✓	✓	A customized hybrid algorithm
Chapter 4 (Study II)	Compensation and service route optimization for OT-based CS service considering collaborative delivery for shared customers	Minimize UDS provider's costs and carbon emissions	✓	✓	✓	A customized decomposition-based iterative method

*UDS providers: Urban delivery service providers, such as retailers, logistics service providers, and parcel delivery service providers in these studies compensation rate (also named by cost coefficient). However, in practice, the FRPT operator and urban delivery service (UDS) provider as two independent business parties may have different and potentially conflict goals regarding the FRPT-based CM transportation collaboration. To our knowledge, there has not been any investigation into service price optimization for the FRPT-based CM transportation service that coordinates FRPT vehicles and accounts for the dynamic interactions among participants. Table 2.2 presents a detailed comparison of problem characteristics, objective, decision, and solution techniques between the studies in Chapters 5 and representative studies on FRPT-based CM transportation service.

2.5.3 Research gap of OMS-based CM delivery

All the aforementioned studies on OMS-based CM delivery service focused on operational-level decision-making problems, e.g., routing optimization. A high-level decision, i.e., the service price, which is fundamentally important to the formulation and sustainable operation of the OMS-based CM delivery service, has not been investigated so far. In fact, most previous studies have investigated this from the perspective of the OMP only. The OMS-based CM delivery service model, however, entails the close collaboration of OMP and UDS provider. To establish the collaboration, the UDS provider needs to offer an attractive outsourcing service price for serving the request to the OMP. The OMP will then make the decision to determine which parcel requests are profitable to serve. The unserved parcel requests have to be fulfilled by the UDS provider's self-operating delivery fleet. In this context, the UDS provider needs to determine the outsourcing service price while considering the OMP's decisions. In this context, the UDS provider should serve as the leader aiming to find an optimal outsourcing service price, and the OMP should be as the follower aiming to figure out the parcel requests to serve under the offered price. To the best of our knowledge, no study has ever considered the interaction and gameplay between UDS provider and OMP in OMS-based CM delivery service. Table 2.3 presents a detailed comparison of problem characteristics, decision-making, model formulation, and solution techniques between the study in Chapter 6 and representative studies on OMS-based CM delivery service.

In summary, despite the successful outcomes of previous studies, the optimization of compensation or service price has been overlooked in all the three forms of IPG transportation service. Furthermore, several critical considerations, such as the interactive game between participants, the integration of collaborative delivery and crowd-shipping service, and the coordination of passenger transport vehicles, the joint optimization of dedicated vehicle and crowd-courier service routes, are absent in prior research. To address these research gaps, Chapter 3 will investigate a compensation and crowd-courier and vehicle service route joint optimization problem

Table 2.2. A detailed comparison between studies III and studies on co-modal transportation service based on fixed-route public transport

Reference	Problem characteristics	Objective	Model decision			Solution method
			Coordination of vehicles	Bi-level	Gameplay of participants	
Ghilas et al. (2013)	Parcel delivery by FRPT-based CM in terminals	Minimize total delivery time	×	×	×	CPLEX
Ghilas et al. (2016b)	Parcel delivery by FRPT-based CM in terminals	Minimize total cost	×	×	×	ALNS
Ghilas et al. (2016a)	Parcel delivery by FRPT-based CM under stochastic demands	Minimize total expected cost	×	×	×	ALNS with sample method
Masson et al. (2017)	Parcel delivery by FRPT-based CM considering multiple stops for parcel unloading	Minimize total travel cost and number of freighters	×	×	×	ALNS
Behiri et al. (2018)	Freight-rail-transport-scheduling problem considering rail station storage capacity	Minimize total cost	×	×	×	Decomposition-based heuristics
Cheng et al. (2018)	Network design for the FRPT-based CM service	Minimize total delivery time	×	×	×	A genetic algorithm-based heuristic
Ji et al. (2020)	Hub location selection problem for FRPT-based CM service	Minimize total cost	×	×	×	Genetic algorithm
Delle Donne et al. (2023)	Network design for the FRPT-based CM service	Maximize covered demands	×	×	×	A column generation-based heuristic
Kızıl and Yıldız (2023)	FRPT-based CM service with backup transfers	Minimize total cost	×	×	×	Branch-and-price method
Chapter 5 (Study III)	Service pricing and bus working scheduling optimization for public transit-based CM considering gameplay between CM service participants	Minimize UDS provider's costs considering maximization of FRPT operator's total profits	✓	✓	✓	A customized decomposition-based iterative method

Table 2.3. A detailed comparison between study IV and studies on co-modal delivery service based on on-demand mobility services

Reference	Problem characteristics	Decision	Objective	Model		Solution method
				Bi-level	Gameplay	
Li et al. (2014)	SARP	Routing optimization	Maximize OMP*'s total profits	×	×	GUROBI solver
Li et al. (2016a)	SARP	Routing optimization	Maximize OMP's total profits	×	×	ALNS
Li et al. (2016b)	SARP with stochastic travel times and delivery locations	Routing optimization	Maximize OMP's total profits	×	×	ALNS
Ren et al. (2021)	Specific SARP for last-mile delivery	Routing optimization	Minimize OMP's total costs	×	×	Genetic Algorithm
Yu et al. (2018)	General SARP with ridesharing (multiple passengers) and without ride duration restriction	Routing optimization	Maximize OMP's total profits	×	×	Simulated Annealing
Beirigo et al. (2018)	SARP with parcel locker and heterogeneity of vehicle's compartments	Routing optimization	Maximize OMP's total profits	×	×	GUROBI solver
Lu et al. (2022)	SARP with a mixed fleet (electric and gasoline vehicles)	Routing optimization and vehicle assignment	Maximize OMP's total profits	×	×	A network partitioning-based heuristic
Chen et al. (2016)	Parcel delivery by the relay of taxis	Parcel path and taxi scheduling optimization	Minimize the total delivery time	×	×	Taxi scheduling algorithm
Chen et al. (2017)	Returned goods collection by the relay of taxis	Parcel path and taxi scheduling optimization	Minimize the total delivery time	×	×	Taxi scheduling algorithm
Zhan et al. (2023)	Parcels and passengers shared transportation with a mixed fleet for multi-types of parcel requests	Routing optimization and vehicle assignment	Maximize the platform's total profits and minimize OMP's total costs	× (multi-objective model)	×	Artificial Bee Colony algorithm
Chapter 6 (Study IV)	Transportation with price optimization and considering game play between CM service partipants	Pricing and routing optimization	Minimize the UDS's total cost considering the maximization of OMP's total profits	✓	✓	A customized IH algorithm

*OMP providers: On-demand mobility service providers, such as taxi and ride-hailing service providers in these studies for a hybrid delivery system considering heterogeneous crowd-couriers. Chapter 4 will extend the study in Chapter 3 and examine a collaboration alliance, order allocation, compensation, and service route joint optimization problem for a collaborative delivery system with OT-based CS services and shared customers. Chapter 5 will explore the optimal service price and dedicated delivery vehicle routes, and the optimal served parcel requests by FRPT vehicles as well as the corresponding working schedules. Chapter 6 will investigate an outsourcing service price for the OMS-based CM delivery service model considering the gameplay between the service participants, and the service routes for the two participants of the CM delivery collaboration.

Chapter 3 Compensation Optimization for Crowd-Shipping based on Ordinary Travelers

This chapter investigates a compensation and service routing (C&R) problem for a hybrid delivery system with dedicated delivery vehicles and ordinary travelers as crowd-couriers while considering heterogeneous service requirements of crowd-couriers. Two compensation schemes are considered, i.e., a uniform and a differentiated compensation mode, under which the crowd-couriers are compensated according to a universal and individual-specific compensation rate, respectively. An MINLP model is formulated for the C&R problem under the uniform compensation (C&R-U), and linearization techniques are employed to transform the MINLP model to an MILP model. In addition, the optimal uniform compensation rate for the C&R-U problem is proved to belong to a finite set of candidate values. Given a specific candidate value, the C&R-U problem will reduce to a crowd-courier and dedicated vehicle routing problem, referred to as R-C&R-U problem. This chapter then develops a customized hybrid algorithm, namely, H-ILS-VNS, to determine the optimal uniform compensation and service routes of crowd-courier and dedicated vehicle. The algorithm will iteratively solve the R-C&R-U problem via VNS with a nested TS (VNS-TS) and update the compensation rate with iterated local search (ILS). For the C&R problem under differentiated compensation modes (C&R-D), we explore the problem feature and formulate it as an MILP model. Moreover, the C&R-D problem can be solved by the adjusted VNS-TS. Numerical experiments are carried out on test instances to assess the efficacy of the models and solution techniques.

The rest of this chapter is structured as follows. The studied problems as well as assumptions and notations are elaborated in Section 3.1. Two MIP models are formulated in Section 3.2. A hybrid algorithm integrating ILS and VNS-TS is elaborated in Section 3.3. Numerical experiments are conducted in Section 3.4. Conclusions are discussed in Section 3.5. Notations used in this chapter is listed in Section 3.6 for readability.

3.1 Problem Statement

Consider that a retailer operates dual shopping channels including online channel on a platform and offline channel on a physical store. The online channel facilitates customers place orders electronically and then receive their purchased products offline through delivery services from the retail store to the customer's location, generally known as O2O orders, whereas the offline channel offers a conventional in-store shopping experience for those who prefer shopping in brick-and-mortar establishments. Within the O2O commerce, an online customer browse and select products from a retail store's inventory on an online platform, such as Meituan in China, and place an order online. Then, the order is transmitted to the physical retail store, where in-store personnel packages products into a parcel and dispatch dedicated delivery vehicles, e.g., self-operating delivery vehicles, to deliver the parcel to the designated location of the online customer. Consider the retailer who provides parcel delivery service for its O2O orders from the retail store to customer locations. Let $\mathcal{S}$ denote the set of the O2O orders. Each order $i \in \mathcal{S}$ is associated with a delivery location, a load q_i, a delivery time window $[e_i, l_i]$, where e_i and l_i denote the earliest and latest time to deliver the products to location $i \in \mathcal{S}$, and the service duration for unloading s_i. For convenience of presentation, we also employ $\mathcal{S}$ to denote the set of delivery locations of all O2O orders.

To fulfill the O2O orders, the retailer employs a hybrid delivery system with both its self-operating dedicated vehicles in set $\mathcal{V}$ and in-store customers in set $\mathcal{K}$ as crowd-couriers. Each vehicle $v \in \mathcal{V}$ is associated with a maximum loading capacity Q_v and a fixed vehicle cost c^{f}. The transportation cost and travel time of the vehicles from location i to j are represented by c_{ij} and r_{ij}, respectively. Each crowd-courier $k \in \mathcal{K}$ specifies their destination d_k, the earliest departure time e_k from the retail store, the latest arrival time l_k at the destination, and the maximum carrying capacity Q_k. Let $\mathcal{D}$ denote the set of destinations of crowd-couriers in set $\mathcal{K}$. The provision of crowd-shipping services may entail detour for crowd-couriers compared with their original trips. Therefore, each crowd-courier $k \in \mathcal{K}$ will also declare the expect-to-be-paid (ETP) per unit of detour time, denoted by E_k. The crowd-couriers will accept the delivery tasks only when the compensation rate offered by the retailer is higher than their ETPs. The travel time of the crowd-couriers from location i to j is t_{ij}.

Given the heterogeneous ETPs of crowd-couriers, the retailer considers two compensation rate settings: (i) a universal compensation rate p for all crowd-couriers, referred to as the uniform compensation mode, and (ii) an individual-specific compensation rate p_k for crowd-courier $k \in \mathcal{K}$, referred to as the differentiated compensation mode. The objective of the C&R-U/C&R-D problem is to jointly determine the uniform/differentiated compensation rates and service routes of crowd-couriers and dedicated vehicles such that (i) all O2O orders are satisfied subject to the time window constraint, (ii) the available time period, carrying capacity, ETPs of employed crowd-couriers and the carrying capacity of the dedicated vehicles are accommodated, and (iii) the total costs, encompassing fixed vehicle cost, transportation cost, and compensation cost is minimized.

3.2 Optimization Model Formulation

In this section, we formulate MIP models for C&R-U and C&RD problems. For ease of modeling, we define the problems on a complete direct graph $\mathcal{G} = (\mathcal{N}, \mathcal{A})$, where $\mathcal{N} = \mathcal{S} \cup \mathcal{D} \cup \{0, \sigma+1\}$, and nodes 0 and $\sigma+1$ represent the retail store, which is physically the same location. In particular, $\sigma := |\mathcal{S}| + |\mathcal{D}|$, where $|\mathcal{S}|$ and $|\mathcal{D}|$ are the number of nodes in sets $\mathcal{S}$ and $\mathcal{D}$, respectively. Each node $i \in \mathcal{N}$ is associated with a service time window $[e_i, l_i]$, a service duration s_i, and a load q_i, with $s_i = 0$ and $q_i = 0$, $\forall i \in \{0, \sigma+1\} \cup \mathcal{D}$. Each arc $(i,j) \in \mathcal{A}$ is associated with vehicle transportation cost c_{ij}, vehicle travel time r_{ij}, and crowd-courier travel time t_{ij}. The notations employed in this chapter are outlined in Section 3.6.

3.2.1 Model for C&R-U problem

To formulate the C&R-U problem, we define the following variables:

- p: Continuous variable to denote the compensation paid for employing crowd-couriers for per unit of detour time.
- x_{ijv} : Binary decision variable that equals 1 if vehicle $v \in \mathcal{V}$ travels directly from node i to j, $\forall i, j \in \mathcal{N}$, and 0 otherwise;
- y_{ijk} : Binary decision variable that equals 1 if crowd-courier $k \in \mathcal{K}$ travels directly from node i to j, $\forall i, j \in \mathcal{N}$, and 0 otherwise;
- τ_i^v : Continuous variable to denote the time epoch when vehicle $v \in \mathcal{V}$ starts service at node $i \in \mathcal{N}$. Note that τ_0^v represents the time at which vehicle $v \in \mathcal{V}$ departs from the retail store, while $\tau_{\sigma+1}^v$ indicates the time when vehicle $v \in \mathcal{V}$ returns to retail store;
- τ_i^k : Continuous variable to denote the time epoch when crowd-courier $k \in \mathcal{K}$ starts service at node $i \in \mathcal{N}$. Note that τ_0^k represents the time at which crowd-courier $k \in \mathcal{K}$ departs from retail store, while $\tau_{d_k}^k$ indicates the time of crowd-courier $k \in \mathcal{K}$ at destination d_k.

With the above notations, the C&R-U problem can be formulated as follows:

[C&R-U]

$$\begin{aligned}\min_{\{\mathbf{p},\mathbf{x},\mathbf{y},\boldsymbol{\tau}\}} TC^U = c^{\mathrm{f}} \sum_{v\in\mathcal{V}} \sum_{j\in\mathcal{S}} x_{0jv} + \sum_{v\in\mathcal{V}} \sum_{i\in\mathcal{N}\setminus\mathcal{D}} \sum_{j\in\mathcal{N}\setminus\mathcal{D}} c_{ij} x_{ijv} \\ + p \sum_{k\in\mathcal{K}} \left(\sum_{i\in\mathcal{S}\cup\{0\}} \sum_{j\in\mathcal{S}\cup\{d_k\}} t_{ij} y_{ijk} - t_{0d_k} \right)\end{aligned} \tag{3.1}$$

subject to

$$\sum_{v\in\mathcal{V}}\sum_{j\in\mathcal{S}\setminus\{\sigma+1\}} x_{ijv} + \sum_{k\in\mathcal{K}}\sum_{j\in\mathcal{S}\bigcup\{d_k\}} y_{ijk} = 1, \qquad \forall i\in\mathcal{S} \tag{3.2}$$

$$\sum_{v\in\mathcal{V}}\sum_{j\in\mathcal{S}\cup\{\sigma+1\}} x_{ijv} = \sum_{v\in\mathcal{V}}\sum_{j\in\mathcal{S}\cup\{0\}} x_{jiv}, \qquad \forall i\in\mathcal{S} \tag{3.3}$$

$$\sum_{k\in\mathcal{K}}\sum_{j\in\mathcal{S}\cup\{d_k\}} y_{ijk} = \sum_{k\in\mathcal{K}}\sum_{j\in\mathcal{S}\cup\{0\}} y_{jik}, \qquad \forall i\in\mathcal{S} \tag{3.4}$$

$$\sum_{j\in\mathcal{S}\cup\{\sigma+1\}} x_{0jv} = 1, \qquad \forall v\in\mathcal{V} \tag{3.5}$$

$$\sum_{i\in\mathcal{S}\cup\{0\}} x_{i(\sigma+1)v} = 1, \qquad \forall v\in\mathcal{V} \tag{3.6}$$

$$\sum_{j\in\mathcal{S}\cup\{d_k\}} y_{0jk} = 1, \qquad \forall k\in\mathcal{K} \tag{3.7}$$

$$\sum_{i\in\mathcal{S}\cup\{0\}} y_{id_kk} = 1, \qquad \forall k\in\mathcal{K} \tag{3.8}$$

$$\tau_i^v + s_i + r_{ij} \le \tau_j^v + M\left(1 - x_{ijv}\right), \qquad \forall i\in\mathcal{S}\cup\{0\}, j\in\mathcal{S}\cup\{\sigma+1\}, v\in\mathcal{V} \tag{3.9}$$

$$e_i \le \tau_i^v \le l_i, \qquad \forall i\in\mathcal{S}, v\in\mathcal{V} \tag{3.10}$$

$$\sum_{i\in\mathcal{S}\cup\{0\}}\sum_{j\in\mathcal{S}} q_j x_{ijv} \le Q_v, \qquad \forall v\in\mathcal{V} \tag{3.11}$$

$$E_k y_{ijk} \le p, \qquad \forall i\in\mathcal{S}\cup\{0\}, j\in\mathcal{S}, k\in\mathcal{K} \tag{3.12}$$

$$\tau_i^k + s_i + t_{ij} \le \tau_j^k + M\left(1 - y_{ijk}\right), \qquad \forall i\in\mathcal{S}\cup\{0\}, j\in\mathcal{S}\cup\{d_k\}, k\in\mathcal{K} \tag{3.13}$$

$$\tau_0^k \ge e_k, \qquad \forall k\in\mathcal{K} \tag{3.14}$$

$$\tau_{d_k}^k \le l_k, \qquad \forall k\in\mathcal{K} \tag{3.15}$$

$$e_i \le \tau_i^k \le l_i, \qquad \forall i\in\mathcal{S}, k\in\mathcal{K} \tag{3.16}$$

$$\sum_{i\in S\cup\{0\}}\sum_{j\in\mathcal{S}} q_j y_{ijk} \le Q_k, \qquad \forall k\in\mathcal{K} \tag{3.17}$$

$$p \ge 0 \tag{3.18}$$

$$x_{ijv}, y_{ijk} \in \{0,1\}, \qquad \forall (i,j)\in\mathcal{A}, v\in\mathcal{V}, k\in\mathcal{K} \tag{3.19}$$

$$\tau_i^v, \tau_i^k \ge 0, \qquad \forall i\in\mathcal{N}, k\in\mathcal{K}, v\in\mathcal{V} \tag{3.20}$$

Objective function (3.1) is to achieve the minimization the total cost TC^U under the uniform compensation mode. Constraint (3.2) suggests that an O2O order should be fulfilled either by a dedicated delivery vehicle/crowd-courier. Constraint (3.3)–(3.4) impose the flow balance constraints of the vehicles and crowd-couriers, respectively. Constraints (3.5)–(3.6) indicate that the dedicated delivery vehicle departs from the retail store and finally arrive at the store. Constraints (3.7)–(3.8) define the starting and ending points for the crowd-couriers. Constraint (3.9) updates the service time epoch of dedicated vehicle along the route, where M is a large number. Constraint (3.10) guarantees the service time window by vehicles. Constraint (3.11) imposes the loading capacity of dedicated vehicles. Constraint (3.12) indicates that crowd-couriers will undertake the delivery task only if their ETPs are met. Constraint (3.13) updates the service time epoch of crowd-couriers along the route. Constraints (3.14)–(3.15) impose the departure and arrival time constraints of crowd-couriers. Constraint (3.16) guarantees the service time window by crowd-couriers. Constraint (3.17) imposes the carrying capacity of the crowd-couriers. Constraints (3.18)–(3.20) establish the domain for the decision variables.

We can see that the model [C&R-U] is an MINLP model due to the inclusion of nonlinear term py_{ijk} in Eq. (3.1). We thus linearize it by introducing an auxiliary variable $z_{ijk} = py_{ijk}$ and imposing the following constraints:

$$z_{ijk} \leq p_{\max} y_{ijk}, \qquad \forall i \in \mathcal{S} \cup \{0\}, j \in \mathcal{S} \cup \{d_k\}, k \in \mathcal{K} \tag{3.21}$$

$$z_{ijk} \leq p, \qquad \forall i \in \mathcal{S} \cup \{0\}, j \in \mathcal{S} \cup \{d_k\}, k \in \mathcal{K} \tag{3.22}$$

$$z_{ijk} \geq p - p_{\max}(1 - y_{ijk}), \qquad \forall i \in \mathcal{S} \cup \{0\}, j \in \mathcal{S} \cup \{d_k\}, k \in \mathcal{K} \tag{3.23}$$

$$z_{ijk} \geq 0, \qquad \forall i \in \mathcal{S} \cup \{0\}, j \in \mathcal{S} \cup \{d_k\}, k \in \mathcal{K} \tag{3.24}$$

where $p_{\max}$ is a parameter which can be set as the maximum ETP of all available crowd-couriers, i.e., $p_{\max} = \max_{k \in \mathcal{K}}\{E_k\}$.

With the above linearization, the model [C&R-U] can be equivalently reformulated as an MILP model:

[C&R-U$^{\mathrm{L}}$]

$$\begin{aligned} \min_{\{\mathbf{p},\mathbf{x},\mathbf{y},\mathbf{z},\boldsymbol{\tau}\}} TC^U = c^{\mathrm{f}} \sum_{v \in V} \sum_{j \in \mathcal{S}} x_{0jv} + \sum_{v \in V} \sum_{i \in \mathcal{N} \setminus \mathcal{D}} \sum_{j \in \mathcal{N} \setminus \mathcal{D}} c_{ij} x_{ijv} \\ + \sum_{k \in \mathcal{K}} \sum_{i \in \mathcal{S} \cup \{0\}} \sum_{j \in \mathcal{S} \cup \{d_k\}} t_{ij} z_{ijk} - p \sum_{k \in \mathcal{K}} t_{0d_k} \end{aligned} \tag{3.25}$$

subject to constraints (3.2)–(3.24).

3.2.2 Model for C&R-D problem

For the C&R-D problem with individual-specific compensation rate, the optimal compensation rate p_k^* will be the ETPs of the corresponding crowd-courier E_k; otherwise, the retailer can further reduce the total cost by reducing the compensation rate to E_k while keeping all the others unchanged. In this way, the C&R-D problem will reduce to a crowd-courier and dedicated vehicle routing problem under a specific compensation rate $p_k^* := E_k$, $\forall k \in \mathcal{K}$, which belongs to the special scenario of C&R-U problem. Therefore, the C&R-D problem can be structured as an MILP model [C&R-D]:

[C&R-D]

$$\begin{aligned} \min_{\{\mathbf{x},\mathbf{y},\boldsymbol{\tau}\}} TC^D = c^{\mathrm{f}} \sum_{j\in\mathcal{S}} x_{0jv} + \sum_{v\in\mathcal{V}} \sum_{i\in\mathcal{N}\setminus\mathcal{D}} \sum_{j\in\mathcal{N}\setminus\mathcal{D}} c_{ij}x_{ijv} \\ + \sum_{k\in\mathcal{K}} E_k \left(\sum_{i\in\mathcal{S}\cup\{0\}} \sum_{j\in\mathcal{S}\cup\{d_k\}} t_{ij}y_{ijk} - t_{od_k} \right) \end{aligned} \tag{3.26}$$

subject to constraints (3.2)–(3.11), (3.13)–(3.17), (3.19)–(3.20).

3.3 H-ILS-VNS Solution Method

The MILP models [C&R-U$^{\mathrm{L}}$] and [C&R-D] can be directly solved by commercial solvers, e.g., GUROBI. However, our preliminary experiments found that only small-scale instances with less than 20 orders and 20 crowd-couriers can be solved within one hour. To tackle larger-scale instances of C&R-U problem, we develop a hybrid algorithm, namely, H-ILS-VNS algorithm, which integrates an ILS method and a VNS-TS algorithm. In the proposed H-ILS-VNS algorithm, the ILS method is employed to update the compensation rate, while the VNS-TS algorithm is utilized to optimize the service routes of crowd-couriers and dedicated vehicles. As for the C&R-D problem, since it is a special case of C&R-U, it can also be solved by the proposed method. Subsequently, we will detail the overall framework of the H-ILS-VNS algorithm designed for the generic C&R-U problem, followed by ILS and VNS-TS modules.

3.3.1 Framework of H-ILS-VNS method

For the C&R-U problem, we can see that once the compensation rate is confirmed, the problem will reduce to a crowd-courier and dedicated vehicle routing problem, i.e., the R-C&R-U problem, which is to identify the most cost-efficient service routes for dedicated vehicles and crowd-couriers to fulfill all O2O orders, under the confirmed compensation rate. Motivated by this, we propose a customized H-ILS-VNS algorithm that iteratively solves the reduced C&R-U

problem by VNS-TS and updates the compensation rate via ILS. The H-ILS-VNS integrates ILS and VNS-TS. The ILS is a modular metaheuristic that can generate new solution and yield good-quality solutions by iteratively performing the multiple modular procedures, including local search, perturbation, and acceptance criterion check (Lourenço et al., 2019). The VNS-TS, combining VNS with a nested TS, demonstrated strong performance across a range of combinatorial optimization problems, e.g., vehicle routing problem with time window (VRPTW), owing to the search diversification and intensification enabled by the multiple neighborhood structures and tabu strategy (Belhaiza et al., 2014; Molina et al., 2020).

To solve the C&R-U problem, the H-ILS-VNS algorithm first starts with an initial arbitrary compensation rate. Then the VNS-TS is employed to solve the R-C&R-U problem to obtain the optimal service routes of crowd-couriers and dedicated vehicles under the given compensation rate. After that, the ILS algorithm will be applied to update the compensation rate. The above procedure will iterate until the maximum number of iterations is reached. The optimal compensation and service routes of crowd-couriers and dedicated vehicles will be obtained. The overall framework of the H-ILS-VNS algorithm is illustrated in Figure 3.1.

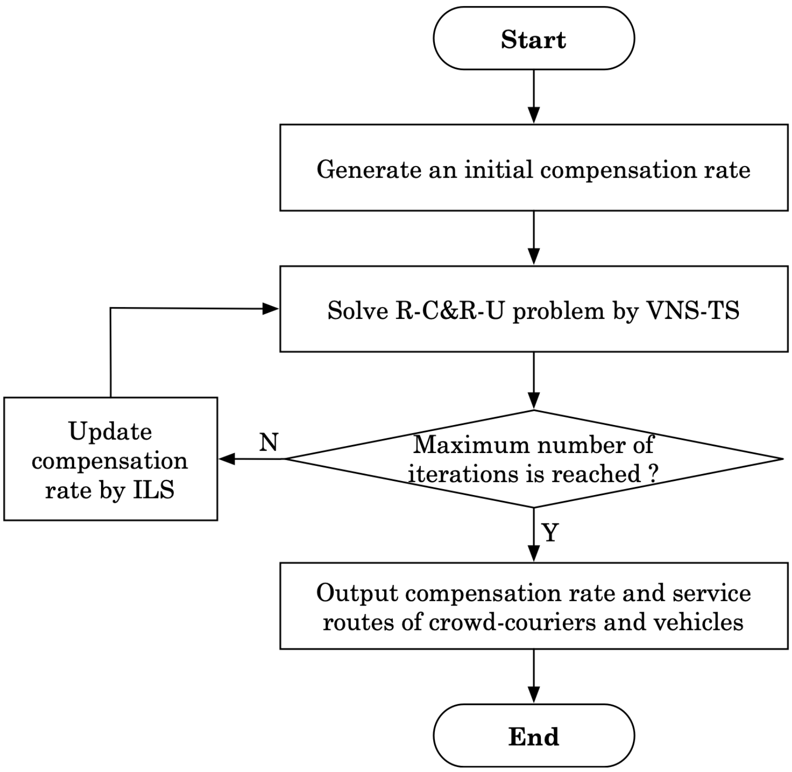

Figure 3.1. Overall framework of H-ILS-VNS algorithm

To enhance the likelihood of finding optimal compensation and service route solutions, we improved the H-ILS-VNS algorithm in accordance with the problem-specific features. Specifically, we have proved that the optimal uniform compensation rate for the C&R-U problem belongs to a finite set of candidate values. Therefore, we only need to update the compensation rate based on those candidate values. This enhances the efficiency of the search process for identifying good-quality compensation rates within a limited computation time and iterations by reducing unnecessary exploration of non-optimal compensation values (Lourenço et al., 2019).

3.3.2 Compensation generation and updating by ILS

In the proposed H-ILS-VNS algorithm, the compensation rate needs to be generated and updated. Theoretically, the retailer can determine the compensation rate as any non-negative value, i.e., $p \geq 0$, resulting in an infinite search space. However, by analyzing the problem characteristics, the search space for compensation rate can be reduced to a set of a finite number of candidate values related to the ETPs of crowd-couriers. Let $\mathcal{P} = \{p_1, \cdots, p_i, \cdots, p_n\}$ denote the set of distinct ETP values of all crowd-couriers; the following proposition is put forth.

Proposition 3.1. *The optimal uniform compensation rate p^* for the C&R-U problem must be 0 or a value in set $\mathcal{P}$, i.e., $p^* \in \{0\} \cup \mathcal{P}$.*

Proof. We prove Proposition 3.1 by contradiction. Since the elements in set $\mathcal{P}$ are distinct, we assume that $p_1 < \cdots < p_i < p_{i+1} < \cdots < p_n$, where $p_1 = \min_{k \in \mathcal{K}} \{E_k\}$ and $p_n = \max_{k \in \mathcal{K}} \{E_k\}$. Suppose that the optimal uniform compensation rate lies in between any two adjacent ETP values in set $\mathcal{P}$, i.e., $p^* \in (p_i, p_{i+1}), \forall i = 1, 2, \ldots, n-1$. Then the retailer can further reduce the total cost by reducing the compensation rate to p_i while keeping all the other decisions unchanged. The same also applies to the cases where assuming $p^* \in (0, p_1)$ or $p^* \in (p_n, \infty)$. Therefore, the optimal compensation rate should be a value in set $\{0\} \cup \mathcal{P}$, i.e., $p^* \in \{0\} \cup \mathcal{P}$. $\square$

According to Proposition 3.1, we can explore the optimal compensation rate in a finite set of candidate values, denoted by $\tilde{\mathcal{P}} = \{0, p_1, p_2, \cdots, p_n\}$. Recall that for each confirmed compensation $p \in \tilde{\mathcal{P}}$, a minimized total cost for serving all O2O orders can be determined by solving the reduced C&R-U problem. We then develop an ILS method to find the optimal compensation rate that can minimize the total cost for retailer, by iteratively searching the compensation that can decrease total cost of the retailer. The specifics of the ILS method are detailed as follows.

The ILS method starts with an initial compensation rate solution. Then, a compensation local search will be executed to obtain the local optimal compensation rate solution p_i^*. For each compensation rate value, a minimized total cost for serving all orders can be determined by solving the R-C&R-U problem to be detailed in the next subsection. Subsequently, a perturbation operation is applied to generate a new compensation rate solution, followed by the execution of the local search procedure again to get the new local optimal compensation solution

p_j^*. Thereafter, the newly identified solution will replace the preceding optimal solution if a lower total cost is achieved. The aforementioned perturbation operation, local search procedure, and solution acceptance check will be iteratively conducted until the maximum number of iterations or if all the candidate values in set $\tilde{\mathcal{P}}$ have been explored. Figure 3.2 illustrates the searching process in one iteration of ILS.

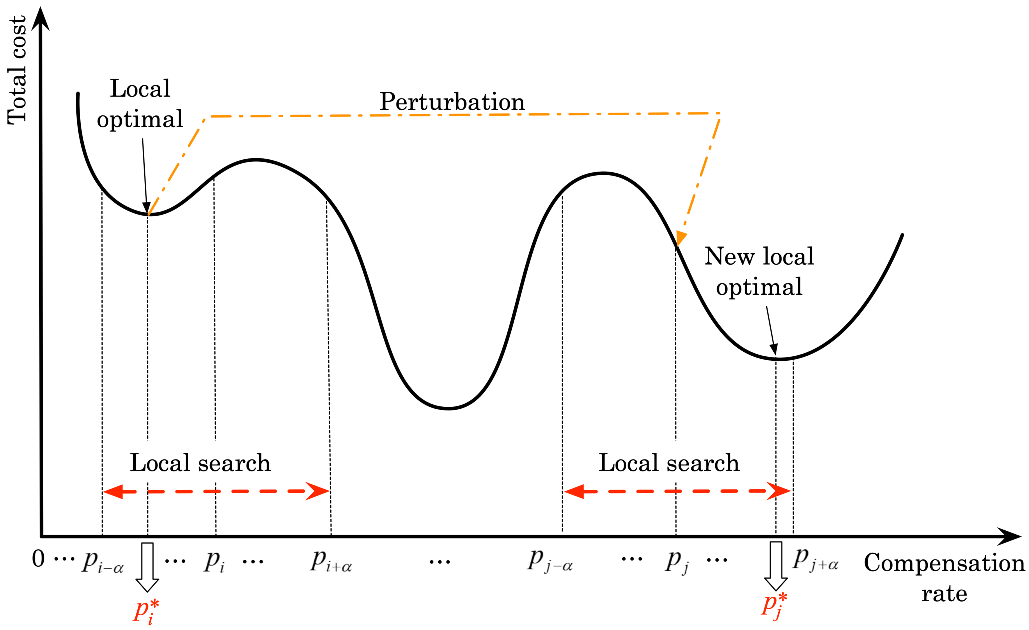

Figure 3.2. An illustrative searching process in one iteration of ILS

As aforementioned, we will search the optimal compensation among a finite number of candidate values in set $\tilde{\mathcal{P}}$ by ILS. The initial compensation rate is randomly chosen from set $\tilde{\mathcal{P}}$. In the local search procedure, we will explore the compensations in α compensation neighbors. For example in Figure 3.2, starting from a compensation rate p_i, we will explore the compensation rates $p_{i-\alpha}, \ldots, p_i, \ldots, p_{i+\alpha}$ in set $\tilde{\mathcal{P}}$. A perturbation operation is employed to generate a new compensation rate solution, aiding in breaking free from local optima. We conduct the perturbation operation by randomly selecting a compensation rate that is not explored in previous iteration. To this end, we will maintain a compensation rate list that has been explored in previous iterations.

3.3.3 Crowd-courier and vehicle routing by VNS-TS

Given a specific compensation rate, the VNS-TS is proposed to solve the R-C&R-U problem to find the good-quality crowd-courier and vehicle routes. The VNS was proposed by Mladenović and Hansen (1997) aiming to obtain optimal solution by iteratively performing the local search procedure with various neighborhood search strategies until the solution cannot be improved by all neighborhood structures (Fleszar et al., 2009). The integration of TS in the VNS will improve the searching intensification and diversification, thus improving the likelihood of finding good-quality solution (Belhaiza et al., 2014; Molina et al., 2020).

Specifically, a set of neighborhood structures is firstly defined, which are employed to generate neighborhood solutions by modifying a given route solution. Let $\mathcal{N}_\lambda$, $\lambda = 1, \cdots, \lambda_{\max}$, denote the λ^{th} neighborhood structure. For example, we can move an order from the current route to another route to get a new route solution by a relocation neighborhood structure. The optimal route solution θ^* and the optimal total cost f_{best} is also initialized. The VNS-TS algorithm starts with the neighborhood structure $\mathcal{N}_1$ and an initialized route solution generated by an initialization procedure Initial$(\cdot)$ as current route solution. Subsequently, an iterative process is initiated. A shaking operation Shaking$(\cdot)$ with $\mathcal{N}_1$ is applied on current route solution to get a new route solution, followed by a local search procedure performed by TS algorithm TS $(\cdot)$ on the solution with $\mathcal{N}_1$ to determine the local optimal route solution. If the newly obtained local optimal route solution is superior to the current solution, it replaces the current solution, and the search returns to the shaking operation with $\mathcal{N}_1$; otherwise, the search explores the next neighborhood structure $\mathcal{N}_{\lambda+1}$. The iteration will continue until all neighborhood structures have been examined, i.e., $\lambda = \lambda_{\max}$. The optimal route solution under the given compensation can be obtained. The pseudocode of the VNS-TS for R-C&R-U problem is presented in Algorithm 3.1. We can see that the developed VNS-TS framework encompasses three key components: (i) construction of an initial solution, (ii) implementation of a shaking procedure employing various neighborhood structures, and (iii) execution of a local search utilizing the TS. We will introduce the three components in detail.

(i) Route solution initialization and evaluation

The initialization procedure Initial$(\cdot)$ is employed to generate the route solution for the R-C&R-U problem given the compensation rate p. We will first identify feasible crowd-couriers with ETPs lower than the given compensation rate. After this, the initial route solution is constructed by allocating all orders to dedicated vehicles, while feasible crowd-couriers will travel directly from the retail store to their respective destinations. To be more specific, an order is firstly selected from the set of all orders, and a vehicle is assigned to fulfill it. Subsequently, orders are randomly selected from the remaining orders and incorporated into the route of the vehicle following a sequence of the ascend earliest service time epoch, i.e., e_i of the order, ensuring that the capacity is not surpassed; otherwise, the chosen order is allocated to a new vehicle. The process continues until all orders have been arranged.

We can see that the generated route solution encompasses multiple dedicated vehicle routes and crowd-courier routes regardless all those constraints including time windows of orders, car-

Algorithm 3.1 Pseudocode of VNS-TS for solving R-C&R-U problem

Input: Compensation rate p
Output: Route solution θ^* and corresponding total cost f_{best}

Define a set of neighborhood structures $\mathcal{N}_\lambda$, where $\lambda = 1, \cdots, \lambda_{\max}$
$\theta^* \leftarrow \varnothing, f_{\text{best}} \leftarrow \infty$ ▷ Initialize the optimal route solution and corresponding total cost
$\theta \leftarrow \text{Initial}(p)$ ▷ Generate initial route solution under compensation rate p
$\lambda \leftarrow 1$
while $\lambda < \lambda_{\max}$ **do**
    $\theta' = \text{Shaking}(\theta, \mathcal{N}_\lambda)$ ▷ Shaking operation for getting a new route solution
    $\theta'' = \text{TS}(\theta', \mathcal{N}_\lambda)$ ▷ Tabu search procedure for finding local optimal route solution
    if $f(\theta'', p) < f_{\text{best}}$ **then**
        $\theta^* \leftarrow \theta''$
        $f_{\text{best}} \leftarrow f(\theta^*, p)$
    end if
    if $f(\theta'', p) < f(\theta, p)$ **then** ▷ Update the optimal route solution
        $\theta \leftarrow \theta''$
        $\lambda \leftarrow 1$
    else
        $\lambda \leftarrow \lambda + 1$
    end if
end while

rying capacities, and service time period. Instead, we will address these constraints by incorporating penalty costs. Specifically, given a compensation solution p and route solution θ, let $TW(\theta), CC(\theta)$, and $ST(\theta)$ denote the corresponding violations of orders' service time window, carrying capacities of crowd-couriers and dedicated vehicles, and crowd-couriers' service time period, respectively. Let γ_1, γ_2, and γ_3 denote the coefficients of penalty. Under this setting, for the C&R-U problem, the total cost including penalties, for a given a route solution θ and compensation solution p, is given by

$$f(\theta, p) = TC^U(\theta, p) + \gamma_1 TW(\theta) + \gamma_2 CC(\theta) + \gamma_3 ST(\theta) \tag{3.27}$$

(ii) Shaking operation

The shaking operation Shaking$(\cdot)$ is utilized to enhance the diversification of route solution by perturbing a route solution with a given neighborhood structure. By perturbing a solution with a given neighborhood structure, a set of neighborhood solutions can be obtained, and we randomly select a solution from the neighborhood solutions even if it results in a worse total cost. This operation can provide a new start of local search to help to escape from the local optima. The neighborhood structure is an important factor influencing the overall effectiveness of the proposed VNS-TS method. Complicated and diverse neighborhood structures will lead to extended computation time, while limited insufficient neighborhood structures will impede the search for the optimal solution. To balance the diversity of neighborhood structures and the computation time, the following neighborhood structures are considered in our implementation.

Neighborhood structure based on intra-route:

- Intra-route relocate: move an order from current position to different position in the route.
- Intra-route exchange: swap the positions of any two orders in a route.
- 2-opt: randomly select two positions in a route, denoted by i and j, keep the partial route before position i and after position j unchanged, but invert the sequence between position i and position j (Croes, 1958).

Neighborhood structure based on inter-routes:

- Inter-route relocate: remove an order from the current route and insert it to another route (Savelsbergh, 1992).
- Inter-route exchange: swap two orders in two different routes (Kindervater and Savelsbergh, 1997).
- Crossing: swap two segments of orders with less two orders in two different routes (Taillard et al., 1997).

Total six neighborhood structures, i.e., $\lambda_{\max} = 6$, are employed for our proposed VNS-TS, and these neighborhood structures will be utilized in shaking operation and the local search procedure by TS.

(iii) Local search by TS algorithm

The new route obtained through the shaking operation will be fed into the local search procedure to identify the optimal route solution under current neighborhood structure $\mathcal{N}_\lambda$ and compensation p. In this chapter, we apply the TS procedure TS$(\cdot)$ to achieve the goal. TS is a widely used meta-heuristic proposed by (Glover, 1986) that can yield good-quality solutions by allowing non-improving solutions and a tabu strategy to avoid cycling iterations. Specifically, the TS procedure TS$(\cdot)$ starts with the given route solution derived from the shaking operation, and set it as current solution and optimal solution. Then, an iterative process is initiated. A series of neighborhood solutions are first generated by performing neighbourhood search on current route solution with the given neighborhood structure. Note that when generating neighborhood solutions, a memory structure named tabu list, will be employed to avoid cyclic exploration and escape from local optima (Glover, 1986). To be more specific, each time a neighborhood solution is obtained, the service relation will be recorded in the tabu list in a certain number of previous iterations, and then any operation to generate a solution that the service relation included in the tabu list is forbidden unless it can generate a better solution than the current optimal solution. Later on, the current solution will be replaced by the best neighborhood solutions even if the objective value of best neighborhood solution is deteriorated, and the optimal route solution will be updated if the objective value of best neighborhood solution is better than the incumbent one. The iterative procedure will be executed until the maximum number of iterations of TS procedure is achieved. The optimal solution will be identified and output for further iteration in the proposed VNS-TS.

3.4 Numerical Experiments

In this section, a series of instances is utilized to validate the effectiveness and efficiency of our proposed H-ILS-VNS algorithm and hybrid delivery system. We will begin by presenting the generation of instances and the setup of parameters. Subsequently, the performance of the algorithm will be evaluated on a range of small-scale instances by comparing the results obtained by the commercial solver GUROBI with those obtained by our proposed algorithm. Later on, a series of instances with various numbers of O2O orders and crowd-couriers will be employed to explore the benefits of the hybrid delivery system. Finally, sensitivity analysis will be conducted to explore the impact of the ETP and the carrying capacity of crowd-couriers on the hybrid delivery system. The solution method are implemented in MATLAB 2021a, calling GUROBI 9.1.2 on a MAC running MacOS Monterey 12.6, equipped with an Apple M1 3.2GHz CPU and 16GB RAM.

3.4.1 Test instance generation and parameter setting

In the C&R problem, O2O orders need to be delivered from retail stores to customers within specified time windows using a hybrid delivery system that includes crowd-couriers. The Solomon instances are widely used for the vehicle routing problem with time windows and its variants (Solomon, 1987), which aim to deliver goods from a depot to a series of customers; however, there is no information about crowd-couriers in the Solomon instances. Therefore, we will generate customized instances by augmenting Solomon instances with crowd-courier data. Specifically, the depot in a selected Solomon instance, originally defined with a specific location and opening time window, is treated as the retail store. The delivery demands in the Solomon instance, characterized by customer location, service time window, parcel load, and service time, are defined as the O2O orders. For dedicated delivery services using traditional vehicles, we assign a vehicle carrying capacity of 200 kg, a fixed usage cost of $50, and a transportation cost of $10 per unit of time. To incorporate crowd-couriers, we generate a group of crowd-couriers originating from the retail store and randomly assign their destinations within the order area. Each crowd-courier is assigned a carrying capacity randomly generated between 10 kg and 30 kg, a randomly generated available time window, and a randomly generated ETP between $1 and $10 per unit of detour time.

Based on the above rules, we then generate a series of instances ranging from small to large scale, with varying numbers of O2O orders and crowd-couriers for testing the proposed solution methods and the hybrid delivery system. For small cases, we select three scales of O2O orders, i.e., $|\mathcal{S}|$=10, 15, and 20, from Solomon instance R201, and generate different number of crowd-couriers according to four different courier-to-order ratios, i.e., $|\mathcal{K}|/|\mathcal{S}|$=0.8, 1, 1.2, 1.5. For larger-scale instances, we select O2O order scales of 100, 200, and 300 from the extended Solomon instance R1-4-10, again varying the number of crowd-couriers based on the above four different ratios.

Regarding algorithm parameters, we set penalty costs $\gamma_1 = 100$, $\gamma_1 = 10$, $\gamma_1 = 15$, the maximum number of iterations for the ILS algorithm $N_{ILS} = 10$, the number of compensation rate neighbors $\alpha = 5$, the maximum iterations in the tabu search procedure $N = 200$, the tabu tenure $\omega = 20$ in the TS procedure.

3.4.2 Algorithm performance evaluation of solution methods

To evaluate the efficiency and reliability of H-ILS-VNS and VNS-TS in solving the C&R-U and C&R-D problems, we compare the results obtained by the developed H-ILS-VNS algorithm with those obtained by solving the models $^{\mathrm{L}}$ [C&R-U$^{\mathrm{L}}$] and [C&R-D] with the solver GUROBI. We first present the objective function values (Obj) and computation times (Time) achieved by both the H-ILS-VNS algorithm and GUROBI for the C&R-U problem in Table 3.1. Objective values that are optimal and best are marked in bold and denoted with an asterisk, respectively. In addition, we calculated the relative gap (RelGap), defined as (Obj$^{\mathrm{H}}$–Obj$^{\mathrm{G}}$)/Obj$^{\mathrm{G}}$, where Obj$^{\mathrm{H}}$ and Obj$^{\mathrm{G}}$ denote the objective values achieved by H-ILS-VNS and GUROBI, respectively.

Table 3.1 shows the comparative efficiency of the H-ILS-VNS algorithm, which in most cases surpasses the performance of the commercial solver GUROBI (except the instance 6 with the gap less than 1%) in finding the optimal solution for the C&R-U problem, and does so in significantly less computation time—for example, the average computation time for the H-ILS-VNS is only 50 s. Conversely, GUROBI struggles to find optimal solutions within 1 h for instances where

Table 3.1. Results of H-ILS-VNS and GUROBI for solving C&R-U problem

Instance	$\|\mathcal{S}\|$	$\|\mathcal{K}\|/\|\mathcal{S}\|$	H-ILS-VNS		GUROBI		RelGap
			Obj ($)	CPU (s)	Obj ($)	CPU (s)	
1	10	0.8	**1,493***	3	**1,493***	603	0.00%
2		1.0	**1,493***	3	**1,493***	880	0.00%
3		1.2	**893***	4	**893***	1,340	0.00%
4		1.5	**739***	4	**739***	2,002	0.00%
5	15	0.8	**1,429***	38	**1,429***	3,093	0.00%
6		1.0	1,234	45	**1,230***	3,383	0.33%
7		1.2	**1,170**	54	1,227	3,600	–4.65%
8		1.5	**962**	65	1,181	3,600	–18.52%
9	20	0.8	**2,458**	68	3,242	3,600	–24.18%
10		1.0	**2,370**	82	3,220	3,600	–26.40%
11		1.2	**2,102**	102	2,994	3,600	–29.79%
12		1.5	**1,904**	133	2,860	3,600	–33.43%
Average	–	–	–	50	–	–	–

the number of O2O orders is 15, particularly as the number of crowd-couriers increases. In contrast, our H-ILS-VNS algorithm consistently finds good-quality solutions quickly, such as delivering a good-quality solution for a scenario with 20 orders and 30 crowd-couriers in 133 s. Moreover, the increased number of orders and crowd-couriers correlates with a rise in the relative gap, demonstrating the H-ILS-VNS algorithm's capability to effectively search for good-quality solutions. Moreover, we also conducted numerical experiments to compare the performance of the VNS-TS algorithm with GUROBI for the C&R-D problem, as shown in Table 3.2.

Table 3.2. Result of VNS-TS and GUROBI for solving C&R-D problem

Instance	$\|\mathcal{S}\|$	$\|\mathcal{K}\|/\|\mathcal{S}\|$	VNS-TS		GUROBI		RelGap
			Obj ($)	CPU (s)	Obj ($)	CPU (s)	
1	10	0.8	**837***	1	**837***	275	0.00%
2		1.0	**837***	1	**837***	316	0.00%
3		1.2	**321***	1	**321***	467	0.00%
4		1.5	**210***	1	**210***	698	0.00%
5	15	0.8	**779***	7	**779***	1,474	0.00%
6		1.0	**532***	8	**532***	1,734	0.00%
7		1.2	**384***	9	**384***	2,064	0.00%
8		1.5	**268***	10	**268***	2,421	0.00%
9	20	18	**1,037**	12	1,247	3,600	–16.84%
10		1.0	**1,000**	12	1,240	3,600	–19.37%
11		1.2	**874**	17	1,233	3,600	–29.12%
12		1.5	**709**	22	1,202	3,600	–41.04%
Average	–	–	–	9	–	–	–

The results in Table 3.2 also demonstrate that VNS-TS effectively produces good-quality solutions for C&R-D problem. Notably, VNS-TS outperforms H-ILS-VNS in solving the C&R-D problem compared to the C&R-U problem, achieving optimal solutions for scenarios with up to

15 orders and 23 crowd-couriers. Additionally, the difference in objective values between VNS-TS and GUROBI is more pronounced for the C&R-D problem, reaching up to 41.04%, compared to the C&R-U problem.The comparative evaluation of our proposed method and GUROBI across both the C&R-U and C&R-D problems underscores the effectiveness and reliability of the H-ILS-VNS and VNS-TS algorithms in identifying good-quality solutions with short computation time. Moreover, we have visualized the objective values for both the C&R-U and C&R-D problems achieved by our method, as illustrated in Figure 3.3. The results demonstrate that the differentiated compensation mode is superior to the uniform compensation mode, as indicated by the orange dotted line being below the blue dashed line.

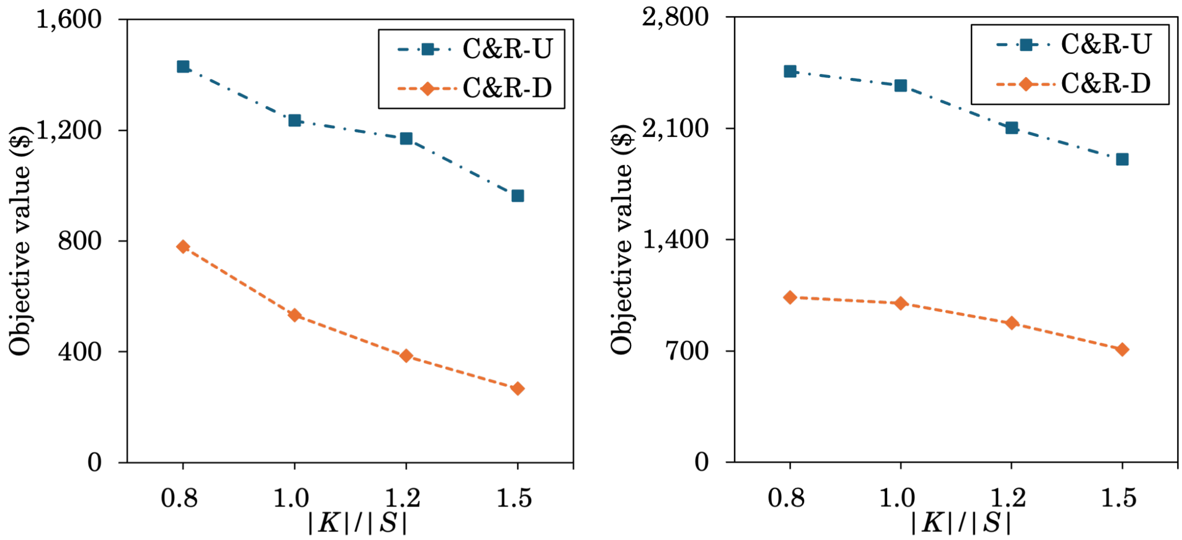

(a) Objective value under $\mathcal{S} = 15$

(b) Objective value under $\mathcal{S} = 20$

Figure 3.3. Comparison of objective value under C&R-U and C&R-D problems

To assess the effectiveness of the H-ILS-VNS/VNS-TS methods for larger-scale C&R-U/C&R-D problems, we tested their performance on instances with 100 to 200 orders and 100 to 300 crowd-couriers. Figure 3.4 illustrates the computation time for solving various scales of C&R-U and C&R-D problems.

The results indicate that H-ILS-VNS efficiently handles a C&R-U problem with 200 orders and 300 crowd-couriers within 211.5 min, while a C&R-D problem of the same size is solved in 22 min. This also implies the greater computational challenges of the C&R-U problem, mainly due to the exploration of the various compensation rates. Notably, as the number of O2O orders increases, the computation time does not grow exponentially, demonstrating the scalability of H-ILS-VNS in tackling large-scale problems and finding good-quality solutions beyond the capabilities of commercial solvers. Furthermore, for a given number of orders, computation time rises as the number of crowd-couriers increases, as illustrated in Figure 3.4(a) and Figure 3.4(b).

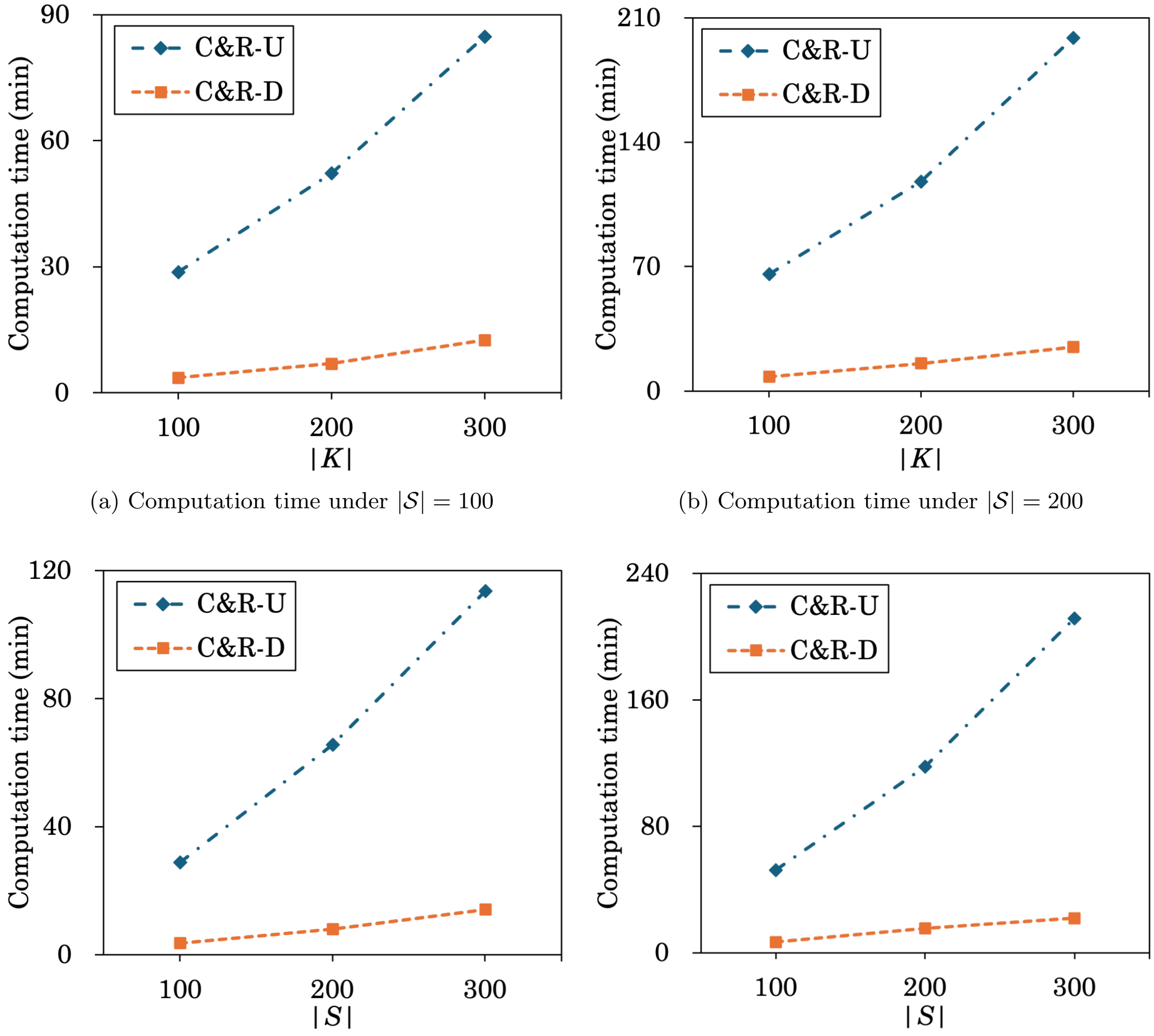

(a) Computation time under $|\mathcal{S}| = 100$

(b) Computation time under $|\mathcal{S}| = 200$

(c) Computation time under $|\mathcal{K}| = 100$

(d) Computation time under $|\mathcal{K}| = 200$

Figure 3.4. Computational efficiency of our proposed methods for solving C&R-U and C&R-D problems

Similarly, more orders lead to longer computation times, with a fixed number of crowd-couriers, as illustrated in Figure 3.4(c) and Figure 3.4(d). Interestingly, computational efficiency is more affected by the number of orders than by the number of crowd-couriers. For example, increasing the crowd-couriers from 100 to 200 with 100 orders results in an 81.6% rise in computation time, whereas increasing the orders from 100 to 200 with 100 crowd-couriers leads to a 127.7% increase in computation time.

3.4.3 Impact analysis of hybrid delivery systems

This section first evaluates the benefits of the hybrid delivery systems with crowd-shipping services through the comparison of some economic indicators and subsequently explores the impact of ETP and carrying capacity on the operation and management of the hybrid delivery system via sensitivity analysis.

To explore the benefit of the hybrid delivery system with crowd-shipping service, we conduct experiments on instances with 100, 200, and 300 O2O orders and various numbers of crowd-couriers at order-to-crowd-courier ratios of 0.8, 1, 1.2, and 1.5. Three delivery models are compared: the traditional dedicated delivery service without crowd-shipping, a hybrid system with crowd-shipping under uniform compensation (C&R-U), and a hybrid system under differentiated compensation (C&R-D). We evaluate the total cost (TC), the average cost per kilogram by dedicated vehicles (AveSlf), the average cost per kilogram by crowd-couriers (AveCrd), the number of crowd-couriers employed (CC), and the fleet size of dedicated vehicles (FS). The results are summarized in Table 3.3.

Table 3.3 shows that the hybrid delivery system with crowd-shipping can significantly reduce total costs for fulfilling orders compared to traditional dedicated delivery model. For example, the average total cost of the dedicated delivery model is \$24,153, while the hybrid delivery system with uniform compensation lowers it to \$20,419, achieving a 15.5% cost saving. Under a given number of orders, e.g., the total cost further decreases from \$22,902 to \$19,199 as the courier-to-order ratio increases from 0.8 to 1.5, highlighting the cost efficiency of utilizing crowd-shipping services and engaging more crowd-couriers. Moreover, there is a reduction in the dedicated vehicle fleet size, from an average of 28 vehicles in the traditional delivery model to 15 vehicles in the hybrid delivery system under a uniform compensation mode. The average cost per kilogram for parcels delivered by crowd-couriers is also lower than that of using dedicated vehicles. The deceased total cost could result from the reduction of the cost associated with the utilization of dedicated vehicle particularly the fixed cost burden of maintaining a large fleet of vehicles, and the adoption of more cost-efficient crowd-shipping services.

The hybrid delivery system under the differentiated compensation mode offers the same benefits as the system under the uniform compensation mode, such as reducing total cost, dedicated vehicle fleet size, and average delivery cost. However, compared to the uniform compensation mode, the differentiated compensation mode further decreases the total cost from \$20,419 to \$19,387. It achieves a lower average delivery cost per kilogram through crowd-couriers (averaged at \$5.8/kg), reduces the dedicated vehicle fleet size (averaged at 13 vehicles), and increases the number of employed crowd-couriers (averaged at 145 persons). This is because the differentiated compensation mode allows the delivery service provider to employ more crowd-couriers at lower individual-specific compensation rates, reducing reliance on dedicated vehicles.

To examine the effects of ETP and the carrying capacity of crowd-couriers on hybrid delivery systems with crowd-shipping services. We evaluate this by exploring the former indicators, e.g.,

Table 3.3. Performance of traditional dedicated delivery and hybrid delivery models under uniform and differentiated compensation modes

Instance	$\lvert\mathcal{S}\rvert$	$\lvert\mathcal{K}\rvert/\lvert\mathcal{S}\rvert$	Dedicated delivery			C&R-U				C&R-D			
			TC (\$)	AveSlf (\$/kg)	FS	TC (\$)	AveCrd (\$/kg)	CC	FS	TC (\$)	AveCrd (\$/kg)	CC	FS
1	100	0.8	11,531	6.8	13	10,535	5.5	47	8	9,330	5.4	56	7
2	100	1.0	11,531	6.8	13	9,391	5.0	64	7	8,803	5.2	72	6
3	100	1.2	11,531	6.8	13	9,049	5.0	89	6	7,803	5.2	83	5
4	100	1.5	11,531	6.8	13	8,458	5.2	94	5	7,195	5.1	106	5
5	200	0.8	24,698	7.2	29	22,902	6.3	111	18	21,665	6.2	122	17
6	200	1.0	24,698	7.2	29	22,033	6.4	120	17	20,763	5.9	143	15
7	200	1.2	24,698	7.2	29	21,098	6.2	139	14	19,127	5.8	163	12
8	200	1.5	24,698	7.2	29	19,199	6.0	163	12	18,591	5.8	184	11
9	300	0.8	36,230	7.0	42	32,157	6.5	161	26	31,468	6.3	170	23
10	300	1.0	36,230	7.0	42	31,425	6.4	184	24	29,860	6.2	199	21
11	300	1.2	36,230	7.0	42	30,402	6.4	197	23	29,351	6.2	210	20
12	300	1.5	36,230	7.0	42	28,384	6.2	221	20	27,692	6.1	230	19
Average	–	–	24,153	7.0	28	20,419	5.9	133	15	19,304	5.8	145	13

TC, AveCrd, CC, and FS via sensitivity analysis on the aforementioned instance with 300 O2O orders and 300 crowd-couriers.

<u>*Expects-to-be-paid of the available crowd-couriers (ETP)*</u>

The ETP of crowd-couriers may significantly influence the DSP's decision-making on the optimal compensation rate and choice between dedicated vehicles or crowd-couriers for parcel deliveries. We examine the impact of ETP of crowd-couriers on hybrid delivery systems under uniform and differentiated compensation modes. To this end, we assign random ETP values to crowd-couriers within different ETP intervals, such as [0,2] and [2,4]. Figure 3.5 illustrates the impact of ETP under two compensation modes.

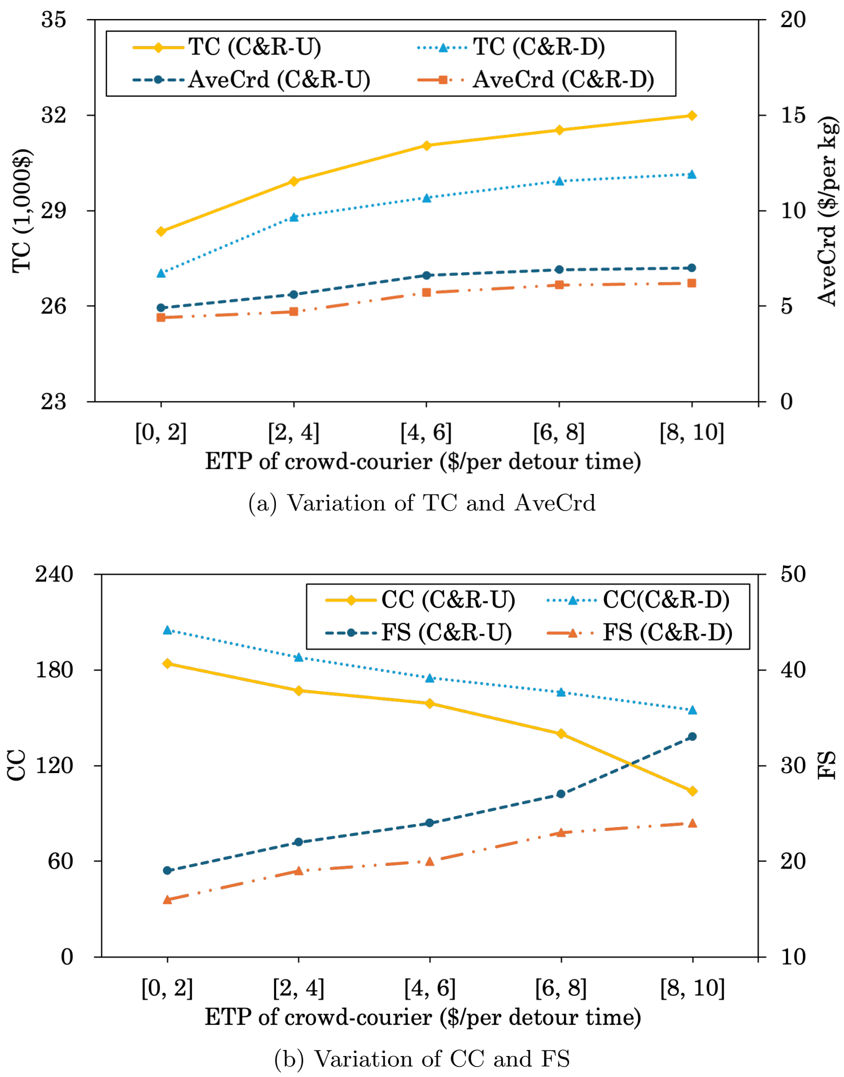

(a) Variation of TC and AveCrd

(b) Variation of CC and FS

Figure 3.5. Effect of ETP on the hybrid delivery system under different compensation modes

Figure 3.5 indicates that under the uniform compensation mode, an increase in the ETP results in a corresponding increase in total cost incurred by the retailer for fulfilling the O2O orders. This is due to a decrease in the utilization of crowd-couriers and an increase in the reliance on dedicated vehicles. From one perspective, the escalation of unit cost for employing crowd-couriers causes a reduction of employing crowd-couriers employed, as shown in Figure 3.5(b), thereby obligating the retailer to incur increased self-operating cost through the usage of dedicated delivery vehicles. From another viewpoint, the rise in the unit cost of engaging crowd-couriers induces a corresponding increase in the overall cost of CS service, as illustrated in Figure 3.5(a). The differentiated compensation mode demonstrates similar results, but it still exhibits superiority over the uniform compensation mode in terms of total cost.

Carrying capacity of crowd-couriers (Cap)

We then analyze how the carrying capacity of crowd-couriers affects the performance of hybrid delivery systems under uniform and differentiated compensation models. To achieve this, we assign random carrying capacities to crowd-couriers within different intervals such as [10 kg, 20 kg] and [30 kg, 40 kg]. Figure 3.6 illustrates the impact of carrying capacity on the system under the two compensation modes.

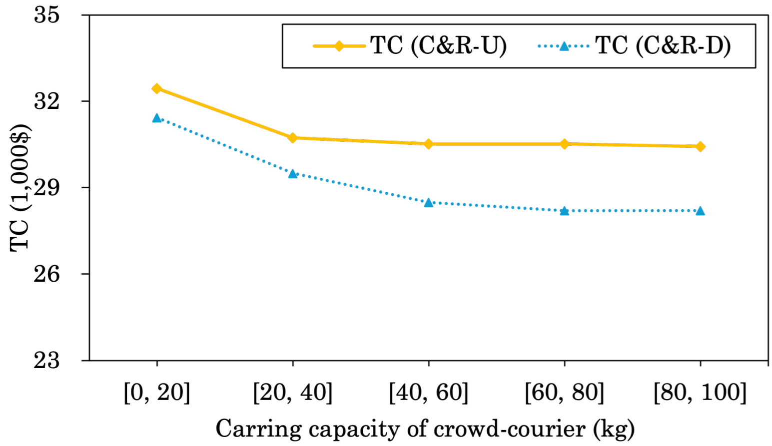

(a) Variation of TC

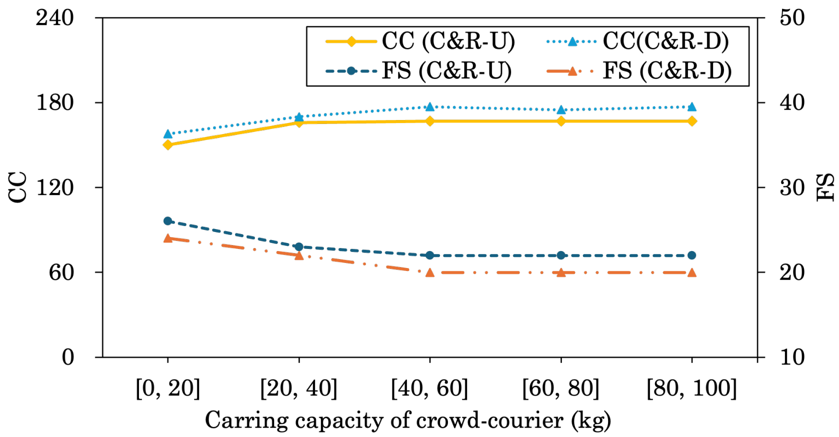

(b) Variation of CC and FS

Figure 3.6. Effect of carrying capacity on the hybrid delivery system under different compensation modes

Under uniform compensation mode, Figure 3.6(a) shows that the increase in carrying capacity results in reduced total costs from \$32,452 to \$30,442, stabilizing when carrying capacity reaches 60 kg. This occurs because crowd-couriers with greater carrying capacity can handle more deliveries, reducing the need to employ a large number of crowd-couriers, as indicated by the downward trend in Figure 3.6(b). Meanwhile, the fleet size also decreases slightly because fewer dedicated vehicles are needed. However, once the carrying capacity reaches 60 kg, cost efficiency maximizes due to participation constraints related to the available time period and ETP requirements. A similar pattern also appears in the differentiated compensation mode, but the cost impact of increased carrying capacity is more pronounced, as shown by the steeper decline in Figure 3.6(a). This analysis suggests that DSPs should also conduct thorough market surveys of potential crowd-couriers' carrying capacities and maintain an optimal fleet size of dedicated vehicles to minimize total costs.

3.5 Concluding Remarks

This chapter investigates the joint optimization of compensation rate and service routes of crowd-courier and dedicated vehicle for the hybrid delivery system incorporating the OT-based CS services and taking into account the heterogeneous service requirements of the crowd-couriers in carrying capacity, available time period, and ETP. The retailer has the option to utilize crowd-couriers or dedicated vehicles to deliver O2O orders while adhering to the heterogeneous service requirements of the employed crowd-couriers. Faced with the available service by crowd-couriers as well as the requirements, the retailer aims to determine the optimal compensation rate and the service routes of crowd-couriers and dedicated vehicles to minimize the total cost. To achieve the objectives, we formulate the studied problems as an MINLP model and an MILP models for the uniform compensation mode and differentiated compensation mode, respectively. Then, linearization techniques are applied to transform the MINLP model to an MILP model that can be solved by commercial solvers. A hybrid algorithm integrating a customized ILS and VNS with a nested TS algorithms is also developed to obtain good-quality solutions for the large-scale instances. Numerical experiments on a series of instances by modified Solomon benchmark instances are carried out to validate the performance of the proposed models and solution methods. Results indicates that the CS model with well-designed compensation rate can save cost for the retailers. Meanwhile, differentiated compensation mode is superior to the uniform mode in cost-saving. Sensitivity analysis is also conducted to explore the factors influencing the CS model and derive managerial insights for stockholders.

3.6 Appendix: Notations

Set	
$\mathcal{S}$	Set of the O2O orders
$\mathcal{V}$	Set of vehicles, $v \in \mathcal{V}$
$\mathcal{K}$	Set of crowd-couriers, $k \in \mathcal{K}$
$\mathcal{D}$	Set of destinations of crowd-couriers
$\tilde{\mathcal{P}}$	Set of candidate compensation rates
Parameters	
q_i	Load of ordered products of O2O order i
s_i	Service time for O2O order i
$[e_i, l_i]$	Time window at node i
Q_v	Loading capacity of each vehicle $v \in \mathcal{V}$
Q_k	Carrying capacity of the crowd-courier $k \in \mathcal{K}$
d_k	Destination of the crowd-courier $k \in \mathcal{K}$
e_k	Earliest departure time of crowd-courier $k \in \mathcal{K}$ from the retail store
l_k	Latest arrival time of the crowd-courier k at the destination
E_k	Expects-to-be-paid of crowd-courier $k \in \mathcal{K}$ per unit of detour time
$r_{i,j}$	Travel time from node i to j by the dedicated vehicle
c^{f}	Fixed cost for per unit of using a dedicated vehicle
c_{ij}	Transportation cost incurred by the dedicated vehicles from location i to j
t_{ij}	Travel time from node i to j by the crowd-courier
$0/\sigma + 1$	Retail store
M	A very large number
$p_{\max}$	A parameter defined as the maximum ETP of all available crowd-couriers
Variables	
p	Continuous variable to denote the compensation paid for employing crowd-couriers for per unit of detour time.
p_k	Continuous variable to denote an individual-specific compensation rate for employing crowd-courier $k \in \mathcal{K}$ for per unit of detour time.
x_{ijv}	Binary variable that is set to 1 if vehicle $v \in \mathcal{V}$ travels from node i to node j for all i, j in set $\mathcal{N}$, and it is set to 0 otherwise.
y_{ijk}	Binary variable that is set to 1 if crowd-courier $k \in \mathcal{K}$ travels from node i to node j for all i, j in set $\mathcal{N}$, and it is set to 0 otherwise.
z_{ijk}	Auxiliary variable, which defined by $z_{ijk} = py_{ijk}$.

τ_i^v	Continuous variable representing the time at which vehicle $v \in \mathcal{V}$ begins service at node $i \in \mathcal{N}$.
τ_i^k	Continuous variable representing the time at which crowd-courier $k \in \mathcal{K}$ starts service at node $i \in \mathcal{N}$.

Chapter 4 Compensation Optimization for Crowd-Shipping based on Ordinary Travelers Considering Collaborative Delivery for Shared Customers

This chapter extends the investigations of Chapter 3 by examining a collaboration alliance, allocation of delivery orders, compensation rate, and routes of vehicle and crowd-courier joint optimization (CACR) problem within a collaborative hybrid delivery system. This system integrates ordinary travelers as crowd-couriers and dedicated vehicles, specifically considering the collaborative deliveries for shared customers. A bi-objective optimization model is formulated for the CACR problem to minimize the total operational cost and carbon emissions of the delivery system. By exploring characteristics of the CACR problem, this problem is later effectively decomposed into a series of bi-objective sub-problems, which aim to find Pareto-optimal service routes for both dedicated vehicles and crowd-couriers under the predefined collaboration alliance and compensation rate. Motivated by this, a decomposition-based iterative optimization (DIO) method is developed to find Pareto-optimal solutions for the CACR problem by iteratively solving a series of sub-problems with updated candidate compensation rate and collaboration alliance. A cluster-first route-second approach is adopted to solve the bi-objective sub-problems. Specifically, a customized spatiotemporal clustering (STC) technique is proposed to achieve the allocation of O2O orders, and an enhanced non-dominated sorting genetic algorithm-II (NSGA-II) that incorporates the Clarke and Wright saving (CW) method, referred to as CW-NSGA-II, is then applied to find the routing solutions. Numerical experiments using adapted benchmark instances and a simulated case in Chongqing, China are conducted to assess our proposed solution method as well as delivery system.

The rest of this chapter is organized in the following manner. Problem description as well as assumptions and notations are provided in Section 4.1. A bi-objective optimization model for the CACR problem is developed in Section 4.2. To solve the problem, a DIO method is developed in Section 4.3. Numerical experiments on adapted benchmark instances and a simulated case in Chongqing, China are performed in Section 4.4. Conclusions of this chapter are summarized in Section 4.5. Notation used in this chapter is listed in Section 4.6 for readability.

4.1 Problem Statement

Consider multiple homogeneous retailers, e.g., supermarkets of the same brand, that each provides dual-shopping channels including an online channel on a platform and an offline channel on a physical store within a same urban area. We consider that each retailer receives a group of O2O orders that each order is associated with a delivery location, e.g., customer's home, a time window that the customer can accept delivery services, load of the ordered products, and service duration for unloading products to customers. Let $\mathcal{R}$ denote the set of retailers, $r \in \mathcal{R}$. We also use $\mathcal{R}$ to denote the set of retail stores. Let $\mathcal{C}^r$ denote the set of all O2O orders received by retailer $r \in \mathcal{R}$. For ease of presentation, we also use $\mathcal{C}^r$ to denote the set of corresponding delivery locations of the O2O orders. We define $\mathcal{C} := \bigcup_{r \in \mathcal{R}} \mathcal{C}^r$. Let $[e_i, l_i]$ denote the delivery time window of O2O order $i \in \mathcal{C}^r$, where e_i and l_i denote the earliest time epoch and latest time epoch for delivery at location $i \in \mathcal{C}^r$, respectively. The load of ordered products of O2O order $i \in \mathcal{C}^r$ is denoted by q_i. The service duration for unloading order i's products to the customer is denoted by σ_i.

We assume that the O2O orders can be shared between different retailers if collaboration is established between them. In other words, if collaboration is formed between different retailers, the O2O order of a retailer can be fulfilled by its collaborative counterpart. This is rational particularly in instances where the retailers are supplied by the same entity, more so under a brand that exhibits similar product and operating costs (Fernández et al., 2018). Nonetheless, the split of demand for a single O2O order is not permissible, indicating that each O2O order must be exclusively serviced by a singular retailer. Let π_{rs} denote the presence of collaboration between two retailers $r \in \mathcal{R}$ and $s \in \mathcal{R}$, where $\pi_{rs} = 1$ if collaboration is formed between them and $\pi_{rs} = 0$ otherwise. Note that $\pi_{rs} = \pi_{sr}, \forall r, s \in \mathcal{R}$ and we set $\pi_{rr} = 1, \forall r \in \mathcal{R}$. Then, let Π^r denote the set of retailers engaged in a collaborative delivery arrangement with retailer r, which can be determined by $\Pi^r = \{s \in \mathcal{R} : \pi_{rs} = 1\}, \forall r \in \mathcal{R}$. In this context, an O2O order $i \in \mathcal{C}^r$ of retailer $r \in \mathcal{R}$ can be fulfilled by any one of the retailers in set Π^r including retailer r itself. Let $\mathcal{C}^r(\Pi^r)$ denote the O2O orders that can be served by retailer r under the collaboration Π^r, where $\mathcal{C}^r(\Pi^r) := \bigcup_{s \in \Pi^r} \mathcal{C}^s, \forall r \in \mathcal{R}$.

Consider that each retailer can fulfil O2O orders through the dedicated delivery service by utilizing self-operating dedicated delivery vehicles and the OT-based CS service by employing ordinary travelers, e.g., in-store customers, as crowd-couriers. Specifically, each retailer $r \in \mathcal{R}$ can provide dedicated delivery services utilizing a fleet of self-operating vehicles in set $\mathcal{V}^r$ to deliver the products from its retail store $r_v \in \mathcal{R}$ while respecting the maximum loading capacity Q_v of each vehicle. Each used vehicle is associated with a fixed cost, a transportation cost, and the corresponding carbon emission. Let c^{f} denote the fixed cost, and c_{ij}, t_{ij}, and m_{ij} denote the transportation cost, travel time, and carbon emission incurred by the dedicated vehicles from location i to j. Besides the dedicated delivery service, the retailer can also employ crowd-couriers to serve the orders during their personal itineraries from the retail store to the itinerary destinations. Let $\mathcal{K}^r$ denote the set of all available crowd-couriers who depart from retail store $r_k \in \mathcal{R}$, and $\mathcal{D}^r$ denote the set of destinations of all crowd-couriers in set $\mathcal{K}^r$. We define $\mathcal{D} := \bigcup_{r\in\mathcal{R}} \mathcal{D}^r$. Each crowd-courier $k \in \mathcal{K}^r$ with an original itinerary from the retail store $r_k \in \mathcal{R}$ to their destination $d_k \in \mathcal{D}^r$ specifies their the earliest departure time e_k from the retail store, the latest arrival time l_k at the destination, as well as the maximum carrying capacity Q_k. Meanwhile, since CS services may cause detour to crowd-couriers compared with their original itineraries, each crowd-courier $k \in \mathcal{K}^r$ puts forth an ETP E_k for per unit of detour time. Let μ_{ij} and ε_{ij} denote the travel time and carbon emission by the crowd-courier k from location i to j, respectively.

Given the O2O orders and dedicated delivery fleets operated by each retailer as well as the available crowd-couriers, a CACR problem is formulated for a multi-retailer collaborative delivery system with OT-based CS services. The CACR problem is to jointly i) establish the collaborative delivery system by determining the optimal collaboration alliance among retailers, ii) allocate the O2O orders to different retailers, iii) determine the optimal compensation, denoted by p, for employing crowd-couriers per unit of detour time, and iv) determine the delivery tasks to either dedicated vehicles or crowd-couriers an associated service routes so that i) all O2O orders are satisfied with respecting the requirements of the O2O orders, ii) the available time period, carrying capacity, ETPs of all employed crowd-couriers are met, and iii) the total costs including the cost paid for dedicated delivery service and the compensation cost paid for employing CS service and the generated carbon emissions are minimized. Notations employed throughout this chapter are outlined in Section 4.6 for readability.

4.2 Bi-Objective Programming Model Formulation

For ease of modeling for the CACR problem, all locations in set $\mathcal{R}$, $\mathcal{C}$, and $\mathcal{D}$ are grouped into a node set $\mathcal{N}$, i.e., $\mathcal{N} = \mathcal{R}\cup\mathcal{C}\cup\mathcal{D}$, and the arcs associated with node set $\mathcal{N}$ are grouped into an arc set $\mathcal{A}$, which is defined as all the arcs possibly traversed by the dedicated vehicles and crowd-couriers. We found that the dedicated delivery vehicles and crowd-couriers in a specific retail store is associated with a set of possibly visiting nodes and traversing arcs with respect to the retailer r's collaboration alliance Π^r with other retailers. In other words, a dedicated vehicle or crowd-courier will only visit a set of nodes and traverse a set of arcs. In this context, we define a subset of nodes $\mathcal{N}_v^r(\Pi^r) \subset \mathcal{N}$ as the set of nodes that are possibly visited by the dedicated vehicle $v \in \mathcal{V}^r$ departing from retail store $r_v \in \mathcal{R}$ under the collaboration of Π^r, i.e., $\mathcal{N}_v^r(\Pi^r) = \{r_v\} \cup \mathcal{C}^r(\Pi^r) \cup \{r'_v\}$, where r'_v is a duplication of r_v for ease of modeling. Furthermore, we denote $\mathcal{A}_v^r(\Pi^r)$ as the set of arcs that possibly traversed by the dedicated vehicle $v \in \mathcal{V}^r$ departing from retail store $r_v \in \mathcal{R}$ under the collaboration of Π^r, i.e., $\mathcal{A}_v^r(\Pi^r) = \{(r_v, j)|v \in \mathcal{V}^r, j \in \mathcal{C}^r(\Pi^r)\} \cup \{(i,j)\,|i, j \in \mathcal{C}^r(\Pi^r)\} \cup \{(i, r'_v)|i \in \mathcal{C}^r(\Pi^r), v \in \mathcal{V}^r\}$. In addition, let $\mathcal{N}_k^r(\Pi^r) \subset \mathcal{N}$ denote the set of nodes that are possibly visited by the crowd-courier $k \in \mathcal{K}^r$

departing from retail store $r_k \in \mathcal{R}$ under the collaboration of Π^r, i.e., $\mathcal{N}_k^r(\Pi^r) = \{r_k\} \cup \mathcal{C}^r(\Pi^r) \cup \{d_k\}$. The set of arcs that possibly traversed by the crowd-courier $k \in \mathcal{K}^r$ departing from retail store $r_k \in \mathcal{R}$ under the collaboration of Π^r is defined as $\mathcal{A}_k^r(\Pi^r) = \{(r_k, j) \,|k \in \mathcal{K}^r, j \in \mathcal{C}^r(\Pi^r)\} \cup \{(i,j) \,|i \in \mathcal{C}^r(\Pi^r), j \in \mathcal{C}^r(\Pi^r)\} \cup \{(i, d_k) \,|i \in \mathcal{C}^r(\Pi^r), k \in \mathcal{K}^r\} \cup \{(r_k, d_k) \,|i \in \mathcal{C}^r, k \in \mathcal{K}^r\}$. We define that $\mathcal{A}^r(\Pi^r) = \mathcal{A}_v^r(\Pi^r) \cup \mathcal{A}_k^r(\Pi^r)$ and $\mathcal{A} = \bigcup_{r\in\mathcal{R}} \mathcal{A}^r(\Pi^r)$. Each node $i \in \mathcal{N}$ is associated with a service time window $[e_i, l_i]$, a service duration σ_i, and a parcel load q_i, with the following information: service duration $\sigma_i = 0, \forall i \in \mathcal{R} \cup \mathcal{D}$ and parcel load $q_i = 0, \forall i \in \mathcal{R} \cup \mathcal{D}$. Each arc $(i,j) \in \mathcal{A}$ is associated with a transportation cost c_{ij}, travel time t_{ij}, and carbon emission m_{ij} by dedicated vehicle from node i to j, and associated with a travel time μ_{ij} and carbon emission ε_{ij} by the crowd-courier from node i to j.

Given the O2O orders, available crowd-couriers, and dedicated vehicles, an bi-objective optimization model [CACR] will be formulated for the CACR problem to determine the optimal collaboration alliance, O2O orders allocation among retailers, compensation rate for employing crowd-couriers, and service routes for dedicated delivery vehicles and employed crowd-couriers. In addition to before-mentioned variable p and π, we define the following variables:

- x_{ijv}: Binary decision variable that equals 1 if dedicated vehicle $v \in \mathcal{V}^r$, $\forall r \in \mathcal{R}$ travels directly from node i to j, $\forall (i,j) \in \mathcal{A}_v^r(\Pi^r)$, and 0 otherwise;
- y_{ijk}: Binary decision variable that equals 1 if crowd-courier $k \in \mathcal{K}^r$, $\forall r \in \mathcal{R}$ travels directly from node i to j, $\forall (i,j) \in \mathcal{A}_k^r(\Pi^r)$, and 0 otherwise;
- τ_i^v: Continuous variable to denote the time epoch when vehicle $v \in \mathcal{V}^r$ starts service at node $i \in \mathcal{N}_v^r(\Pi^r)$. Note that $\tau_{r_v}^v$ represents the time at which vehicle $v \in \mathcal{V}^r$ departs from the retail store, while $\tau_{r_v'}^v$ indicates the time when vehicle returns to retail store;
- τ_i^k: Continuous variable to denote the time epoch when crowd-courier $k \in \mathcal{K}^r$ starts service at node $i \in \mathcal{N}_k^r(\Pi^r)$. Note that $\tau_{r_k}^k$ represents the time at which crowd-courier $k \in \mathcal{K}^r$ departs from the retail store, while $\tau_{d_k}^k$ indicates the time at their destination.

With the above notations, the bi-objective programming model for the studied CACR problem can be formulated as follows:

[CACR]

$$\begin{aligned} \min_{\{\boldsymbol{\pi},\mathbf{p},\mathbf{x},\mathbf{y},\boldsymbol{\tau}\}} TC = c^{\mathrm{f}} \sum_{r\in\mathcal{R}} \sum_{v\in\mathcal{V}^r} \sum_{j\in\mathcal{C}^r(\Pi^r)} x_{r_v jv} + \sum_{r\in\mathcal{R}} \sum_{v\in\mathcal{V}^r} \sum_{(i,j)\in\mathcal{A}_v^r(\Pi^r)} c_{ij} x_{ijv} \\ + p \sum_{r\in\mathcal{R}} \sum_{k\in\mathcal{K}^r} \left(\sum_{(i,j)\in\mathcal{A}_k^r(\Pi^r)} \mu_{ij} y_{ijk} - \mu_{r_k d_k} \right) \end{aligned} \tag{4.1}$$

$$\min_{\{\boldsymbol{\pi},\mathbf{p},\mathbf{x},\mathbf{y},\boldsymbol{\tau}\}} CE = \sum_{r\in\mathcal{R}}\sum_{v\in\mathcal{V}^r}\sum_{(i,j)\in\mathcal{A}_v^r(\Pi^r)} m_{ij}x_{ijv} + \sum_{r\in\mathcal{R}}\sum_{k\in\mathcal{K}^r}\left(\sum_{(i,j)\in\mathcal{A}_k^r(\Pi^r)} \varepsilon_{ij}y_{ijk} - \varepsilon_{r_k d_k}\right) \tag{4.2}$$

subject to

$$\sum_{r\in\Pi^r}\sum_{v\in\mathcal{V}^r}\sum_{j\in\mathcal{C}^r(\Pi^r)\cup\{r'_v\}} x_{ijv} + \sum_{r\in\Pi^r}\sum_{k\in\mathcal{K}^r}\sum_{j\in\mathcal{C}^r(\Pi^r)\cup\{d_k\}} y_{ijk} = 1, \qquad \forall i\in\mathcal{C}^r, r\in\mathcal{R} \tag{4.3}$$

$$\sum_{j\in\mathcal{C}^r(\Pi^r)\cup\{r'_v\}} x_{r_v jv} = 1, \qquad \forall v\in\mathcal{V}^r, r\in\mathcal{R} \tag{4.4}$$

$$\sum_{j\in\mathcal{C}^r(\Pi^r)\cup\{r'_v\}} x_{ijv} = \sum_{j\in\mathcal{C}^r(\Pi^r)\cup\{r_v\}} x_{jiv}, \qquad \forall i\in\mathcal{C}^r\left(\Pi^r\right), v\in\mathcal{V}^r, r\in\mathcal{R} \tag{4.5}$$

$$\sum_{i\in\mathcal{C}^r(\Pi^r)\cup\{r_v\}} x_{ir'_v v} = 1, \qquad \forall v\in\mathcal{V}^r, r\in\mathcal{R} \tag{4.6}$$

$$\sum_{j\in\mathcal{C}^r(\Pi^r)\cup\{d_k\}} y_{r_k jk} = 1, \qquad \forall k\in\mathcal{K}^r, r\in\mathcal{R} \tag{4.7}$$

$$\sum_{j\in\mathcal{C}^r(\Pi^r)\cup\{d_k\}} y_{ijk} = \sum_{j\in\mathcal{C}^r(\Pi^r)\cup\{r_k\}} y_{jik}, \qquad \forall i\in\mathcal{C}^r\left(\Pi^r\right), k\in\mathcal{K}^r, r\in\mathcal{R} \tag{4.8}$$

$$\sum_{i\in\mathcal{C}^r(\Pi^r)\cup\{r_k\}} y_{id_k k} = 1, \qquad \forall k\in\mathcal{K}^r, r\in\mathcal{R} \tag{4.9}$$

$$\tau_i^v + \sigma_i + t_{ij} \le \tau_j^v + M_1\left(1 - x_{ijv}\right), \qquad \forall (i,j)\in\mathcal{A}_v^r(\Pi^r), v\in\mathcal{V}^r, r\in\mathcal{R} \tag{4.10}$$

$$e_i \le \tau_i^v \le l_i, \qquad \forall i\in\mathcal{C}^r\left(\Pi^r\right), v\in\mathcal{V}^r, r\in\mathcal{R} \tag{4.11}$$

$$\sum_{i\in\mathcal{C}^r(\Pi^r)\cup\{r_v\}}\sum_{j\in\mathcal{C}^r(\Pi^r)} q_j x_{ijv} \le Q_v, \qquad \forall v\in\mathcal{V}^r, r\in\mathcal{R} \tag{4.12}$$

$$p \ge E_k y_{ijk}, \qquad \forall (i,j)\in\mathcal{A}_k^r(\Pi^r), k\in\mathcal{K}^r, r\in\mathcal{R} \tag{4.13}$$

$$\tau_i^k + \sigma_i + \mu_{ij} \le \tau_j^k + M_2\left(1 - y_{ijk}\right), \qquad \forall (i,j)\in\mathcal{A}_k^r(\Pi^r), k\in\mathcal{K}^r, r\in\mathcal{R} \tag{4.14}$$

$$\tau_{r_k}^k \ge e_k, \qquad \forall k\in\mathcal{K}^r, r\in\mathcal{R} \tag{4.15}$$

$$\tau_{d_k}^k \le l_k, \qquad \forall k\in\mathcal{K}^r, r\in\mathcal{R} \tag{4.16}$$

$$e_i \le \tau_i^k \le l_i, \qquad \forall i\in\mathcal{C}^r\left(\Pi^r\right), k\in\mathcal{K}^r, r\in\mathcal{R} \tag{4.17}$$

$$\sum_{i\in\mathcal{C}^r(\Pi^r)\cup\{r_k\}}\sum_{j\in\mathcal{C}^r(\Pi^r)} q_j y_{ijk} \le Q_v, \qquad \forall k\in\mathcal{K}^r, r\in\mathcal{R} \tag{4.18}$$

$$\pi_{rs} = \pi_{sr}, \qquad \forall r,s\in\mathcal{R} \tag{4.19}$$

$$\pi_{rr} = 1, \qquad \forall r \in \mathcal{R} \tag{4.20}$$

$$\Pi^r = \{s \in \mathcal{R} : \pi_{rs} = 1\}, \qquad \forall r \in \mathcal{R} \tag{4.21}$$

$$p \geq 0 \tag{4.22}$$

$$x_{ijv} \in \{0, 1\}, \qquad \forall (i,j) \in \mathcal{A}_v^r(\Pi^r), v \in \mathcal{V}^r, r \in \mathcal{R} \tag{4.23}$$

$$y_{ijk} \in \{0, 1\}, \qquad \forall (i,j) \in \mathcal{A}_k^r(\Pi^r), k \in \mathcal{K}^r, r \in \mathcal{R} \tag{4.24}$$

$$\pi_{rs} \in \{0, 1\}, \qquad \forall r, s \in \mathcal{R} \tag{4.25}$$

$$\tau_i^v \geq 0, \qquad \forall i \in \mathcal{N}_v^r(\Pi^r), v \in \mathcal{V}^r, r \in \mathcal{R} \tag{4.26}$$

$$\tau_i^k \geq 0, \qquad \forall i \in \mathcal{N}_k^r(\Pi^r), k \in \mathcal{K}^r, r \in \mathcal{R} \tag{4.27}$$

The objectives (4.1) and (4.2) are to reduce the overall costs and carbon emissions associated with fulfilling all O2O orders received by multiple retailers, respectively. Specifically, objective (4.1) seeks to minimize total cost, which includes expenses incurred from utilizing dedicated delivery services and compensating crowd-couriers. Objective (4.2) specifically targets the reduction of carbon emissions, taking into account the emissions resulting from dedicated delivery vehicles and the additional emissions caused by the detouring of crowd-couriers providing crowd-shipping services. Constraint (4.3) ensures that each O2O order received by a retailer is appropriately handled, either by the retailer's dedicated delivery vehicle, a crowd-courier, or through the service provided by its collaborative retailers. Constraints (4.4)–(4.6) impose the flow balance constraint on the dedicated delivery vehicles, while Constraints (4.7)–(4.9) impose a similar constraint on the potential crowd-couriers. Constraint (4.10) updates the service time epoch of a dedicated vehicle along the route, where M_1 denotes a large number. Constraint (4.11) ensures adherence to the service time window specified for O2O orders by the dedicated vehicles. Constraint (4.12) enforces the loading capacity of dedicated vehicles. Constraint (4.13) stipulates that the individuals can be employed to provide crowd-shipping services only if their ETPs are met. Constraint (4.14) updates the service time epoch of crowd-couriers along the route, with M_2 denoting a large number. Constraints (4.15)–(4.16) impose time constraints on crowd-couriers for their departure and arrival times. Constraint (4.17) guarantees that the service time window specified for O2O orders is respected by the employed crowd-couriers. Constraint (4.18) sets the carrying capacity limit for the crowd-couriers. Constraints (4.19)–(4.20) defines the collaboration between two retailers. Constraint (4.21) defines the set of collaborative retailers for each individual retailer. Constraints (4.22)–(4.27) establish the feasible domain for the decision variables.

4.3 DIO Solution Method

The CACR problem indicates significant computational complexities due to the multi-objective combinatorial optimization with various decision components, such as determining collaboration alliance, allocating O2O orders for multiple retailers, designing compensation rate for employing crowd-couriers, and optimizing service routes of dedicated delivery vehicles and crowd-couriers, making the problem unsolvable with off-the-shelf solvers. Therefore, we propose a customized DIO method. This section initially introduce the DIO method framework, and subsequently elaborates on the detailed procedures of the proposed DIO method.

4.3.1 Framework of DIO method

In this chapter, the original CACR problem aims to identify Pareto-optimal solutions of the decisions for collaboration alliance π_{rs}, compensation rate p, dedicated vehicle routes x_{ijv}, and crowd-courier routes y_{ijk} that can achieve a good balance between total cost and carbon emission objectives. Before the introduction of details of the DIO method, we firstly introduce some definitions for the better understanding of solutions of bi-objective optimization problem. Let $\boldsymbol{\theta}$ denote the solution including all above decisions, and $\boldsymbol{\Theta}$ be the set of solutions, where each solution $\boldsymbol{\theta} \in \boldsymbol{\Theta}$ is evaluated based on two objective values, i.e., total costs $TC(\boldsymbol{\theta})$ and total carbon emissions $CE(\boldsymbol{\theta})$. For our bi-objective optimization problem $\min_{\boldsymbol{\theta}\in\boldsymbol{\Theta}}(TC(\boldsymbol{\theta}), CE(\boldsymbol{\theta}))$ subjecting to the constraints, we have the following definitions:

Definition 4.1. ***(Cover and Dominate)*** *A solution $\boldsymbol{\theta} \in \boldsymbol{\Theta}$ is defined to cover a solution $\boldsymbol{\theta}' \in \boldsymbol{\Theta}$ (denoted by $\boldsymbol{\theta} \preceq \boldsymbol{\theta}'$) if $TC(\boldsymbol{\theta}) \leq TC(\boldsymbol{\theta}')$ and $CE(\boldsymbol{\theta}) \leq CE(\boldsymbol{\theta}')$. A solution $\boldsymbol{\theta}$ dominates $\boldsymbol{\theta}'$ (denoted by $\boldsymbol{\theta} \prec \boldsymbol{\theta}'$) if and only if $\boldsymbol{\theta} \preceq \boldsymbol{\theta}'$ and $TC(\boldsymbol{\theta}) < TC(\boldsymbol{\theta}')$ or $CE(\boldsymbol{\theta}) < CE(\boldsymbol{\theta}')$. A solution $\boldsymbol{\theta} \in \boldsymbol{\Theta}$ is non-dominated if there is no solution $\boldsymbol{\theta}' \in \boldsymbol{\Theta}$ such that $\boldsymbol{\theta}' \prec \boldsymbol{\theta}$.*

Definition 4.2. ***(Pareto-optimal and Pareto front)*** *A solution $\boldsymbol{\theta} \in \boldsymbol{\Theta}$ is said to be Pareto-optimal if it is non-dominated. The Pareto-optimal solution set is defined as $\boldsymbol{\Theta}^* = \{\boldsymbol{\theta} \in \boldsymbol{\Theta} : \boldsymbol{\theta}$ is Pareto-optimal$\}$. The Pareto front is defined as $\mathcal{O} = \{TC(\boldsymbol{\theta}), CE(\boldsymbol{\theta}) : \boldsymbol{\theta} \in \boldsymbol{\Theta}^*\}$.*

We can see that once the collaboration alliance is confirmed, the CACR problem becomes a bi-objective multi-depot vehicle and crowd routing problem with compensation optimization, referred to as the BO-MVCRP-C problem, which aims to find Pareto-optimal solutions of compensation rate and service routes for dedicated deliver vehicles or crowd-couriers under a given collaboration alliance. Furthermore, the BO-MVCRP-C problem can be further decomposed to a BO-MVCRP problem that aims to find Pareto-optimal solutions of routes for dedicated vehicles and crowd-couriers if the compensation rate is also determined. Motivated by this, we can solve the master CACR problem by solving the BO-MVCRP problem, referred to as the sub-problem, under the iteratively updated collaboration alliance and compensation until the stop condition is reached. To this end, we propose the DIO method, see Figure 4.1.

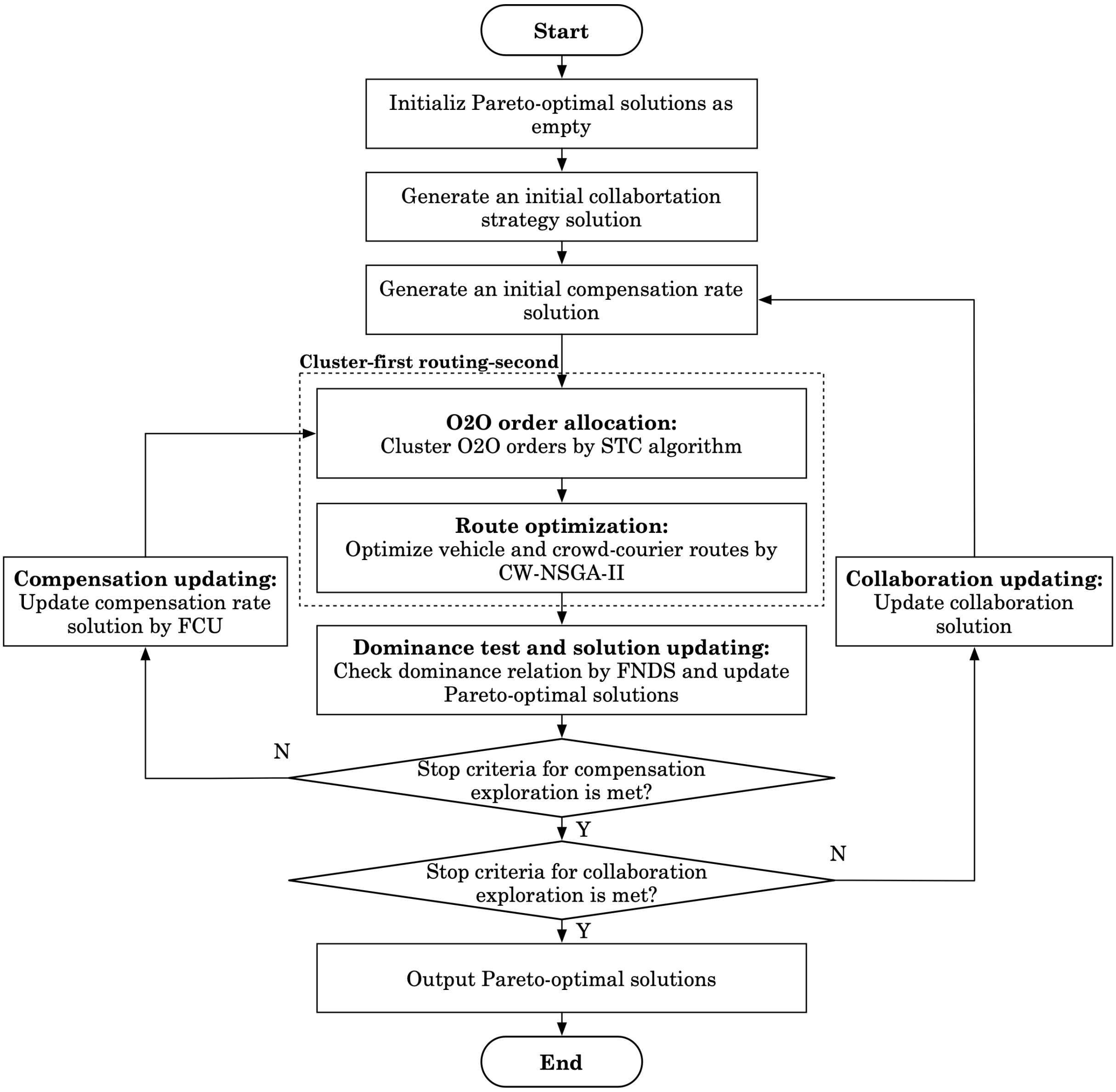

Figure 4.1. Framework of the DIO method

The DIO method starts with the initialization of the global Pareto-optimal solutions with all decisions as empty set. Initially, a collaboration alliance and compensation rate are generated as the current collaboration alliance and compensation rate solutions. As previously mentioned, with these solutions in place, the master CACR problem is reduced to a BO-MVCRP problem, i.e., the sub-problem. To solve the sub-problem, we employ the widely used *cluster-first route-second* philosophy, which is a prevalent approach in solving multi-depot VRPs (Dondo and Cerdá, 2007). Specifically, we first employ a spatiotemporal clustering (STC) method to allocate the O2O orders to multiple retailers based on spatiotemporal proximity. Subsequently, we develop an enhanced NSGA-II that incorporates the CW method, referred to as CW-NSGA-II, to find the routing solutions for dedicated vehicles and crowd-couriers. We can then derive Pareto-optimal solutions under current collaboration alliance and compensation. A fast non-dominated sorting (FNDS) procedure is then applied to check the dominance relation and update the global Pareto-optimal solutions that encompass all decisions. Subsequently, the collaboration alliance and compensation rate will be updated. The limited number of potential collaboration strategies collaboration alliance, among retailers allows for a comprehensive exploration of all feasible options. As for the compensation rate, which varies within a continuous positive range, a frequency-based compensation updating (FCU) procedure is employed for its update. This iterative process continues until the termination criteria are satisfied, culminating in the acquisition of the final Pareto-optimal solutions.

4.3.2 Compensation generation and updating by FCU procedure

In the proposed DIO method, a compensation needs to be generated and updated. Similar to Chapter 3, while compensation rate can be theoretically any non-negative value, i.e., $p > 0$, leading to an infinite search space for compensation, we can reduce this to a finite set of candidate compensation rates by analyzing the problem's characteristics. let $\mathcal{P} = \{p_1, \cdots, p_i, \cdots, p_n\}$ represent the set of unique ETPs of all crowd-couriers, and we have Proposition 4.1.

Proposition 4.1. *The optimal compensation rate denoted by p^* for the CACR problem must be either one of the ETPs of all crowd-couriers or zero, i.e., $p^* \in \{0\} \cup \mathcal{P}$.*

Proof. We prove proposition 4.1 by contradiction. We assume that $p_1 < \cdots < p_i < p_{i+1} < \cdots < p_n$, where $p_1 = \min_{k \in \mathcal{K}^r, r \in \mathcal{R}} E_k$ and $p_n = \max_{k \in \mathcal{K}^r, r \in \mathcal{R}} E_k$. Suppose that the optimal compensation rate is $(p_i + \Delta p) \notin \mathcal{P}$ such that $(p_i + \Delta p) < p_{i+1}, \forall \Delta p > 0$. However, by setting the compensation rate to p_i instead of $(p_i + \Delta p)$, we can reduce costs and maintain the carbon emissions without altering the delivery service plan for O2O orders. That means the compensation rate $(p_i + \Delta p)$ is dominated by p_i. Additionally, this also applies to the cases where assuming $0 < p^* < p_1$ and $p_n < p^* < \infty$. Therefore, the optimal compensation rate must be one of the ETPs of crowd-couriers or zero, i.e., $p^* \in \{0\} \cup \mathcal{P}$. $\square$

With Proposition 4.1, we can limit the search of compensation solution to a finite set of candidate compensation rate denoted as $\tilde{\mathcal{P}} = \{0\} \cup \mathcal{P}$. We found that the optimal compensation rate is influenced by the ETPs declared by available crowd-couriers, especially those declared most frequently. Motivated by this, we will generate and update the compensation rate based on the descending order of ETP frequency, referred to as the ETP frequency-based compensation updating (FCU) procedure. Specifically, let $\lambda(p_i)$ denote the frequency of ETP p_i declared among all crowd-couriers. To generate and update the compensation rate, we start by setting the compensation rate as $p \leftarrow \arg\max_{p_i \in \tilde{\mathcal{P}}} \lambda(p_i)$ and update $\tilde{\mathcal{P}}$ by $\tilde{\mathcal{P}} \leftarrow \tilde{\mathcal{P}} \backslash p$. The compensation rate is then iteratively updated using this procedure until the maximum number of iterations is reached. It is noted that if multiple p_i values exist under $\arg\max_{p_i \in \tilde{\mathcal{P}}} \lambda(p_i)$, one is randomly selected for further exploration.

4.3.3 Order allocation by STC algorithm

Given a collaboration alliance and a compensation rate, each retailer is associated with a group of O2O orders that can be served. Inspired by the observation that effective solutions for vehicle routing problems rarely include long delivery routes (Toth and Vigo, 2003), we propose a spatiotemporal clustering (STC) method to allocate O2O orders to retailers based on spatiotemporal-related proximity. Unlike traditional vehicle routing problems where O2O orders are allocated solely based on distance to a depot (a retail store in our study), our approach also considers the availability and spatiotemporal proximity of crowd-couriers. Specifically, we also consider to allocate an O2O order to a retail store whose available crowd-couriers are close to the order in terms of time availability and geographic proximity. Let D_{ik} denote the proximity between an O2O order $i \in \mathcal{C}^r$ and and a crowd-couriers $k \in \mathcal{K}^s, s \in \Pi^r$. If the O2O order and the crowd-courier are compatible in time windows (i.e., $e_k < e_i$ and $l_i < l_k$), and the ETP of the crowd-courier is acceptable to the retailer (i.e., $E_k < \hat{E}$, where $\hat{E}$ is the acceptable compensation parameter), we define D_{ik} as the distance between the crowd-courier's destination and the O2O order's delivery location; otherwise, let $D_{ik} \leftarrow \infty$. Let $\hat{D}$ denote the distance threshold for allocating an O2O order to a crowd-courier. Additionally, let D_{is} denote the distance between the delivery location of an O2O order and a retail store. We then employ the STC method to allocate O2O orders to retailers. Let Ξ^r denote the set of orders allocated to retail store $r \in \mathcal{R}$. The STC method procedure for order allocation is outlined as follows:

- ***Step 1: (Cluster definition and initialization)***
  - ***Step 1.1:*** Set all retail store $r \in \mathcal{R}$ as the cluster centers;
  - ***Step 1.2:*** Initialize O2O order allocations as $\Xi^r \leftarrow \varnothing, \forall r \in \mathcal{R}$;
- ***Step 2: (Distance calculation)***
  - ***Step 2.1:*** For each O2O order $i \in \mathcal{C}^r, \forall r \in \mathcal{R}$, calculate the distance D_{is} between the order and the retail store $s \in \Pi^r$ that can provide dedicated delivery service;
  - ***Step 2.2:*** For each O2O order $i \in \mathcal{C}^r, \forall r \in \mathcal{R}$, calculate the closeness D_{ik} between the order and available crowd-couriers $k \in \mathcal{K}^s, s \in \Pi^r$;

- ***Step 3: (O2O order allocation)***
  - ***Step 3.1:*** For each O2O order $i \in \mathcal{C}^r$ received by $r \in \mathcal{R}$, find the crowd-courier $k \in \mathcal{K}^s, s \in \Pi^r$ with the minimized D_{ik}. If $D_{ik} < \hat{D}$, allocate the O2O order to s and include the O2O order to Ξ^r; otherwise go to ***Step 3.2***;
  - ***Step 3.2:*** Find the retail store $s \in \Pi^r$ with the minimized D_{is} and allocate O2O order to s and include the O2O order to Ξ^r, then return to ***Step 3.1***.
- ***Step 4: (Output)*** Output the O2O orders allocation $\Xi^r, \forall r \in \mathcal{R}$.

4.3.4 Vehicle and crowd-courier routing by CW-NSGA-II

With the allocation of O2O orders, we then develop CW-NSGA-II algorithm to find the routing solutions under the given compensation rate p, collaboration alliance Π^r, and O2O order allocation Ξ^r for each $r \in \mathcal{R}$. The NSGA-II, an evolutionary algorithm that is population-based and known for its improved solution distribution and enhanced convergence to the true Pareto front, is commonly employed in addressing multi-objective optimization problems (Deb et al., 2002). The objective is to derive Pareto-optimal routing solutions, which illustrate the balance between TC and CE objectives. The algorithm initiates with a starting set of candidate route solutions, known as the parent population P_g under current generation g. These solutions are encoded as chromosomes and performed with genetic operation $\text{GO}(P_g)$, including selection, crossover, and mutation, to produce offspring populations denoted by O_g. The solutions in the combined parent and offspring populations $I_g \leftarrow \{P_g\} \cup \{O_g\}$ are then ranked using a fast non-dominated sorting procedure $\text{FNDS}(I_g)$, which assigns each solution to a front, e.g., $F_1, F_2, \cdots$, based on dominance relationships. The algorithm assigns a fitness value to each solution by considering both its front rank and its crowding distance, which is calculated by a crowding-distance calculation algorithm $\text{CDA}(F_i)$. Solutions possessing greater fitness values are chosen to constitute the subsequent parent population, and the process repeats until the maximum number of generations is met. The Pareto-optimal solutions, i.e., solutions in F_1, will be output. Figure 4.2 displays an instance of a generation evolving through NSGA-II.

Following the NSGA-II framework, we further enhance NSGA-II by integrating CW saving method to generate promising initial populations, thereby improving the search for optimal solutions. The method identifies pairs of customers whose combined routes result in cost savings through distance reduction. These savings are ranked in descending order, and the algorithm iteratively merges the routes of the corresponding customers while ensuring capacity constraints are maintained. This procedure is repeated until all customers have been allocated to routes, yielding an initial solution that can be refined through local search procedures. In

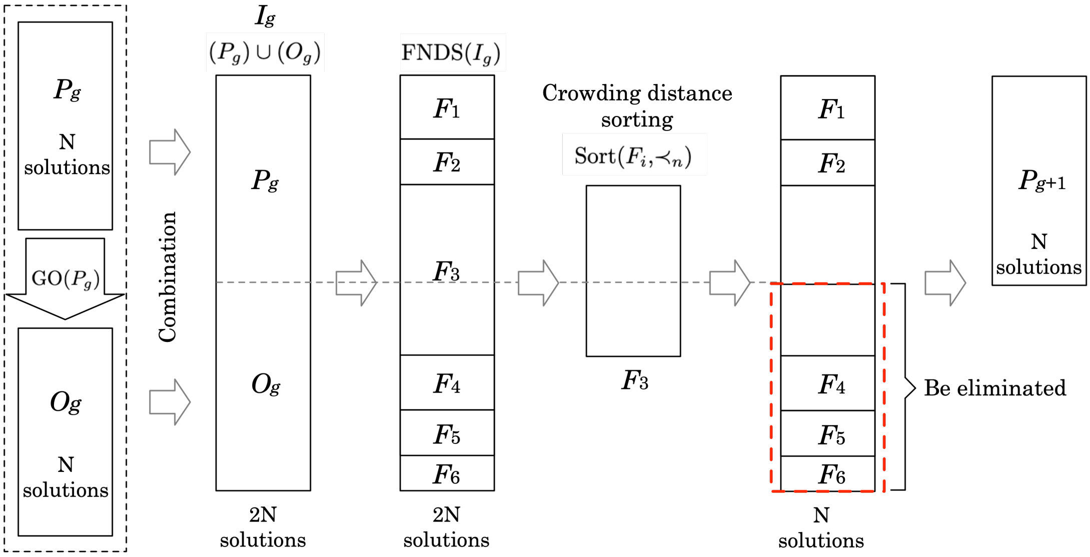

Figure 4.2. An illustrative evolutionary process in one generation of NSGA-II method

our implementation, we employ the CW savings method to generate initial routing solutions by exclusively serving all O2O orders with dedicated delivery vehicles. Concurrently, all available crowd-couriers are arranged to travel directly from the retail store to their respective destinations. By utilizing this CW-NSGA-II framework, a set of Pareto-optimal routing solutions can be obtained. The pseudocode for the CW-NSGA-II algorithm is summarized in Algorithm 4.2.

4.3.5 Dominance test for Pareto solutions

In our study, we utilize the FNDS procedure of the NSGA-II algorithm to conduct dominance test and identify Pareto-optimal solutions from a given set of Pareto solutions. The FNDS procedure for our problem is outlined as follows:

Step 1: (Initialization) For each solution $\boldsymbol{\theta} \in \boldsymbol{\Theta}$, initialize: i) the number of solutions that dominate $\boldsymbol{\theta}$, denoted by $n_{\boldsymbol{\theta}}$, ii) and the set of solutions that $\boldsymbol{\theta}$ dominates, denoted by $\boldsymbol{\Theta}_{\boldsymbol{\theta}}$.

Step 2: (Domination Count and Dominated Set Calculation)

- For each solution $\boldsymbol{\theta} \in \boldsymbol{\Theta}$:
  - Set $n_{\boldsymbol{\theta}} \leftarrow 0$ and $\boldsymbol{\Theta}_{\boldsymbol{\theta}} \leftarrow \varnothing$.
  - For each other solution $\boldsymbol{\theta}' \in \boldsymbol{\Theta}$: If $\boldsymbol{\theta}$ dominates $\boldsymbol{\theta}'$ (i.e., $TC(\boldsymbol{\theta}) \leq TC(\boldsymbol{\theta}')$ and $CE(\boldsymbol{\theta}) \leq CE(\boldsymbol{\theta}')$ with at least one strict inequality), then add $\boldsymbol{\theta}'$ to $\boldsymbol{\Theta}_{\boldsymbol{\theta}}$. Conversely, if $\boldsymbol{\theta}'$ dominates $\boldsymbol{\theta}$, let $n_{\boldsymbol{\theta}} \leftarrow n_{\boldsymbol{\theta}} + 1$.

Step 3: (Identify the First Front)

- Initialize the first front $F_1 \leftarrow \varnothing$.

- For each solution $\boldsymbol{\theta} \in \boldsymbol{\Theta}$: If $n_{\boldsymbol{\theta}} = 0$ (i.e., $\boldsymbol{\theta}$ is not dominated by any other solution), add $\boldsymbol{\theta}$ to F_1 and set its rank by $\text{rank}(\boldsymbol{\theta}) \leftarrow 1$.

Step 4: (Subsequent Fronts)

- Initialize the front counter $i \leftarrow 1$.
- While F_i is not empty:
  - Initialize the next front $F_{i+1} \leftarrow \varnothing$.
  - For each solution $\boldsymbol{\theta} \in F_i$:
    * For each solution $\boldsymbol{\theta}' \in \boldsymbol{\Theta}_{\boldsymbol{\theta}}$: Let $n_{\boldsymbol{\theta}'} \leftarrow n_{\boldsymbol{\theta}'} - 1$. If $n_{\boldsymbol{\theta}} = 0$, add $\boldsymbol{\theta}$ to F_{i+1} and set its rank $\text{rank}(\boldsymbol{\theta}) \leftarrow i + 1$.
  - Increment the front counter i and set $F_i \leftarrow F_{i+1}$.

Step 5: (Output) The solutions are sorted into different fronts $F_1, F_2, \ldots$, where F_1 contains the Pareto-optimal routing solutions.

Algorithm 4.2 Pseudocode of CW-NSGA-II

Input: p, Π^r, $\mathcal{K}^r$, $\mathcal{R}$, Ξ^r

Output: F_1

$g = 1$ ▷ Initialize the number of generations
$P_g \leftarrow$CW$(\Xi^r, \mathcal{K}^r)$ ▷ Generate initial populations (parent population) using CW method
while $g < G$ **do**
  $O_g \leftarrow$GO(P_g) ▷ Generate offspring populations using genetic operators (GO)
  $I_g \leftarrow \{P_g\} \cup \{O_g\}$ ▷ combine parent and offspring populations
  $F \leftarrow$FNDS(I_g) ▷ $F = (F_1, F_2, \cdots)$
  $P_{g+1} \leftarrow \varnothing, i = 1$
  while $|P_{g+1}| + |F_i| \leq N$ **do** ▷ Fill the parent population
    CDA(F_i) ▷ Calculate crowding-distance in F_i
    $P_{g+1} \leftarrow P_{g+1} \cup F_i$
    $i \leftarrow i + 1$
  end while
  Sort(F_i) ▷ Sort the solutions in F_i in descending order
  $P_{g+1} \leftarrow P_{g+1} \cup F_i[1 : (N - |P_{g+1}|)]$ ▷ Keep the size of population as N
  $g \leftarrow g + 1$
end while

It is noted that to determine the global Pareto-optimal solutions, we focus on conducting Steps 1 to 3 of the dominance test on the obtained the solutions in F_1. This ensures that we accurately identify the solutions that are not dominated by any other, thereby achieving a good balance between costs and carbon emissions.

4.4 Numerical Experiments

In this section, we first test the performance of our proposed solution method on a series of adapted benchmark instances, and then examine the benefits of our proposed delivery system through a simulated case in Chongqing, China. The experiments were performed using MATLAB 2021a on a personal computer with macOS Sonoma 14.3, equipped with an Apple M1 3.2GHz CPU and 16GB RAM.

4.4.1 Test instances generation and parameter setting

This chapter introduces a DIO method to address the CACR problem, utilizing a CW-NSGA-II heuristic to to address sub-problem. Typically, the effectiveness of heuristic for multi-objective problems is assessed by examining how close the achieved solutions are to the true Pareto front, i.e., Pareto approximation, and the diversity of these solutions, i.e., coverage of the Pareto front. To demonstrate the superiority of the CW-NSGA-II heuristic in solving the bi-objective sub-problem, we evaluate the metrics *hypervolume*, as proposed by Zitzler and Thiele (1998), and *coverage*, as proposed by Zitzler et al. (2000), which are widely utilized metrics for evaluating the aforementioned objectives. Specifically, we compare the performance of CW-NSGA-II with classic NSGA-II and multi-objective particle swarm optimization (MOPSO) methods. Additionally, we compare the best objective values, i.e., TC and CE, achievable with the three methods. To provide a clear demonstration, this section first introduces the instance details and parameter setting and then analyzes the results obtained from our experiments.

The CACR problem aims to fulfil all orders received by multiple retailers using the collaborative delivery system with OT-based CS services. The data for the instances should include multiple retailers, each associated with a retail store, a set of orders, a fleet of dedicated vehicles, and a group of available crowd-couriers. Given the absence of off-the-shelf benchmark instances for our particular problem, we generate test instances by making adjustments on the widely used VRPTW benchmark instances provided by Homberger and Gehring (2005). The specific instance generation is elaborated as follows.

For the retail stores, we use the depot in a selected VRPTW instance as one of the retail stores and randomly select other two locations within the instance to represent the remaining retail stores, resulting in a total of three retail stores. Each retail store is associated with a pair of coordinates indicating its location and an opening time window. For the orders, we utilize the customer delivery demands in the VRPTW instances, where each order is associated with coordinates indicating the customer's location, a service time window, the load of the products or goods, and the service time required for unloading. The orders are allocated to a retail store according to the distance. To generate crowd-couriers data, we randomly select a group of customer demands from the VRPTW instances and make necessary adjustments. Specifically, for each chosen demand, the coordinates are assumed to be the crowd-courier's destination, and each crowd-courier is assumed to be initially located at the retail store which is nearest to the destination. The time window of the chosen demand is considered the available time period for a crowd-courier to provide delivery services, with the left side of the time window indicating the earliest departure time from the retail store and the right side indicating the latest arrival time at the destination. The load of the chosen demand is used as the carrying capacity of the crowd-courier, and the service time is removed. Instead, we randomly generate a number from 1 to 10 as the ETP of the crowd-courier. We implement the DIO method to solve the CACR problem with the parameter setting as: the population size of each generation $N = 10$, the number of iterations for compensation updating $I_{\max} = 20$, crossover probability of the NSGA-II $P_c = 0.8$, mutation probability of the NSGA-II $P_m = 0.1$, and the maximum number of generation $G = 200$.

4.4.2 Algorithm performance evaluation on test instances

We first assess the Pareto approximation by computing the hypervolume metric, denoted as $\mathrm{M_H}$. For our studied CACR problem with TC and CE objectives, $\mathrm{M_H}$ is defined as the covered size by all Pareto-optimal solutions with a reference point, typically the maximal values of each objective. Interested readers may access more details for the two metrics from Garcia-Najera and Bullinaria (2011). When using this metric to evaluate multiple solution methods, the method that yields solutions encompassing the greatest hypervolume, i.e.,$\mathrm{M_H}$, is considered superior. Table 4.1 presents the hypervolume values achieved by our proposed CW-NSGA-II, classic NSGA-II, and MOPSO methods under different numbers of orders and crowd-couriers. The results in Table 4.1 indicate that CW-NSGA-II achieves the greatest hypervolume value in most instances, with an average hypervolume value of 0.721 compared to 0.711 for NSGA-II and 0.621 for MOPSO. This demonstrates the strong performance of the proposed method in Pareto approximation.

Next, we evaluate the coverage of the Pareto front by computing the coverage metric, denoted as $\mathrm{M_C}$. Specifically, let $\mathrm{M_C}(A \prec B)$ denote the ratio of solutions obtained by method B that are dominated by those achieved by method A. For example, $\mathrm{M_C}$(CW-NSGA-II $\prec$ NSGA-II) =1 indicates that all solutions obtained by NSGA-II are dominated by those obtained by CW-NSGA-II. A method is considered superior if it is associated with the largest coverage value, i.e.,$\mathrm{M_C}$, compared to other methods. Table 4.2 presents the coverage values from paired com-

Table 4.1. Hypervolume value M_H achieved by CW-NSGA-II, NSGA-II, and MOPSO methods

Instances	CW-NSGA-II	NSGA-II	MOPSO
C_10_10	0.729	0.720	0.640
C_15_15	0.719	0.715	0.608
C_20_20	0.726	0.718	0.614
C_25_25	0.719	0.720	0.630
C_30_30	0.720	0.701	0.604
C_35_35	0.721	0.702	0.612
C_40_40	0.712	0.705	0.635
C_45_45	0.718	0.725	0.613
C_50_50	0.726	0.700	0.637
Average	**0.721**	0.711	0.621

parisons between CW-NSGA-II and NSGA-II, and CW-NSGA-II and MOPSO.

Table 4.2. Coverage value M_C by comparing CW-NSGA-II, NSGA-II, and MOPSO methods

Instances	CW-NSGA-II $\prec$ NSGA-II	NSGA-II $\prec$ CW-NSGA-II	CW-NSGA-II $\prec$ MOPSO	MOPSO $\prec$ CW-NSGA-II
C_10_10	0.92	0.93	0.93	0.87
C_15_15	1.00	0.88	1.00	0.71
C_20_20	0.93	0.88	1.00	0.81
C_25_25	0.93	0.93	1.00	0.80
C_30_30	0.93	0.81	0.90	0.69
C_35_35	0.93	0.93	1.00	0.87
C_40_40	1.00	0.87	0.92	0.67
C_45_45	1.00	0.71	0.92	0.65
C_50_50	0.93	0.80	1.00	0.67
Average	**0.95**	0.86	**0.96**	0.75

Table 4.2 indicates that the coverage value of CW-NSGA-II to NSGA-II is greater than that of NSGA-II to CW-NSGA-II in most instances, with an average coverage value of 0.95 versus 0.86. Similarly, the coverage value of CW-NSGA-II to MOPSO is also greater than that of MOPSO to CW-NSGA-II in most instances, with an average coverage value of 0.96 versus 0.75. This demonstrates the robust performance of CW-NSGA-II with respect to solution diversity.

In addition to the hypervolume and coverage metrics, we also present the best single objective values achieved by CW-NSGA-II, NSGA-II, and MOPSO. Table 4.3 presents the objectives of total costs (Obj_1), total carbon emissions (Obj_2), and the computation time (CPU) by the three methods. Table 4.3 indicates that CW-NSGA-II method outperforms classic NSGA-II and MOPSO in minimizing total costs and carbon emissions in most instances, while maintaining competitive computation times. Although CW-NSGA-II incorporates the CW method for generating initial solutions, it does not exhibit a significant increase in computation time compared to classic NSGA-II. This is attributed to the efficient performance of the CW method in constructing the initial population. Additionally, the comparison indicates that improving the initial population can lead to better objective values.

4.4.3 Case study

We first introduce a simulated case in Chongqing, China, which involves six retail stores, a set of O2O orders, and crowd-couriers, as illustrated in Figure 4.3. Specifically, we select six supermarkets operating online and offline shopping channels in Chongqing, China, denoted as $\mathcal{R} = \{\mathrm{R1}, \mathrm{R2}, \cdots, \mathrm{R6}\}$. We generate a bunch of O2O orders, i.e., $\mathcal{C} = \{\mathrm{C1}, \cdots, \mathrm{C210}\}$, and a group of available crowd-couriers $\mathcal{K} = \{\mathrm{K1}, \cdots, \mathrm{K210}\}$ located within a 10 km radius of each retail store. In Figure 4.3, we use the same icon to represent the location of the retail store and the delivery locations of its orders, and use the same icon with a red box to denote the destinations of the available crowd-couriers. The opening time window for each retail store is set from 14:00 to 18:00. The service time window for each O2O order is randomly selected within this period, with a minimum duration of 60 minutes. The parcel load for each order is randomly generated between 10 kg and 30 kg. In order to mitigate the unavailability of crowd-couriers due to randomly generated service time periods, we extend the time window of the nearest location of an order to generate the available time period for a crowd-courier. The ETP for a crowd-courier is a randomly generated number between \$1 and \$10. The capacity of a dedicated vehicle is set at 200 kg. The fixed cost per unit of using a dedicated vehicle is set as \$30. To calculate the average transportation cost and carbon emission, we consider the gas consumption rate of 15 L/100km. We estimate carbon emissions according to the framework proposed by Xiao et al. (2012), given by the equation $Y = 0.0000793X - 0.026$, where Y represents the fuel consumption rate (L/kg) and X denotes the weight of the vehicle (kg).

4.4.4 Benefit analysis of the collaborative delivery system

To assess the benefits of the collaborative delivery system with OT-based CS services, we provide comparative examples of the total costs and carbon emissions between our proposed system, which involves collaboration among retailers, and a traditional independent delivery model, see Figure 4.4. The independent delivery model is both less cost-efficient and less environmentally friendly. This is evident as the Pareto front for the independent non-collaborative model is dominated by that of the collaborative model. The collaborative delivery model demonstrates significant cost savings and reductions in carbon emissions. Furthermore, the delivery system that entails full collaboration among all retailers demonstrates a predominant effect over partial collaboration. These improvements could be attributed to the sharing of O2O orders among multiple retailers, optimized scheduling of dedicated vehicles, and the maximized utiliza-

Table 4.3. Best objective value and computation time achieved by CW-NSGA-II, NSGA-II, and MOPSO

Instance	CW-NSGA-II			NSGA-II			MOPSO		
	Obj_1 (\$)	Obj_2 (kg)	CPU (s)	Obj_1 (\$)	Obj_2 (kg)	CPU (s)	Obj_1 (\$)	Obj_2 (kg)	CPU (s)
C_10_10	745.7	4.1	8.5	805.9	5.0	9.9	870.8	5.4	23.2
C_15_15	1156.9	7.8	10.1	1285.4	9.5	10.7	1428.2	10.6	24.0
C_20_20	1562.2	11.2	11.5	1912.0	15.5	12.1	2340.3	19.1	24.2
C_25_25	2169.7	15.6	13.8	2623.2	21.9	13.4	3171.4	26.7	25.1
C_30_30	2596.1	19.4	14.8	3393.8	30.5	15.5	4436.6	40.0	27.4
C_35_35	3345.4	27.1	16.8	4301.8	40.1	17.4	5531.6	52.0	27.4
C_40_40	3991.2	32.6	19.6	5217.9	49.7	19.3	6821.5	65.1	27.9
C_45_45	4555.8	38.4	20.4	6358.8	63.5	20.8	8875.4	89.4	29.2
C_50_50	5245.6	43.8	22.6	7386.6	73.6	22.4	9801.4	97.3	29.1
Average	**2818.7**	**22.2**	**15.3**	3698.4	34.4	15.7	4808.6	45.3	26.2

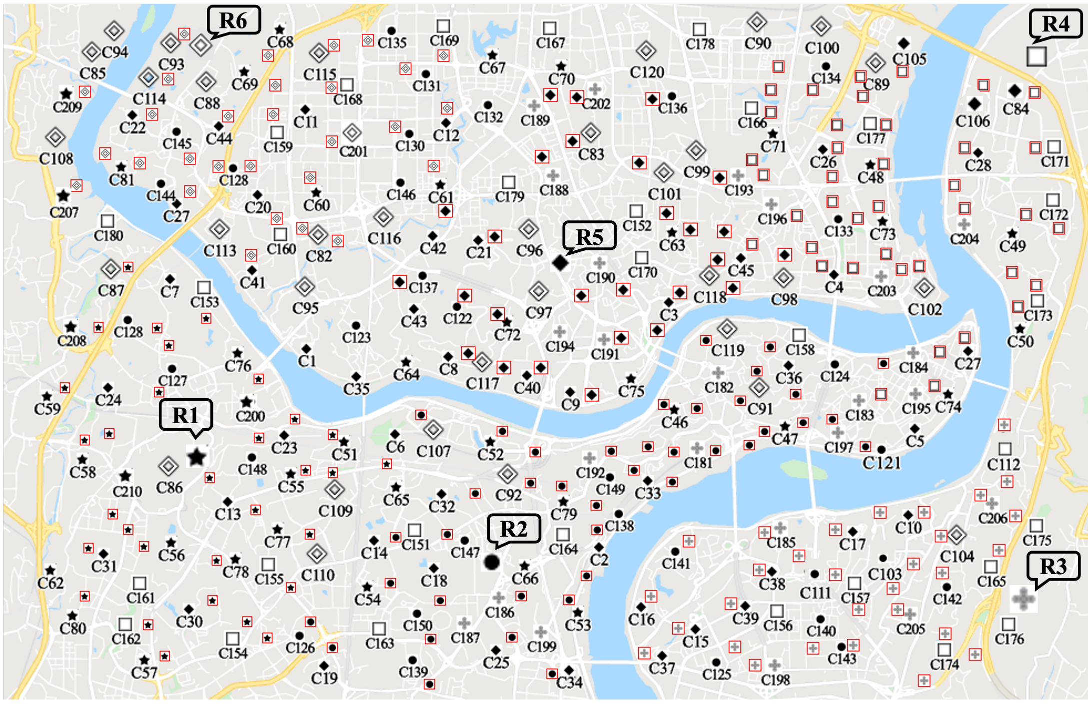

Figure 4.3. Distribution of retail stores, delivery locations, and destinations of crowd-couriers

tion of available crowd-couriers. Notably, some orders fulfilled by crowd-couriers result in very low carbon emissions due to hitch-hike deliveries with little detour. In addition, the figure also highlights a conflict between minimizing total cost and minimizing carbon emissions. This underscores the importance of considering both factors in the decision-making process for delivery service providers.

To further examine the impact of the collaborative delivery system with OT-based CS services on individual retailers, we compare several indicators of each retailer under the collaborative delivery model and the traditional independent delivery model. Specifically, we compare the total cost averaged over all Pareto solutions (ATC), average total carbon emissions (ACE), average number of dedicated vehicles (#Veh), average cost (AC), and average service price for employing crowd-couriers (Price) as shown in Table 4.4. Figure 4.5 visualizes the results.

Table 4.4. Comparison of non-collaborative and full-collaborative delivery models

Instance	Non-Collaborative				Full-Collaborative			
	ATC ($)	ACE (kg)	#Veh	AC($)	ATC ($)	ACE (kg)	#Veh	Price ($)
R1	1365.9	22.3	4	2.01	935.0	20.6	2	5.0
R2	1248.6	19.2	3	2.12	1184.3	18.8	2	4.6
R3	1149.6	18.9	3	2.13	1012.1	14.6	2	4.7
R4	841.3	15.9	2	2.34	671.8	11.8	1	4.7
R5	2318.7	32.4	6	2.23	2345.3	24.0	5	5.2
R6	1099.5	16.2	3	2.11	786.5	11.3	2	4.8
All retailers	8023.6	124.8	21	–	**6935.1**	**101.1**	**14**	–

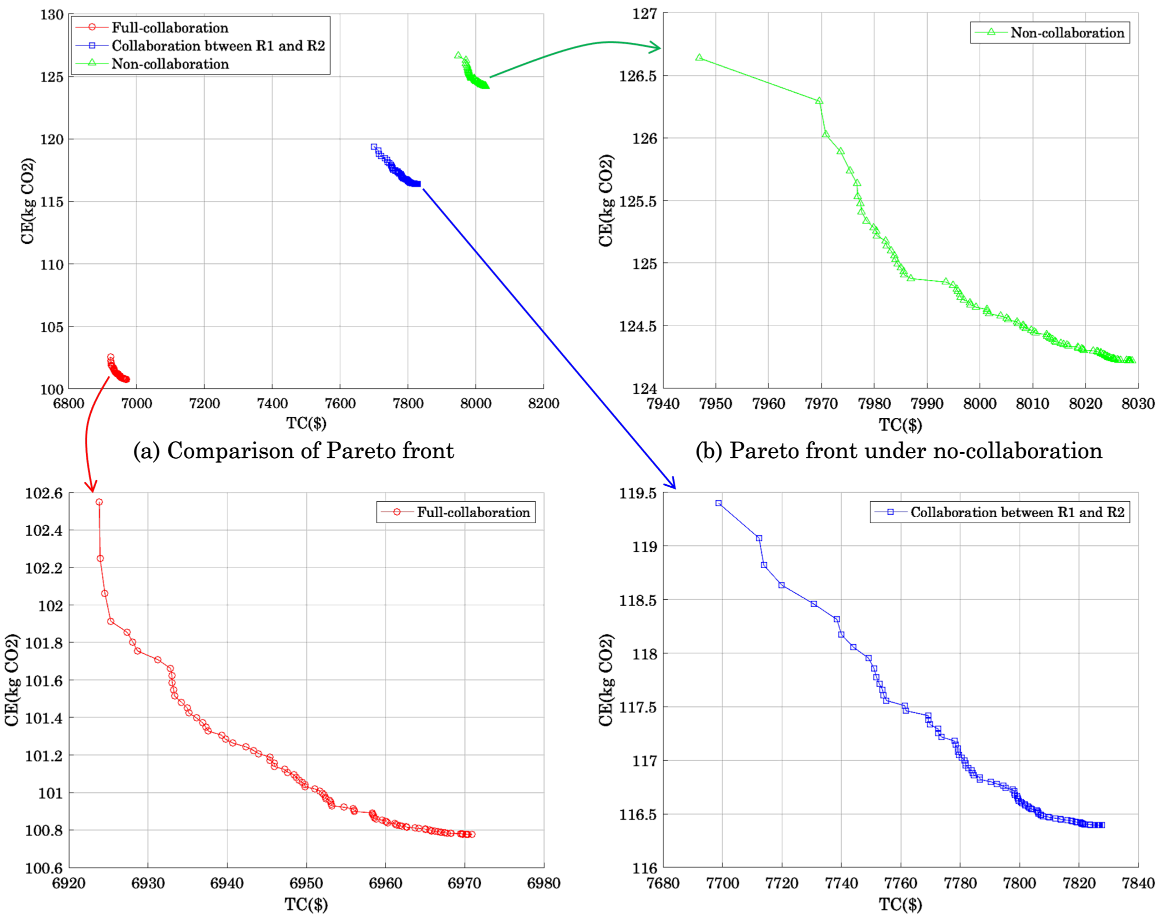

(a) Comparison of Pareto front

(b) Pareto front under no-collaboration

(c) Pareto front under full-collaboration

(d) Pareto front under collaboration R1 and R2

Figure 4.4. Pareto front under various collaboration strategies

Table 4.4 indicates that most retailers benefit from using a collaborative hybrid delivery system with full collaboration among all retailers as opposed to managing deliveries independently without CS service. These benefits include lower total costs, as illustrated in 4.5(a), and reduced carbon emissions, as illustrated in 4.5(b), which can be attributed to the improved efficiency of using both crowd-couriers and dedicated vehicles in a cooperative manner. Furthermore, the use of fewer vehicles, as shown in 4.5(c), has been noted as another benefit of the collaborative CS model. This reduction is partly due to more crowd-couriers being engaged not just for individual retailer's deliveries but for managing collective orders, which further decreases costs and emissions. Notably, increasing the compensation for crowd-couriers has led to higher employment rates, with a corresponding decrease in emissions and no significant cost increase. This trend suggests a strategic advantage in expanding the use of crowd-couriers under the collaborative framework. However, Retailer R5 has experienced a slight increase in these metrics, likely due to handling a larger order volume. From a broader perspective, while the system-wide benefits are clear, individual participants may face increased delivery responsibilities. This highlights a potential trade-off between optimizing for the entire system and optimizing for individual

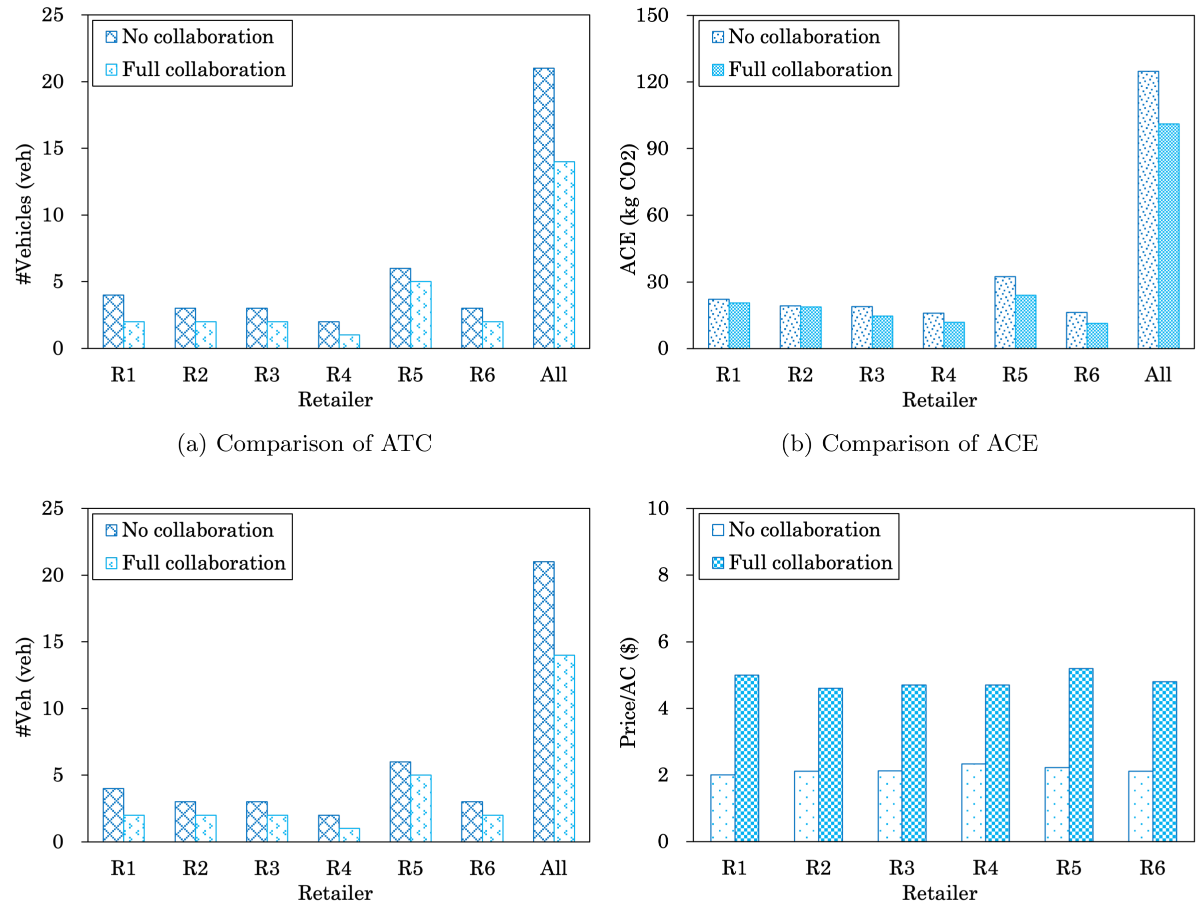

(a) Comparison of ATC

(b) Comparison of ACE

(c) Comparison of #Veh

(d) Comparison of AC and Price

Figure 4.5. Comparison of ATC, ACE, #Veh, AC, and Price under no collaboration and full collaboration

stakeholders. To ensure the sustainability of such a collaborative system, it may be necessary to develop a alliance for distributing costs and benefits among participants. This particular aspect, however, falls outside the scope of this study and is recommended for future exploration.

4.5 Concluding Remarks

This chapter studies the joint optimization of collaboration alliance, order allocation, compensation rate determination, and service routes for a collaborative delivery system with OT-based CS services. It considers the potential collaboration among multiple retailers and the diverse service requirements of available crowd-couriers. In addition to minimizing the total cost of the collaborative delivery system, we also aim to minimize total carbon emissions, resulting in a bi-objective optimization problem. A bi-objective optimization model is formulated, and a customized DIO method is developed to solve the problem. The DIO method seeks to find Pareto-optimal solutions for the problem by solving a series of sub-problems under iteratively updated collaboration strategies and compensation rates until a stopping condition is met. Particularly, a tailored frequency-based compensation updating procedure is proposed to adjust the compensation rate. Additionally, a spatiotemporal clustering method is developed to allocate orders to specific retailers, and a CW-NSGA-II method is utilized to find Pareto-optimal solutions. Numerical experiments on a set of adapted benchmark instances and a simulated case in Chongqing are conducted to evaluate the performance of the proposed DIO method and the benefits of the collaborative delivery system. The results indicate that a collaborative delivery system can decrease the total cost of fulfilling delivery orders and reduce carbon emissions. The results also demonstrate a significant conflict between the objectives of minimizing total cost and minimizing carbon emissions.

4.6 Appendix: Notations

Set	
$\mathcal{R}$	Set of retailers/retail stores, $r \in \mathcal{R}$
Π^r	Set of retailers engaged in a collaborative delivery arrangement with retailer r, $\Pi^r = \{s \in \mathcal{R} : \pi_{rs} = 1\}, \forall r \in \mathcal{R}$
$\mathcal{V}^r$	Set of dedicated vehicles departing from retail store $r \in \mathcal{R}$, $v \in \mathcal{V}^r$
$\mathcal{K}^r$	Set of crowd-couriers departing from retail store $r \in \mathcal{R}$, $k \in \mathcal{K}^r$
$\mathcal{C}^r$	Set of O2O orders received by retailer $r \in \mathcal{R}$
$\mathcal{C}$	Set of all O2O orders/delivery locations of O2O orders, $\mathcal{C} := \bigcup_{r\in\mathcal{R}} \mathcal{C}^r$
$\mathcal{C}^r(\Pi^r)$	Set of O2O orders that can be served by retailer r under the collaboration Π^r
$\mathcal{K}^r$	Set of all available crowd-couriers who depart from retail store $r_k \in \mathcal{R}$
$\mathcal{D}^r$	Set of destinations of all available crowd-couriers in set $\mathcal{K}^r$
$\mathcal{D}$	Set of destinations of all available crowd-couriers, $\mathcal{D} := \bigcup_{r\in\mathcal{R}} \mathcal{D}^r$
$\mathcal{N}_v^r(\Pi^r)$	Set of nodes that are possibly visited by the dedicated vehicle $v \in \mathcal{V}^r$ departing from retail store $r_v \in \mathcal{R}$ under the collaboration of Π^r
$\mathcal{A}_v^r(\Pi^r)$	Set of arcs that possibly traversed by the dedicated vehicle $v \in \mathcal{V}^r$ departing from retail store $r_v \in \mathcal{R}$ under the collaboration of Π^r
$\mathcal{N}_k^r(\Pi^r)$	Set of nodes that are possibly visited by the crowd-courier $k \in \mathcal{K}^r$ departing from retail store $r_k \in \mathcal{R}$ under the collaboration of Π^r
$\mathcal{A}_k^r(\Pi^r)$	Set of arcs that possibly traversed by the crowd-courier $k \in \mathcal{K}^r$ departing from retail store $r_k \in \mathcal{R}$ under the collaboration of Π^r
$\mathcal{A}^r(\Pi^r)$	Set of arcs that possibly traversed by the dedicated vehicles and crowd-courier departing from retail store $r \in \mathcal{R}$ under the collaboration of Π^r
$\mathcal{N}$	Set of all nodes, $\mathcal{N} = \mathcal{R} \cup \mathcal{C} \cup \mathcal{D}$
$\mathcal{A}$	Set of all arcs, $\mathcal{A} = \bigcup_{r\in\mathcal{R}} \mathcal{A}^r$
Parameters	
$[e_i, l_i]$	Delivery time window of O2O order $i \in \mathcal{C}^r, r \in \mathcal{R}$
q_i	Load of ordered products of O2O order $i \in \mathcal{C}^r, r \in \mathcal{R}$
σ_i	Service duration for unloading order i's products to the customer
r_v	Retail store from which the dedicated vehicle v depart
r'_v	The duplication of retail store r_v
r_k	Retail store from which the crowd-courier k depart
d_k	Destination of the crowd-courier k
e_k	Earliest departure time of the crowd-courier k from the retail store

l_k	Latest arrival time of the crowd-courier k at the destination
Q_v	Maximum carrying capacity of the dedicated delivery vehicle v
Q_k	Maximum carrying capacity of the crowd-courier k
c^{f}	Fixed cost for per unit of using a dedicated vehicle
c_{ij}	Transportation cost incurred by the dedicated vehicles from location i to j
t_{ij}	Travel time incurred by the dedicated vehicles from location i to j
m_{ij}	Carbon emission incurred by the dedicated vehicles from location i to j
μ_{ij}	Travel time incurred by the crowd-courier from location i to j
ε_{ij}	Carbon emission incurred by the dedicated vehicles from location i to j
E_k	ETP of crowd-courier k
M_1/M_2	A large positive number
Variables	
p	Continuous variable to denote the compensation paid for employing crowd-couriers for per unit of detour time.
π_{rs}	Binary variable to denote the collaboration between two retailers $r \in \mathcal{R}$ and $s \in \mathcal{R}$, where $\pi_{rs} = 1$ if collaboration is formed between them and $\pi_{rs} = 0$ otherwise.
x_{ijv}	Binary variable that equals 1 if dedicated vehicle $v \in \mathcal{V}^r$, $\forall r \in \mathcal{R}$ travels directly from node i to j, $\forall (i,j) \in \mathcal{A}_v^r(\Pi^r)$, and 0 otherwise.
y_{ijk}	Binary variable that equals 1 if crowd-courier $k \in \mathcal{K}^r$, $\forall r \in \mathcal{R}$ travels directly from node i to j, $\forall (i,j) \in \mathcal{A}_k^r(\Pi^r)$, and 0 otherwise.
τ_i^v	Continuous variable to denote the time epoch when vehicle $v \in \mathcal{V}^r$ starts service at node $i \in \mathcal{N}_v^r(\Pi^r)$. Note that $\tau_{r_v}^v$ represents the time at which vehicle $v \in \mathcal{V}^r$ departs from the retail store, while $\tau_{r_v'}^v$ indicates the time when vehicle returns to retail store.
τ_i^k	Continuous variable to denote the time epoch when crowd-courier $k \in \mathcal{K}^r$ starts service at node $i \in \mathcal{N}_k^r(\Pi^r)$. Note that $\tau_{r_k}^k$ represents the time at which crowd-courier $k \in \mathcal{K}^r$ departs from the retail store, while $\tau_{d_k}^k$ indicates the time at their destination.

Chapter 5 Service Price Optimization for Public Transit-based Co-Modal Transportation Service

This chapter investigates a CM transportation service price (CSP) problem for a public transit (PT)-based CM transportation service considering the collaborative gameplay between logistics service providers (LSP) and PT operator (PTO). The PT-based CM transportation service aims to leverages the spare capacity of existing bus scheduled trips to carry out parcel deliveries through the coordination of multiple buses with fixed timetables. A bilevel path-based programming model is formulated based on the interactive dynamics between LSP and the PTO, and a tailored iterated three-stage hybrid (ITH) method combining two granular tabu search (GTS) algorithms and an artificial bee colony (ABC) algorithm is developed to solve the studied problem. Numerical experiments on a series of randomly generated instances and simulated cases in Chongqing, China are performed to evaluate the performance of the ITH method and benefits of the introduction of PT-based CM transportation service. Results indicate that PT-based CM transportation service can reduce up to 30% total cost for LSP while generating additional profits for PTO.

The rest of this chapter are organized as follows. Problem description as well as assumptions and notations are elaborated in Section 5.1. A bilevel path-based programming model for the studied problem is developed in Section 5.2. To solve the problem, an ITH algorithm is developed in Section 5.3. Numerical experiments on randomly generated instances and simulated cases in Chongqing, China are conducted in Section 5.4. Conclusions of this chapter are summarized in Section 5.5. Notation used in this chapter is listed in Section 5.6 for readability.

5.1 Problem Statement

We consider an LSP who provides parcel delivery service using a fleet of dedicated vehicles (e.g., trucks) in set $\mathcal{V}$ subject to a carrying capacity Q_v of each vehicle $v \in \mathcal{V}$ within a city. Consider that the LSP receives a bunch of parcel delivery requests that parcels need to be delivered from a urban consolidation and distribution center (CDC) to several regional delivery stations (RDSs) geographically distributed in the city. Specifically, each parcel delivery request is associated with a delivery location, i.e., RDS, service duration for parcel deliveries on the RDS, and parcel load. The RDSs as well as the CDC are associated with an opening time window for parcel services. Let $\mathcal{H}$ denote the set of parcel delivery requests. For ease of presentation, we also use $\mathcal{H}$ to denote the set of delivery locations of the all the parcel delivery requests, i.e., RDSs. Let σ_h and q_h denote the service duration and parcel load of the parcel delivery request

$h \in \mathcal{H}$, respectively. Furthermore, let $[E_h, L_h]$ denote the opening time window during which RDS accepts parcel deliveries, where E_h and L_h indicate the earliest and latest time epoch, respectively. In addition, we denote 0 as the location of CDC, and $[E_0, L_0]$ denote the opening time window of CDC.

In the city, we consider a PTO who provides passenger transportation service using a fleet of buses in set $\mathcal{B}$ serving a series of fixed routes adhering to fixed timetables. To be more specific, each bus $b \in \mathcal{B}$ serving a route will fulfill a set of scheduled trips, denoted the by $\mathcal{L}^b = \{1, 2, \cdots, |\mathcal{L}^b|\}$, where $|\mathcal{L}^b|$ denotes the last trip that bus $b \in \mathcal{B}$ serves. We define $\mathcal{L} := \bigcup_{b \in \mathcal{B}} \mathcal{L}^b$. Each scheduled trip $l \in \mathcal{L}^b$ of bus $b \in \mathcal{B}$ is characterized by two bus terminals, referred to as the origin terminal and destination terminal of each trip, respectively, and corresponding departure time and arrival time at the terminals. Note that we do not consider the case of 'circular trip', i.e., a trip that starts and ends at a same terminal station. However, this trip can be easily modeled as two trips. Then, each bus b will serve the scheduled trips $l \in \mathcal{L}^b$ following the departure and arrival timetable, and there is a time interval between two consecutive scheduled trips, according to the practical operations. Let $s^{\mathrm{o}}_{b,l}$ and $s^{\mathrm{d}}_{b,l}$ denote the origin terminal and destination terminal of the bus b's l-th trip, respectively, and $t^{\mathrm{o}}_{b,l}$ and $t^{\mathrm{d}}_{b,l}$ be the corresponding departure time of bus b from the origin terminal and arrival time of bus b at the destination terminal, respectively. The time interval between two consecutive scheduled trips is defined as the time interval from $t^{\mathrm{d}}_{b,l-1}$ to $t^{\mathrm{o}}_{b,l}$ between trips $l-1$ and l of bus b. The notations used throughout this chapter is summarized in Section 5.6.

To minimize the costs of fulfilling the parcel delivery requests, the LSP will collaborate with the PTO by outsourcing parcel delivery tasks to the PTO. Specifically, the LSP will provide the PTO with the parcel delivery requests and a certain monetary payment, denoted as p, for delivering each unit of parcel load, referred to as the service price. Received these parcel delivery requests, the PTO will then determine which parcel delivery requests it serves by scheduling its buses with spare capacities to maximize its total profits, while adhering to the fixed bus timetable for passenger service. The unserved parcel requests, along with the corresponding outsourcing cost that should be paid to PTO, will be fed back to the LSP. Then the LSP will satisfy these unserved requests using its own dedicated delivery vehicles. We can see that the interactive dynamic between the LSP and PTO gives rise to a Stackelberg game between the LSP and PTO, where the LSP serving as the leader, aims to determine the optimal service price considering the PTO's optimal service decision, whereas the PTO serving as the follower aims to make its optimal decision on the served parcel requests based on the offered price. By collaborating with the PTO, the LSP can fulfill the parcel requests either through the CM transportation service provided by the PTO or its own dedicated delivery service.

To more explicitly elaborate on the new PT-based CM transportation service and dedicated delivery service, we will then introduce (i) pickup, delivery, and transshipment operations and bus trip chain of PT-based CM transportation service, (ii) feasibility, revenue, and cost of a bus trip chain, iii) vehicle route of dedicated delivery service, and iv) feasibility and cost of a dedicated vehicle service route.

5.1.1 Pickup, delivery, transshipment operations, and bus trip chain

We assume that all available buses operated by PTO have a uniform model, type, and carrying capacity for passengers except that each bus $b \in \mathcal{B}$ in the l-th trip has a heterogeneous parcel carrying capacity, denoted by Q_l^b. Since each bus serving specific trips should adhere to a fixed timetable, we assume that the bus can only accommodate parcels during the time interval between consecutive scheduled trips of the bus, e.g., the time interval from $t^{\mathrm{d}}_{b,l-1}$ to $t^{\mathrm{o}}_{b,l}$ (Ghilas et al., 2013). Specifically, during the time interval, the bus can drive to a near CDC or terminal to pick up parcels or drive to another near terminal or RDS to drop off parcels unless the fixed timetable and carrying capacity is not violated. Recognizing that a parcel delivery request from the CDC to a specific RDS may not be able to be directly served by a scheduled bus trip due to the fixed timetable and locations of terminals, we consider a general PT-based CM transportation scenario that a parcel request can be served in the manner of the relay of multiple bus scheduled trips with necessary pickup, delivery, and transshipment operations. Figure 5.1 illustrates an example of a bus trip chain for serving a parcel delivery request from CDC to an RDS.

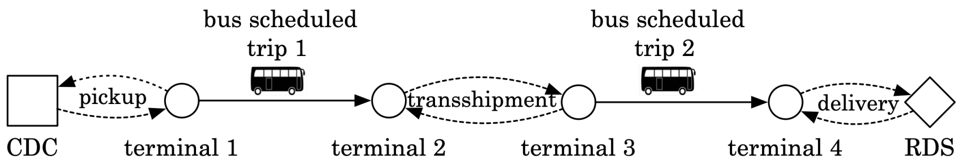

Figure 5.1. An illustrative example of a bus trip chain

In this context, a parcel delivery request may be served by a series of bus scheduled trip with necessary pickup, delivery, and transshipment operations between CDC, terminals, and RDS. For ease of elaboration, we refer to the service route that includes the CDC 0, a series of bus scheduled trips $l \in \mathcal{L}$, and an RDS $h \in \mathcal{H}$ as a bus trip chain, denoted by r_h, which can be represented by

$$r_h = 0 \Leftrightarrow s^{\mathrm{o}}_{b_1,l_1} \rightarrow s^{\mathrm{d}}_{b_1,l_1} \Leftrightarrow s^{\mathrm{o}}_{b_2,l_2} \rightarrow s^{\mathrm{d}}_{b_2,l_2} \cdots s^{\mathrm{o}}_{b_{n_r},l_{n_r}} \rightarrow s^{\mathrm{d}}_{b_{n_r},l_{n_r}} \Leftrightarrow h \tag{5.1}$$

from CDC 0 to an RDS $h \in \mathcal{H}$ with total n_r bus scheduled trips, where $\rightarrow$ denotes the scheduled trip of the bus from the origin terminal to the corresponding destination terminal and $\Leftrightarrow$ denotes the necessary pickup, delivery, and transshipment operation for parcel delivery. Specifically, $0 \Leftrightarrow s^{\mathrm{o}}_{b_1,l_1}$ denote the pickup operation that the bus drives to the CDC to pick up parcels and then back to the terminal of its upcoming scheduled trip, $s^{\mathrm{d}}_{b_i,l_i} \Leftrightarrow s^{\mathrm{o}}_{b_{i+1},l_{i+1}}$ denote the transshipment operation that a bus drives to another terminal to transfer parcels and go back to the terminal of its next scheduled trip, and $s^{\mathrm{d}}_{b_{n_r},l_{n_r}} \Leftrightarrow h$ denote the delivery operation that the bus drives to the RDS h to deliver parcels and then back to the terminal of its next scheduled trip. Note that there may be no transshipment operation between two bus scheduled trips if transfer can be achieved in a same terminal. We can see that the pickup, delivery, and transshipment operations among CDC, terminals, and RDS result in additional travel time and an operating cost for buses. Let $\tau(i, j)$ denote the travel time by the bus from location i to j. Let $C_{l_i,l_{i+1}}$ denote the cost of the transshipment operation between consecutive bus scheduled trips l_i and l_{i+1}, $\forall i = 1, 2, \cdots, n_r - 1$. Particularly, C_{0,l_1} denote the pickup cost incurred for the pickup operation by the bus, and $C_{n_r,h}$ denote the delivery cost incurred by delivery operation.

5.1.2 Feasibility, revenue, and cost of a bus trip chain

It can be seen that a bus trip chain is feasible for serving a parcel delivery request if it fulfills the two conditions: (i) the fixed timetable of each bus involved in the constructed bus trip chain and time window of CDC and RDSs are not violated, referred to as time-related condition; and (ii) the carrying capacity of each bus involved in the constructed bus trip chain is respected, referred to as capacity-related condition.

(i) Time-related condition for a feasible bus trip chain

As aforementioned, the timetable of bus scheduled trips involved in the bus trip chain should be strictly adhered to in order to ensure the primary function of passenger service. Some necessary activities such as vehicle clean and inspection need to be undertaken for the driver at the terminal during the time interval between consecutive scheduled trips of the bus. Moreover, the process of loading or unloading parcels necessitates additional working time. Let δ denote the time duration for necessary activities and σ denote the service time for loading or unloading parcels. Then, for the bus trip chain with the CDC 0, a series of bus scheduled trips $l_1, l_2, \cdots, l_{n_r}$ and the RDS h, the time-related condition for the feasibility of a bus trip chain can be asserted if the following feasibility conditions of the pickup, delivery, and transshipment operations for the related buses can be satisfied.

Pickup operation: the feasibility condition of the pickup operation performed by bus $b_1 \in \mathcal{B}$ in the bus trip chain r_h can be ensured if the timetable of the bus and the time window of the

CDC, i.e., Eq. (5.2) and Eq. (5.3), respectively, can be satisfied.

$$t^{\mathrm{d}}_{b_1,l_1-1} + \tau\left(s^{\mathrm{d}}_{b_1,l_1-1}, 0\right) + \sigma + \tau\left(0, s^{\mathrm{o}}_{b_1,l_1}\right) + \delta \le t^{\mathrm{o}}_{b_1,l_1}, \qquad \forall l_1 \in \mathcal{L}^{b_1}\backslash\{1\}, b_1 \in \mathcal{B} \tag{5.2}$$

$$E_0 \le t^{\mathrm{d}}_{b_1,l_1-1} + \tau(s^{\mathrm{d}}_{b_1,l_1-1}, 0) \le L_0, \qquad \forall l_1 \in \mathcal{L}^{b_1}\backslash\{1\}, b_1 \in \mathcal{B} \tag{5.3}$$

Delivery operation: the feasibility condition of the delivery operation performed by the bus $b_{n_r} \in \mathcal{B}$ in the bus trip chain r_h can be ensured if the timetable of the bus and the time window of the RDS $h \in \mathcal{H}$, i.e., Eq. (5.4) and Eq. (5.5), respectively, can be satisfied.

$$t^{\mathrm{d}}_{b_{n_r},l_{n_r}-1} + \tau\left(s^{\mathrm{d}}_{b_{n_r},l_{n_r}-1}, h\right) + \sigma + \tau\left(h, s^{\mathrm{o}}_{b_{n_r},l_{n_r}}\right) + \delta \le t^{\mathrm{o}}_{b_{n_r},l_{n_r}}, \quad \forall l_{n_r} \in \mathcal{L}^{b_{n_r}}\backslash\{1\}, b_{n_r} \in \mathcal{B}, h \in \mathcal{H} \tag{5.4}$$

$$E_h \le t^{\mathrm{d}}_{b_{n_r},l_{n_r}-1} + \tau(s^{\mathrm{d}}_{b_{n_r},l_{n_r}-1}, h) \le L_h, \qquad \forall l_{n_r} \in \mathcal{L}^{b_{n_r}}\backslash\{1\}, b_{n_r} \in \mathcal{B}, h \in \mathcal{H} \tag{5.5}$$

Transshipment operation: the feasibility condition of the transshipment operation performed by the buses $b_i, b_j \in \mathcal{B}$ in the bus trip chain r_h can be ensured if the timetable of the bus $b_i, b_j \in \mathcal{B}$, i.e., Eq. (5.6) and Eq. (5.7), respectively, can be satisfied.

$$t^{\mathrm{d}}_{b_i,l_i-1} + \tau\left(s^{\mathrm{d}}_{b_i,l_i-1}, s^{\mathrm{o}}_{b_j,l_j}\right) + \sigma + \tau\left(s^{\mathrm{o}}_{b_j,l_j}, s^{\mathrm{o}}_{b_i,l_i}\right) + \delta \le t^{\mathrm{o}}_{b_i,l_i}, \quad \forall l_i \in \mathcal{L}^{b_i}\backslash\{1\}, l_j \in \mathcal{L}^{b_j}, b_i, b_j \in \mathcal{B} \tag{5.6}$$

$$t^{\mathrm{d}}_{b_i,l_i-1} + \tau(s^{\mathrm{d}}_{b_i,l_i-1}, s^{\mathrm{o}}_{b_j,l_j}) + \sigma \le t^{\mathrm{o}}_{b_j,l_j} - \sigma, \qquad \forall l_i \in \mathcal{L}^{b_i}\backslash\{1\}, l_j \in \mathcal{L}^{b_j}, b_i, b_j \in \mathcal{B} \tag{5.7}$$

(ii) Capacity-related condition for a feasible bus trip chain

For each bus trip chain r_h with the CDC 0, bus scheduled trips $l_1, l_2, \cdots, l_{n_r}$ and the RDS h, the carrying capacity of the bus trip chain r_h able to accommodate parcels is limited by the minimum carrying capacity among all the bus trips in the bus trip chain. Let Q_{r_h} denote the capacity of the bus trip chain r_h that can accommodate parcels, which can be presented by

$$Q_{r_h} = \min_{i=1,2,\cdots,n_r, b_i \in \mathcal{B}} \{Q^{b_i}_{l_i}\}, \qquad \forall r_h \in \mathcal{R}^h, h \in \mathcal{H} \tag{5.8}$$

Let z_{r_h} denote the load of parcels served by the bus trip chain r_h. The capacity-related condition for a feasible bus trip chain can be ensured if the following constraint is satisfied:

$$z_{r_h} \leq \min\{Q_{r_h}, q_h\}, \qquad \forall r_h \in \mathcal{R}^h, h \in \mathcal{H} \tag{5.9}$$

It can be seen that a parcel delivery request may not be able to be fulfilled by on bus trip chain due to the limited carrying capacity of each bus trip chain. With loss of generality, we assume that a parcel delivery request can be fulfilled by multiple bus trip chains from the CDC to the RDS. A bus trip chain r_h is feasible only if the time-related and capacity-related conditions are satisfied. Let $\mathcal{R}$ denote the set of all feasible trip chains, and $\mathcal{R}^h$ denote the set of all feasible trip chains that can serve parcel request $h \in \mathcal{H}$, $\mathcal{R} := \bigcup_{h\in\mathcal{H}} \mathcal{R}^h$.

We can see that the revenue obtained by PTO from scheduling bus trip chain r_h to serve z_{r_h} parcels in RDS h is the sum of charge for the served parcels, i.e., $pz_{rh}, \forall h \in \mathcal{H}$, while the additional operating cost paid by PTO for scheduling bus trip chain r_h to serve the parcels can be expressed by the sum of additional cost due to pickup, delivery, and transshipment operations, which can be expressed as

$$c_{r_h} = C_{0,l_i} + \sum_{j=1}^{n_r-1} C_{l_i,l_{i+1}} + C_{l_{n_r},h}, \qquad \forall r_h \in \mathcal{R}^h, h \in \mathcal{H} \tag{5.10}$$

Kindly note that the cost of transporting parcels during the scheduled trips is not taken into account, as these trips are pre-scheduled for passenger service.

5.1.3 Dedicated vehicle service route

Given the parcel delivery requests as well as the service price, some parcel delivery requests may be fully or partially served by the bus trip chains, whereas those requests that are not (fully) served need to be fulfilled by the dedicated delivery service provided by LSP itself. We denote $\tilde{\mathcal{H}}(p)$ as the set of RDSs whose parcel delivery requests are not fully satisfied under the given service price, and use $\tilde{q}_h(p)$ to denote the remaining load of parcels of the request $h \in \mathcal{H}$ that needs to be satisfied under price p, where $\tilde{q}_h(p)$ can be calculated by the subtraction of initial parcel demand q_h and the parcels that have been served by CM transportation service by solving the lower-level BTS problem. Then, the unserved parcel delivery requests will be fulfilled by dedicated delivery services. Specifically, dedicated vehicle $v \in \mathcal{V}$ will load the parcels from the CDC 0, delivers parcels to a series of RDSs $h_1, h_2, \cdots, h_\omega$, and finally returns to the CDC 0, referred to as dedicated vehicle service route ω, which can be represented by

$$\omega = 0 \mapsto h_1 \mapsto h_2 \mapsto \cdots \mapsto h_{n_\omega} \mapsto 0 \tag{5.11}$$

where $\mapsto$ denote the vehicle routes. We can see that each dedicated vehicle service route ω is associated with an operating cost, including the fixed cost and the transportation cost. Let C^{f} denote the fixed cost of using each dedicated vehicle. Let $\phi(i,j)$ and κ_{ij} denote the travel time and transportation cost by the dedicated vehicle from location i to j, respectively. Let ξ_i denote the time epoch that the dedicate vehicle start service at the location i.

5.1.4 Feasibility and cost of a dedicated vehicle service route

It can be seen that a dedicated vehicle service route is feasible for serving the parcel delivery requests if it fulfills the two conditions: (i) time windows of RDSs and the CDC are not violated, referred to as time window condition; and (ii) the carrying capacity of the dedicated vehicle is respected, referred to as vehicle capacity condition.

(i) Time window condition for a feasible dedicated vehicle service route

For a vehicle route starting from the CDC 0, visiting a series of RDSs $h_1, h_2, \cdots, h_\omega$, and ending at CDC 0, the time window condition for the feasibility of dedicated vehicle service route can be asserted if the following time window constraints of RDS and CDC are satisfied. The time window of RDS $h_i, \forall i = 1, 2, \cdots, n_\omega$ can be ensured by

$$\xi_{h_{i-1}} + \sigma_{h_i} + \phi(h_{i-1}, h_i) \leq \xi_{h_i}, \qquad \forall i = 2, 3, \cdots, n_\omega \tag{5.12}$$

$$E_{h_i} \leq \xi_{h_i} \leq L_{h_i}, \qquad \forall i = 2, 3, \cdots, n_\omega \tag{5.13}$$

and the time window of the CDC can be satisfied by

$$E_0 \leq \xi_0 \leq L_0. \tag{5.14}$$

(ii) Vehicle capacity condition for a feasible dedicated vehicle service route

For a dedicated vehicle service route ω, the carrying capacity of a dedicated vehicle can be ensured by

$$\sum_{i=1}^{n_\omega} \tilde{q}_{h_i}(p) \leq Q_v, \qquad \forall v \in \mathcal{V}. \tag{5.15}$$

A dedicated vehicle service route ω is feasible if the above two conditions are satisfied, and we let $\mathbf{\Omega}$ denote all be the set of all feasible routes.

The cost of a dedicated vehicle service route can be calculated by the sum of the fixed cost of utilizing a vehicle and the corresponding transportation cost, which can be calculated by

$$c_\omega = C^{\mathrm{f}} + \kappa_{0h_1} + \sum_{i=1}^{n_\omega-1} \kappa_{h_i h_{i+1}} + \kappa_{h_\omega 0}, \qquad \forall \omega \in \mathbf{\Omega}. \tag{5.16}$$

It can be seen that the PT-based CM transportation service provided by PTO, along with the dedicated delivery service provided by LSP combine to form a hybrid delivery system. Consequently, each parcel delivery request can be accommodated by either the PT-based CM transportation service, the dedicated delivery service, or the hybrid delivery service that incorporates both models. For PTO, given the parcel delivery requests and the service price, the objective of PTO is to determine the optimal parcel requests to serve and the corresponding bus trip chains under the offered service price such that (i) the service time window of the RDS and CDC is not violated; (ii) the bus fixed timetables and the carrying capacity of the buses in the bus trip chains are respected; (iii) the total profit is maximized. For LSP, received with the optimal decision of PTO under the given service price, the objective of LSP is to determine the service price between a lower bound $\underline{p}$ and an upper bound $\overline{p}$, and the dedicated vehicle service routes such that (i) the service time window of the RDS and CDC is satisfied; (ii) the loading capacity of the dedicated vehicle is respected; and (iii) the total cost, including the self-operating cost paid for dedicated delivery service and outsourcing cost paid to PTO, is minimized.

To achieve the objectives, we formulate the CSP problem in a bilevel framework based on the interactive dynamics between LSP and PTO. A lower-level bus trip scheduling problem, referred to as BTS problem, is formulated to determine the PTO's optimal decision, i.e., the served parcel requests and corresponding bus trip chains for maximizing the PTO's total profits under the given a service price. An upper-level dedicated vehicle routing problem with pricing, referred to as VRP-P problem, is formulated to determine the optimal service price and dedicated vehicle routes to minimize the LSP's total costs, which consists of the outsourcing cost paid to PTO and the cost paid for dedicated delivery service.

5.2 Bilevel Path-based Optimization Model Formulation

In this section, we formulate a bilevel optimization model for the studied CSP problem composed of the upper-level VRP-P problem and a lower-level BTS problem. Since the LSP will determine the optimal service price considering the PTO's optimal decision under the offered price, in the next subsections, we will first elaborate on the lower-level BTS model and then the upper-level VRP-P model.

5.2.1 Lower-level BTS model

Given the service price p and outsourced parcel delivery requests $\mathcal{H}$, a profit-maximization model will be formulated to determine the optimal served requests and the bus trip chains that can maximize the PTO's total profits by serving additional parcel requests. In additional to aforementioned notations, we define x_{r_h} as the binary variable that equals 1 if bus trip chain $r_h \in \mathcal{R}^h$ is used for parcel deliveries, and 0 otherwise. Let $\eta^l_{r_h}$ denote the incidence coefficient that equals 1 if bus scheduled trip $l \in \mathcal{L}$ is utilized in the bus trip chain $r_h \in \mathcal{R}^h$, and 0 otherwise.

With the above notations, a path-based model [BTS] for the lower-level BTS problem can be formulated as follows:

[BTS]

$$\max_{\{\mathbf{x},\mathbf{z}\}} TP = \sum_{h\in\mathcal{H}} \sum_{r_h\in\mathcal{R}^h} p z_{r_h} - \sum_{h\in\mathcal{H}} \sum_{r_h\in\mathcal{R}^h} c_{r_h} x_{r_h} \tag{5.17}$$

subject to Eq. (5.9), and

$$\sum_{h\in\mathcal{H}} \sum_{r_h\in\mathcal{R}^h} \eta^l_{r_h} x_{r_h} \leq 1, \qquad \forall l \in \mathcal{L} \tag{5.18}$$

$$x_{r_h} = \{0,1\}, \qquad \forall r_h \in \mathcal{R}^h, h \in \mathcal{H} \tag{5.19}$$

$$z_{r_h} \geq 0, \qquad \forall r_h \in \mathcal{R}^h, h \in \mathcal{H} \tag{5.20}$$

where objective (5.17) is to maximize the total profits obtained by serving the parcel delivery requests, which is the subtraction of the total revenue and the corresponding operating cost. Eq. (5.18) indicates that each bus trip can be at most employed in one bus trip chain. Eqs. (5.19) and (5.20) define the domains of the variables.

5.2.2 Upper-level VRP-P model

Given the set of parcel delivery requests that are not (fully) satisfied $\tilde{\mathcal{H}}(p)$ and the corresponding outsourcing cost for the served parcel delivery requests under the offered price p, a cost-minimization model will be formulated to determine the optimal service price and dedicated vehicle service routes for fulfilling all the unserved parcel requests. In additional to aforementioned notations, we define y_ω as the binary variables that equals 1 if route ω is utilized for parcel delivery service, and 0 otherwise. Let a^ω_h denote the incidence coefficient that equals 1 if RDS $h \in \tilde{\mathcal{H}}(p)$ is served by route ω, and 0 otherwise.

With the above notations, a path-based model [VRP-P] for the upper-level VRP-P problem can be formulated as follows:

[VRP-P]

$$\min_{\{\mathbf{p},\mathbf{y}\}} TC = \sum_{\omega\in\mathbf{\Omega}} c_\omega y_\omega + \sum_{h\in\mathcal{H}} p(q_h - \tilde{q}_h(p)) \tag{5.21}$$

subject to

$$\sum_{\omega\in\Omega} a_\omega^h y_\omega = 1, \qquad \forall h \in \tilde{\mathcal{H}}(p) \tag{5.22}$$

$$y_\omega = \{0,1\}, \qquad \forall \omega \in \mathbf{\Omega} \tag{5.23}$$

$$\underline{p} \leq p \leq \overline{p} \tag{5.24}$$

where objective (5.21) is to minimize the LSP's total costs, including the self-operating cost paid for the dedicated delivery service and the outsourcing cost paid to PTO, which depends on the optimization of the lower-level BTS problem. Eq. (5.22) ensures that the unserved parcel requests should be fulfilled by the dedicated delivery service. Eqs. (5.23) and (5.24) define the domains of the variables.

5.3 ITH Solution Method

The CSP problem consisting of an upper-level VRP-P with a nested lower-level BTS problem is characterized as a hierarchical optimization challenge, which renders it unsolvable by commercial solvers. However, the bilevel framework of the CSP problem reveals that once the service price is confirmed, the upper-level problem is reduced to a vehicle routing problem, i.e., R-VRP-P problem, which is to find vehicle service routes for LSP to fulfil unserved parcel requests obtained by resolving the lower-level BTS problem at the aforementioned price. In light of this observation, we propose a customized iterated three-stage hybrid (ITH) algorithm to obtain good-quality solutions for the CSP problem by iteratively addressing the BTS problem, the R-VRP-P problem, and updating the service price. Specifically, in the first stage, we propose a granular tabu search (GTS) algorithm on an extended bus trip (EBT) network to solve the lower-level BTS problem to obtain the parcel requests served by bus trip chains and the parcel requests that are not (fully) served by PT-based CM transportation service under an initial price. In the second stage, we employ a GTS on an unserved parcel request (UPR) network to solve the upper-level R-VRP-P problem to determine the optimal dedicated service routes at the aforementioned price. In the third stage, an artificial bee colony (ABC) algorithm is employed to update the service price based on performance of the prices. The three-stage optimization is iterated until the maximum number of iterations is reached, and the optimal service price, along with the corresponding bus trip chains and dedicated vehicle routes will be finally determined. The overall framework of the ITH algorithm is illustrated in Figure 5.2.

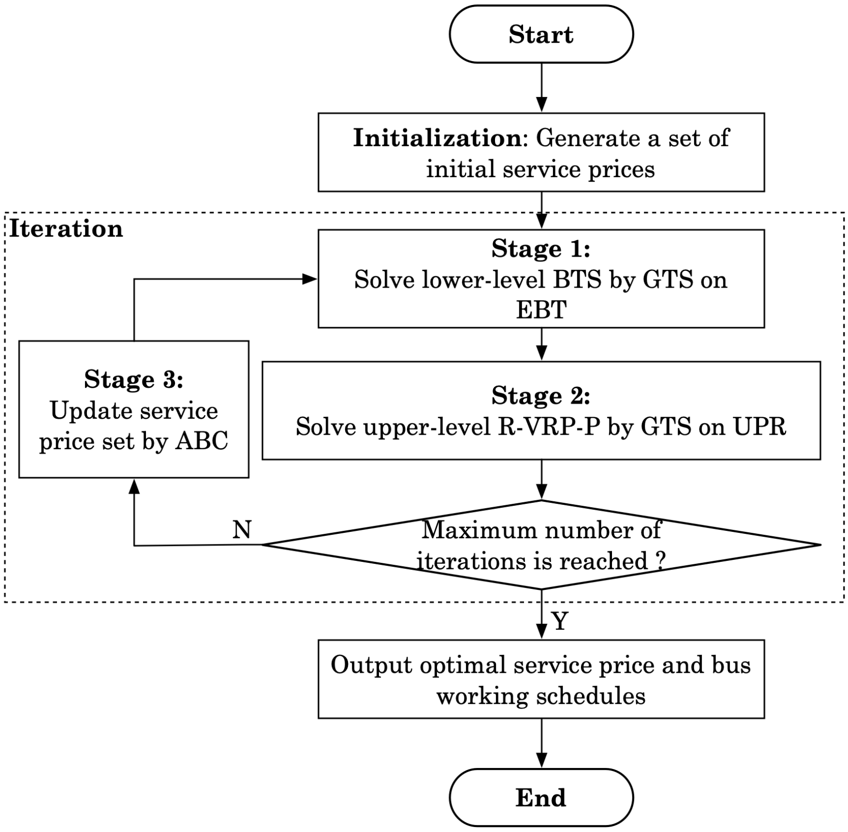

Figure 5.2. Overall framework of the ITH method

We can see that the ITH algorithm integrates two GTS algorithms and an ABC algorithm. The GTS is originated from the TS, which has demonstrated its efficacy in solving vehicle routing problems and related variants through the implementation of tabu strategies and non-improvement solution strategies (Toth and Vigo, 2003; Goeke, 2019). The ABC algorithm is a swarm-based evolutionary algorithm that simulates the nectar searching behavior of honeybees, offering the good ability to explore multiple solutions and yield high-quality solution (Karaboga and Basturk, 2008). In order to increase the likelihood of finding optimal solutions, we have considered two aspects for both the ABC algorithm and TS algorithm: on the one hand, we consider the local search and global search utilizing a memory-based new start strategy in the ABC algorithm to search the good-quality service price. On the other hand, we have proposed two GTS algorithms with a granular strategy based on the EBT and UPR, which is tailored to the characteristics of the lower-level and upper-level problems, to determine the good-quality bus trips chains and dedicated vehicle routes. These strategies enhance computational efficiency by reducing the exploration of low-quality solutions in each iteration. Furthermore, it can be seen that the optimization of the lower-level followed by the optimization upper-level problems can be carried out parallelly under different service prices. The utilization of a swarm-based ABC algorithm facilitates the parallel optimization of the lower-level and upper-level problems under distinct prices in each iteration using multi-thread technology. By combining TS algorithms and the ABC algorithm, we are able to identify a good-quality service price that minimizes the total cost of LSP while considering the interaction between LSP and PTO. In the subsequent subsections, we will provide detailed descriptions of the developed ABC and GTS algorithms.

5.3.1 Price initialization and updating by ABC algorithm

In the proposed ITH algorithm, a set of service prices needs to be generated and updated, which is achieved by ABC algorithm. The main idea behind the ABC algorithm is to simulate the collective intelligence of bee colony to locate optimal positions with abundant nectar, which is achieved by a swarm of artificial bees, namely, employed bees, onlooker bees, and scout bees. Specifically, a group of employed bees initiate the search for nectar from a set of random positions and explore the neighborhoods to discover the positions with more nectar using a local search strategy, referred to as the employed bee phase. Obtained the information shared by the employed bees, a group of onlooker bees select the promising positions with more nectar and further explore the neighborhoods of these selected positions to find better positions with more nectar via a local search strategy, referred to as the onlooker bee phase. If there is always no more nectar can be found after multiple searches around a particular position, the position will be abandoned and a scout bee is dispatched to explore a new random position, known as the scout bee phase. By a certain number of searches by employed bees, onlooker bees, and scout bees, a position characterized by abundant nectar is finally discovered.

To implement the ABC for finding the good-quality service price, a set of service prices in interval $[\underline{p}, \overline{p}]$ needs to be initialized. Specifically, we firstly generate an initialized set of service prices with total P prices by

$$p_i = \underline{p} + rand(0,1)(\overline{p} - \underline{p}), \qquad \forall i = \{1, 2, \cdots, P\} \tag{5.25}$$

where $rand(0,1)$ is a random function to generate a number between 0 and 1. Then, employed bee phase, onlooker bee phase, and scout bee phase are utilized to update the price set based on the performance of the price. In this paper, the performance of a price, namely, fitness value of a price, is defined as the total cost of LSP under the price, i.e., $TC(p)$.

In the employed bee phase, a local search is implemented on current price to generate a new price, which can be achieved by

$$p_i' = p_i + rand(-1,1)(p_i + \Delta p), \qquad \forall i \in \{1, 2, \cdots, P\} \tag{5.26}$$

where $rand(-1,1)$ is random function to generate a number within the range $[-1,1]$, and Δp is the parameter to control the local search range. If the new obtained price is better than current one, i.e., the price with better fitness value, the current price in the price set will be replaced by the new price. Then, the price set will be input to the onlooker bee phase for further exploration.

In the onlooker bee phase, promising prices, i.e., prices with good fitness value, will be selected for further exploration to find a better price. We employ roulette wheel selection to determine the selected prices and implement local search on the selected prices by Eq. (5.26). Also, if the new obtained price is better than current one, the current price will be replaced by the new price. After the onlooker bee phase, a scout bee phase is employed to initiate a new start for the prices with low possibility to become the optimal price. To be more specific, for those prices that has not been update by local search procedure in a certain number of iterations, we will randomly generate a new price by Eq. (5.25). Noted that a record of the explored prices is updated to ensure that the new generated prices have not been examined.

5.3.2 EBT-based GTS algorithm for lower-level BTS problem

In order to address the lower-level BTS problem and the upper-level reduced VRP-P problem, two customized GTS algorithms are proposed. The GTS algorithms in this chapter are derived from the classical TS algorithm, which is a meta-heuristic widely employed for solving diverse combinatorial optimization problems. The TS algorithm begins with an initial solution, which also serves as the current solution and the optimal solution at the beginning. Subsequently, a set of operators defines a series of moves applied to the current solution, resulting in the generation of new solutions known as neighborhood solutions. For example, an insertion operator might involve removing a request from the current route and inserting it into a different route. The various options for requests, routes, and insertion locations correspond to distinct moves. The current solution is then updated to be the best neighborhood solution, while the current optimal solution is updated only if the objective value of the best neighborhood solution surpasses that of the incumbent solution. Notably, to prevent cyclic iterations and escape local optima, a memory structure known as the tabu list is employed while applying moves to the current solution (Glover, 1986). Specifically, when a neighborhood solution is obtained, the corresponding move responsible for generating that solution is declared tabu. Consequently, the inverse operation of this move is prohibited for a specified number of iterations, unless it can generate a superior solution compared to the current optimal solution (Glover, 1986). The classical TS algorithm considers all possible moves during the exploration of neighborhood solutions when applying an operator, resulting in a considerable amount of time being consumed. In order to enhance computational efficiency, Toth and Vigo (2003) proposes a valuable granular strategy to the TS algorithm, which selectively explores moves that hold promise in generating good-quality solutions. This strategy has demonstrated notable effectiveness in achieving good-quality solutions within reduced computation time (Kirchler and Calvo, 2013). In line with the framework of the classical TS algorithm, we also consider a granular strategy that takes into account the distinctive characteristics of the upper- and lower-level problems during the neighborhood search procedure.

Given the service price and the parcel requests, the lower-level BTS problem is to find the optimal bus trip chains for parcel delivery that can maximize the PTO's total profit. To facilitate the exploration of the bus trip chain consisting of the CDC, a series of bus scheduled trips, and an RDS, we introduce an EBT network denoted by $\mathcal{G}_1 = (\mathcal{N}_1, \mathcal{A}_1)$, where $\mathcal{N}_1 = \{0\} \cup \mathcal{L} \cup \mathcal{H}$ denotes the set of network nodes and $\mathcal{A}_1 = \{(0,l) : l \in \mathcal{L}\} \cup \{(l,l') : l, l' \in \mathcal{L}\} \cup \{(l,h) : l \in \mathcal{L}, h \in \mathcal{H}\}$ denotes the set of network arcs representing corresponding pickup/delivery/transshipment operations of a bus. We can see that each node is associated with time-related conditions, such as time windows of the CDC node and RDS nodes and timetable of the bus scheduled trip nodes. In this context, certain arcs within the network may not be viable due to violation on these time-related conditions. To address this issue, we assess the feasibility of each arc by assigning a cost that represents the implementation of the corresponding pickup/delivery/transshipment operations while considering the time-related constraints. Let $\hat{c}_{ij}$ denote the cost associated with the arc $(i,j) \in \mathcal{A}_1$ considering the time-related constraints. If the operation associated with the arc $(i,j) \in \mathcal{A}_1$ do not cause violation on the time-related conditions, the cost of the arc is defined as the operating cost of the corresponding operation, i.e., $\hat{c}_{ij} = C_{ij}, \forall (i,j) \in \mathcal{A}_1$. Conversely, if a violation occurs, the cost is set to a large value, i.e., $\hat{c}_{ij} = M_1, \forall (i,j) \in \mathcal{A}_1$, where M_1 is a large value.

With the established EBT considering the time-related feasibility of the arcs, we then implement the TS to find the optimal bus trip chains. We will first generate an initial solution by generating $|\mathcal{H}| + 1$ bus trip chains, where $|\mathcal{H}|$ is the total number of RDSs. The first $|\mathcal{H}|$ bus trip chains consist of the CDC and an RDS without any bus scheduled trips arranged, and all bus scheduled trips are arranged in the $(|\mathcal{H}|+1)$-th bus trip chain. It is noted that bus trip chains only encompassing the CDC and RDS, as well as the $(|\mathcal{H}|+1)$-th bus trip chain, do not generate any profit or cost. Later on, we will apply the before-mentioned insertion operator to relocate a trip node from current bus trip chain to a different bus trip chain to generate neighborhood solutions following the steps of classical TS. However, unlike the classical TS that considers all moves, i.e., various options for bus trips, bus trip chains, and insertion locations, when applying the insertion operator, we consider a granular strategy that only considers the promising moves during the implementation of neighborhood search with the insertion operator. Specifically, we can see that a smaller value of $\hat{c}_{ij}$ indicates that it would be more cost-effective to schedule the node i exactly before node j. Motivated by this, we define the promising move as the move that can make the node i exactly before node j such that $\hat{c}_{ij} \leq c_{\text{gra\_low}}$, where $c_{\text{gra\_low}}$ is a granular threshold setting for lower-level BTS problem. This granular strategy can improve the efficiency of neighborhood search for a good-quality solution by reducing the exploration for unpromising moves. Figure 5.3 illustrates an example of neighborhood search with a granular strategy for a case with one CDC, two bus trips, and two parcel delivery requests in two RDSs.

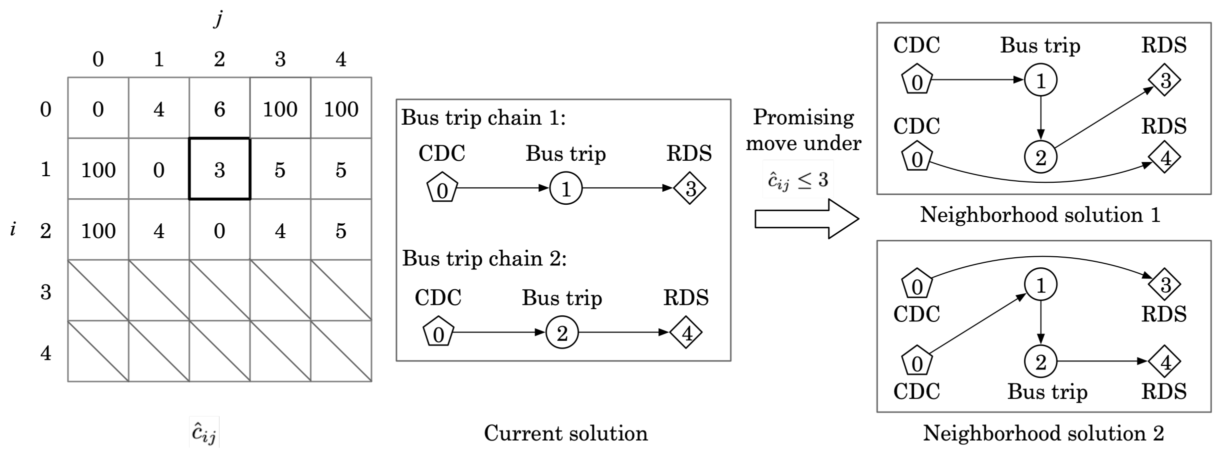

Figure 5.3. An illustrative example of neighborhood search with a granular strategy

In Figure 5.3, compared with the neighborhood search of the current solution with all possible moves, we only consider the promising moves under the granular strategy such that $\hat{c}_{ij} \leq 3$, i.e.,$c_{\text{gra\_low}} = 3$ to get reduced neighborhood solutions with good-probability to find the optimal solution. It can be seen that a higher value of the granular threshold $c_{\text{gra\_low}}$ implies a reduction in the exploration of moves, leading to reduced time consumption but a constrained search for neighborhood solutions. In this chapter, we define a dynamic $c_{\text{gra\_low}}$ through iterative implementation. To be more specific, the granular threshold $c_{\text{gra\_low}}$ is initiated as $c_{\text{gra\_low}} \leftarrow \min_{(i,j)\in\mathcal{A}_1}\{\hat{c}_{ij}\}$ and then gradually increase by $c_{\text{gra\_low}} \leftarrow c_{\text{gra\_low}} + \Delta c_{\text{low}}$ until the upper bound $\bar{c}_{\text{gra\_low}}$ is reached.

Furthermore, it is evident that the aforementioned approach only considers scenarios where each parcel delivery request is served by a maximum of one bus trip chain. However, it is possible for a parcel delivery request to be fulfilled by multiple bus trip chains. To this end, we will iterate the implementation of the EBT-based GTS algorithm multiple times until no parcel requests can be accommodated by bus trip chains. More specifically, after obtaining the bus trip chains for parcel deliveries, we will remove the corresponding parcel requests and the assigned bus trips. Subsequently, we will repeat the EBT-based GTS algorithm to generate new sets of bus trip chains until no parcel requests can be served by the CM transportation service. This iterative approach is justified by the fact that a bus trip chain will always carry the maximum number of parcels it can accommodate. The step-by-step procedures of the EBT-based GTS for solving the lower-level BTS problem are elaborated as follows.

- **Step 0: (Data input and initialization)** Input the parcel requests $\mathcal{H}$, service price p, and bus trip $\mathcal{L}$. Initialize current number of iterations $n \leftarrow 1$, maximum number of iterations N, penalty coefficient γ, adaptive factor for penalty coefficient ϱ, and $TabuList$. Initialize the optimal PT-based CM transportation service solution, i.e., bus trip chains $\Psi \leftarrow \varnothing$, and total profit for PTO $TP(\Psi, p) \leftarrow 0$ under the price p.
- **Step 1: (Generation and evaluation of the initial solution)**
  - **Step 1.1:** Generate an initial bus trip chain solution ψ_0 with requests $\mathcal{H}$ and bus trip $\mathcal{L}$, and compute the parcel load carried by bus trip chains, denoted by $z(\psi_0)$, and profit for PTO, represented by $f(\psi_0, p)$ under solution ψ_0 and price p considering the penalty cost due to violation of the constraints.
  - **Step 1.2:** Initialize current optimal bus trip chain solution by $\psi^* \leftarrow \psi_0$ and PTO's profit under current optimal solution by $f_{\text{best}} \leftarrow f(\psi^*, p)$.
- **Step 2: (Neighborhood search)**
  - **Step 2.1:** Initialize the current bus trip chain solution by $\psi \leftarrow \psi^*$ and the set of neighborhood solutions by $\mathcal{NS}(\psi) \leftarrow \varnothing$.
  - **Step 2.2:** Explore promising $Moves$ with the granular strategy.
    - **Step 2.2.1:** Calculate cost $\hat{c}_{ij}, \forall (i,j) \in \mathcal{A}_1$.
    - **Step 2.2.2:** Initialize granular threshold $c_{\text{gra\_low}}$ as $c_{\text{gra\_low}} \leftarrow \min_{(i,j)\in\mathcal{A}_1}\{\hat{c}_{ij}\}$ and determine the upper bound of granular threshold by $\bar{c}_{\text{gra\_low}}$.
    - **Step 2.2.3:** Obtain the promising $Moves$ such that $\hat{c}_{ij} \leq c_{\text{gra\_low}}$.
  - **Step 2.3:** Obtain neighborhood solutions by applying promising $Moves$ on solution ψ considering the tabu strategy, i.e., $\mathcal{NS}(\psi) = \text{Neighbor}(\psi, Moves, TabuList, f_{\text{best}})$, where Neighbor$(\cdot)$ represents the neighborhood search operation. More specifically, we utilize $Moves$ on current routing solution ψ to generate the neighborhood solutions. Each time we generate a neighborhood solution ψ', we first check if the move

that generates it is prohibited by the $TabuList$. If it is not forbidden, the solution is included in $\mathcal{NS}(\psi)$. However, if the move is forbidden, we examine if the solution satisfies the condition $f(\psi', p) > f_{\text{best}}$: if yes, the solution is included in $\mathcal{NS}(\psi)$.

  - **Step 2.4:** If $\mathcal{NS}(\psi) \neq \varnothing$, go to **Step 2.4.1**, otherwise go to **Step 2.5**.

    * **Step 2.4.1:** Identify the best solution from the set of neighborhood solutions, i.e., $\hat{\psi} = \arg\max_{\psi' \in \mathcal{NS}(\psi)} f(\psi', p)$.

    * **Step 2.4.2:** Perform a feasibility check on solution ψ'. If violation occurs, adjust the associated penalty coefficient by $\gamma \leftarrow \gamma + \varrho$. Conversely, if no violation occurs, update the optimal solution by $\psi^* \leftarrow \hat{\psi}$, $f_{\text{best}} \leftarrow f(\hat{\psi}, p)$ if $f(\hat{\psi}, p) > f_{\text{best}}$.

    * **Step 2.4.3:** Let $\psi \leftarrow \hat{\psi}$ and update $TabuList$ with the $Move$ that generates solution $\hat{\psi}$ and go to **Step 3**.

  - **Step 2.5:** If $c_{\text{gra\_low}} < \bar{c}_{\text{gra\_low}}$, let $c_{\text{gra\_low}} \leftarrow c_{\text{gra\_low}} + \Delta c_{\text{low}}$ and go to **Step 2.2.3**; otherwise go to **Step 3**.

- **Step 3: (Iteration condition)** If $n < N$, let $n \leftarrow n + 1$ and go to **Step 2.3**, otherwise go to **Step 4**.

- **Step 4: (Update of CM transportation solution and request)** If the optimal bus trip chain solution do not include the scenario that parcel requests are served by CM transportation service, go to **Step 5**; otherwise to to **Step 4.1**.

  - **Step 4.1:** Add the optimal bus trip chain solution ψ^* to the CM transportation service solution by $\Psi \leftarrow \Psi \cup \psi^*$ and accumulate the profit of the solution to the total profit for PTO.

  - **Step 4.2:** If the optimal bus trip chain solution ψ^* includes the scenario that parcel requests are served by CM transportation service, obtain the set of remaining parcel requests $\mathcal{H}'$ by removing requests that have been fully served under solution ψ and adjust the parcel load of the request in parcel requests $\mathcal{H}$, let $\mathcal{H} \leftarrow \mathcal{H}'$, remove the used bus trips from $\mathcal{L}$ and go to **Step 0**.

- **Step 5: (Output)** Output PT-based CM transportation service solution Ψ^* and PTO's total profit TP.

Kindly note that the solution ψ^* should not cause any violation on corresponding constraints, which can be guaranteed by a feasibility check in Step 2.4.2. The total profit for PTO TP consists of the profit of all employed optimal bus trip chains obtained by each TS implementation. Meanwhile, by exploring the CM transportation service solution ψ^*, the unserved parcel delivery requests under the offered price p will be grouped in set $\tilde{\mathcal{H}}(p)$, which will be then input for the optimization of the upper-level R-VRP-P problem.

5.3.3 UPR-based GTS algorithm for upper-level R-VRP-P problem

The upper-level R-VRP-P problem is to determine the optimal dedicated vehicle routes for fulfilling the parcel requests that are not (fully) served by the PT-based CM transportation service. To facilitate the exploration of the dedicated vehicle routes, we establish a UPR by $\mathcal{G}_2 = (\mathcal{N}_2, \mathcal{A}_2)$, where $\mathcal{N}_2 = \{0\} \cup \tilde{\mathcal{H}}(p)$ denotes the set of network nodes and $\mathcal{A}_2 = \{(0, h) : h \in \tilde{\mathcal{H}}(p)\} \cup \{(h, h') : h, h' \in \tilde{\mathcal{H}}(p)\} \cup \{(h, 0) : h \in \tilde{\mathcal{H}}(p)\}$ denotes the corresponding arc that can be traveled by the dedicated vehicles. Similar to the construction of EBT network, we denote $\tilde{c}_{ij}$ as the cost associated with the arc $(i, j) \in \mathcal{A}_2$ considering the time and capacity constraints. Specifically, if the vehicle service associated with the arc $(i, j) \in \mathcal{A}_2$ does not cause violation on the time and capacity constraints, the cost of the arc is defined as the transportation cost along the arc, i.e., $\tilde{c}_{ij} = \kappa_{ij}, \forall (i, j) \in \mathcal{A}_2$. Conversely, if a violation occurs, the cost is set to a large value, i.e., $\tilde{c}_{ij} = M_2, \forall (i, j) \in \mathcal{A}_2$, where M_2 is a large value.

With the established UPR network considering the time and capacity feasibility of the arcs, we then implement the TS to find the optimal dedicated vehicle service routes. We will first generate an initial solution by request-to-vehicle assignment method proposed by (Cordeau and Laporte, 2003). More specifically, parcel request randomly selected from all unserved parcel requests is arranged to a vehicle according to the earliest service time of the time window until the vehicle capacity is not available, and the request will be assigned to a new dedicated vehicle. While this method ensures adherence to the vehicle capacity constraint, other constraints may be violated. To address such violations, penalties are imposed on the solutions by introducing a penalty coefficient for each constraint violation and incorporating the penalty cost into the objective function. Then, the insertion operator mentioned earlier is employed to relocate a request node from its current service route to a different service route, thereby generating neighborhood solutions in accordance with the classical TS approach.We will then consider the moves that can make the node i exactly before node j such that $\tilde{c}_{ij} \leq c_{\text{gra\_upp}}$. The granular threshold $c_{\text{gra\_upp}}$ is initiated as $c_{\text{gra\_upp}} \leftarrow \min_{(i,j) \in \mathcal{A}_2} \{\tilde{c}_{ij}\}$ and then gradually increase by $c_{\text{gra\_upp}} \leftarrow c_{\text{gra\_upp}} + \Delta c_{\text{upp}}$ until the upper bound $\bar{c}_{\text{gra\_upp}}$ is reached. The step-by-step procedures of the UPR-based GTS for solving the upper-level R-VRP-P problem are elaborated as follows.

- **Step 0: (Data input and initialization)** Input the parcel requests $\tilde{\mathcal{H}}(p)$ under the price p. Initialize current number of iterations $n \leftarrow 1$, maximum number of iterations N, penalty coefficient γ, adaptive factor for penalty coefficient ϱ, and $TabuList$. Initialize vehicle route solution $\theta^* \leftarrow \varnothing$, and total profit for PTO $TC(\theta^*, p) \leftarrow \infty$.

- **Step 1: (Generation and evaluation of the initial solution)**
  - **Step 1.1:** Create an initial dedicated vehicle routing solution θ_0 with requests $\tilde{\mathcal{H}}(p)$ and compute the total cost for LSP, represented by $g(\theta_0, p)$ under solution θ_0 and price p considering the penalty cost due to violation of the constraints.
  - **Step 1.2:** Initialize current optimal dedicated vehicle routing solution by $\theta^* \leftarrow \theta_0$ and current optimal total cost under current optimal solution by $g_{\text{best}} \leftarrow g(\theta^*, p)$.
- **Step 2: (Neighborhood search)**
  - **Step 2.1:** Initialize the current solution by $\theta \leftarrow \theta^*$ and the set of neighborhood solutions by $\mathcal{NS}(\theta) \leftarrow \varnothing$.
  - **Step 2.2:** Explore promising $Moves$ with the granular strategy.
    * **Step 2.2.1:** Calculate cost $\tilde{c}_{ij}, \forall (i,j) \in \mathcal{A}_2$.
    * **Step 2.2.2:** Initialize granular threshold $c_{\text{gra\_upp}}$ as $c_{\text{gra\_upp}} \leftarrow \min_{(i,j)\in\mathcal{A}_2}\{\tilde{c}_{ij}\}$ and determine the upper bound of granular threshold by $\bar{c}_{\text{gra\_upp}}$.
    * **Step 2.2.3:** Obtain the promising $Moves$ such that $\tilde{c}_{ij} \leq c_{\text{gra\_upp}}$.
  - **Step 2.3:** Obtain neighborhood solutions by applying promising $Moves$ on solution θ considering the tabu strategy, i.e., $\mathcal{NS}(\theta) = \text{Neighbor}(\theta, Moves, TabuList, g_{\text{best}})$, where Neighbor$(\cdot)$ represent the neighborhood search operation. More specifically, we utilize $Moves$ on current routing solution θ to generate the neighborhood solutions. Each time we generate a neighborhood solution θ', we first check if the move that generates it is prohibited by the $TabuList$. If it is not forbidden, the solution is included in $\mathcal{NS}(\theta)$. However, if the move is forbidden, we then examine if the solution satisfies the condition $g(\theta', p) < g_{\text{best}}$: if yes, the solution is included in $\mathcal{NS}(\theta)$.
  - **Step 2.4:** If $\mathcal{NS}(\theta) \neq \varnothing$, go to **Step 2.4.1**, otherwise go to **Step 2.5**.
    * **Step 2.4.1:** Identify the best solution from the set of neighborhood solutions, i.e., $\hat{\theta} = \arg\min_{\theta'\in\mathcal{NS}(\theta)} g(\theta', p)$.
    * **Step 2.4.2:** Perform a feasibility check on solution θ'. If violation occurs, adjust the associated penalty coefficient by $\gamma \leftarrow \gamma + \varrho$. Conversely, if no violation occurs, update the optimal solution by $\theta^* \leftarrow \hat{\theta}, g_{\text{best}} \leftarrow g(\hat{\theta}, p)$ if $g(\hat{\theta}, p) < g_{\text{best}}$.
    * **Step 2.4.3:** Let $\theta \leftarrow \hat{\theta}$ and update $TabuList$ with the $Move$ that generates solution $\hat{\theta}$ and go to **Step 3**.
  - **Step 2.5:** If $c_{\text{gra\_upp}} < \bar{c}_{\text{gra\_upp}}$, let $c_{\text{gra\_upp}} \leftarrow c_{\text{gra\_upp}} + \Delta c_{\text{upp}}$ and go to **Step 2.2.3**; otherwise go to **Step 3**.

- **Step 3: (Iteration condition)** If $n < N$, let $n \leftarrow n + 1$ and go to **Step 2.3**, otherwise go to **Step 4**.
- **Step 4: (Output)** Output current optimal dedicated vehicle routing solution θ and LSP's total profit TC.

Kindly note that the solution θ^* must satisfy all relevant constraints without any violations, which is ensured by the feasibility check performed on in Step 2.4.2. As a result, the total cost of the optimal routing solution θ^* is given by $TC(\theta^*, p)$

5.4 Numerical Experiments

This section will first evaluate the performance of the proposed ITH algorithm on a series of randomly generated instances. Subsequently, a set of simulated cases from Chongqing, China is utilized to perform an implication analysis for the hybrid delivery system incorporating PT-based CM transportation service. The algorithms are implemented using MATLAB 2021a on a personal computer equipped with MacOS Big Sur 11.6 and an Apple M1 3.2 GHz CPU.

5.4.1 Test instance generation and parameter setting

We generate multiple instances with varying numbers of parcel delivery requests, ranging from 10 to 60, and bus scheduled trips, ranging from 10 to 120, within a 50 km×50 km square region. The coordinates for the RDS and bus terminals are randomly generated within the region, while the coordinates for the CDC are set at (25, 25). The distance between two locations is calculated using the Euclidean distance. By setting the speed of buses and dedicated vehicles at 30 km/h, we can obtain the travel time between any two locations. The parcel load for each parcel delivery request is randomly selected from the range of 10 kg to 30 kg, and the opening time window for each RDS is randomly chosen within the interval [10:00, 14:00]. The time window for the CDC is set as [10:00, 14:00]. Regarding the bus trips, the carrying capacity of each bus trip is selected from the range of 20 kg to 40 kg. The departure time of a bus from the origin terminal is randomly generated within the interval [10:00, 13:00], and the arrival time of the bus at the destination terminal is set as the departure time plus the travel time. Each bus has a 20-minute available time interval to carry out pickup, delivery, and relay operations. The service time for loading parcels onto each bus is set as 5 min, and an additional 5 min is allocated for necessary activities for each bus and driver. For dedicated vehicles, the carrying capacity of each vehicle is set as 200 kg, and the service time for loading parcels is set as 5 min.

5.4.2 Performance of ITH method on test instances

We will use the randomly generated instances to evaluate the performance of the proposed ITH algorithm by comparing it with other heuristic methods. Specifically, the effectiveness of the ITH algorithm relies on the integration of the ABC algorithm and the TS algorithm. To evaluate the efficacy of the ABC algorithm and TS algorithm, we will compare their performance with that of the genetic algorithm (GA), which is another evolutionary population-based algorithm, as well as a greedy heuristic by an insertion operation (INS). By combining these four methods to solve the upper-level and lower-level problems, as well as updating the prices, we will compare the performance of four hybrid methods: ABC and TS (our proposed ITH method), ABC-INS, GA-TS, and GS-INS.

We report the results of 10 instances of varying scales, characterized by different numbers of parcel delivery requests (#ParReq) and bus scheduled trips (#BusTrp) in Table 5.1. For each instance, we generate five random instances and compute the average values of the objective value (Obj) and CPU time by different methods. The best objective values among the four methods are indicated in bold. Additionally, to facilitate comparison, we calculate the relative gaps RelGap_1, RelGap_2, RelGap_3, and RelGap_4, which are computed as $\text{RelGap}_1 = (\text{Obj}^* - \text{Obj}_1)/\text{Obj}^* * 100\%$, $\text{RelGap}_2 = (\text{Obj}^* - \text{Obj}_2)/\text{Obj}^* * 100\%$, $\text{RelGap}_3 = (\text{Obj}^* - \text{Obj}_3)/\text{Obj}^* * 100\%$, where Obj^*, Obj_1, Obj_2, and Obj_3 are the objective values obtained by ITH algorithm, ABC-INS, GA-TS, GA-INS, respectively.

It can be seen that our proposed ITH algorithm integrating two TS and an ABC algorithm outperforms the other three methods in finding the minimized objective value. Moreover, the ITH algorithm achieves good-quality solutions with lower CPU time compared to the other three methods, with an average CPU time of 369.4s compared to 517.5s for ABC-INS, 428.7s for GA-TS, and 612.9s for GA-INS. On the one hand, the TS algorithm, incorporating a tabu strategy and a cost-oriented granular strategy, reduces exploration for unpromising moves while enhancing the search for good-quality solutions. This improves the likelihood of identifying optimal bus trip chains and dedicated vehicle routes. It is evident that, using the same method (ABC or GA) for price updating, the TS algorithm yields better objective values than the insertion heuristic (INS). For instance, ABC-TS achieves a superior objective value compared to ABC-INS, with an average relative gap of 3.89%. On the other hand, the ABC algorithm, which combines local and global search for service price determination, assists in finding good-quality prices that lead to improved objective values. Using the same method (TS or INS) for lower- and upper-level optimization, the ABC algorithm outperforms the GA algorithm. For

Table 5.1. Comparison of the proposed ITH, ABC&INS, GA&TS, and GA&INS algorithms

Instance	#ParReq	#BusTrp	ABC-TS (ITH)		ABC&INS		GA&TS		GA&INS		RelGap_1	RelGap_2	RelGap_3
			Obj ($)	CPU (s)	Obj ($)	CPU (s)	Obj ($)	CPU (s)	Obj ($)	CPU (s)			
1	10	10	**861**	9.9	877	10.3	877	**9.5**	876	9.9	1.8%	1.9%	1.8%
2	20	20	**1,750**	**21.7**	1,769	27.3	1,789	**21.7**	1,841	27.7	1.1%	2.2%	5.2%
3	30	30	**2,782**	**48.1**	2,885	58.6	2,903	58.4	2,858	70.4	3.7%	4.4%	2.7%
4	40	40	**3,155**	**116.9**	**3,155**	137.0	3,439	138.8	3,510	168.9	0.0%	9.0%	11.0%
5	50	50	**3,876**	**293.6**	4,057	364.5	4,221	327.2	4,343	413.3	4.7%	8.9%	12.1%
6	60	30	**4,526**	**309.1**	4,663	407.8	4,932	349.8	4,999	475.9	3.0%	9.0%	10.4%
7	60	45	**4,415**	**390.2**	4,564	542.2	4,866	436.2	4,832	609.2	3.4%	10.2%	9.5%
8	60	60	**4,320**	**569.8**	4,457	781.2	4,719	645.1	4,785	875.0	3.2%	9.2%	10.8%
9	60	90	**4,092**	**827.6**	4,305	1,210.1	4,660	985.1	4,676	1,484.7	5.2%	13.9%	14.3%
10	60	120	**3,799**	**1,107.0**	4,286	1,635.6	4,394	1,314.8	4,401	1,993.6	12.8%	15.7%	15.9%
Average	–	–	–	**368.6**	–	517.5	–	428.7	–	612.9	3.9%	8.4%	9.4%

instance, ABC-TS achieves a superior objective value compared to GA-TS, with an average relative gap of 8.44%. Figure 5.4 provides a visual comparison of the objective value and CPU time under different scales of the problem with varying numbers of parcel requests and bus trips. It is evident that as the number of bus scheduled trips and parcel requests increases, our proposed ITH algorithm demonstrates the best objective value performance in Figure 5.4(a) and the smallest increase in computation time in Figure 5.4(b). This comparison highlights the strong performance of the ITH algorithm in finding good-quality solutions for the CSP problem. In addition, our experiments also show that the ITH algorithm is capable of solving the instance with a total of 300 parcel requests and bus trips within one hour. The CPU time does not exhibit exponential growth with an increasing number of parcel requests and bus-scheduled trips, which indicates the algorithm's strong potential for effectively addressing scenarios involving a substantial number of parcel delivery requests and bus-scheduled trips.

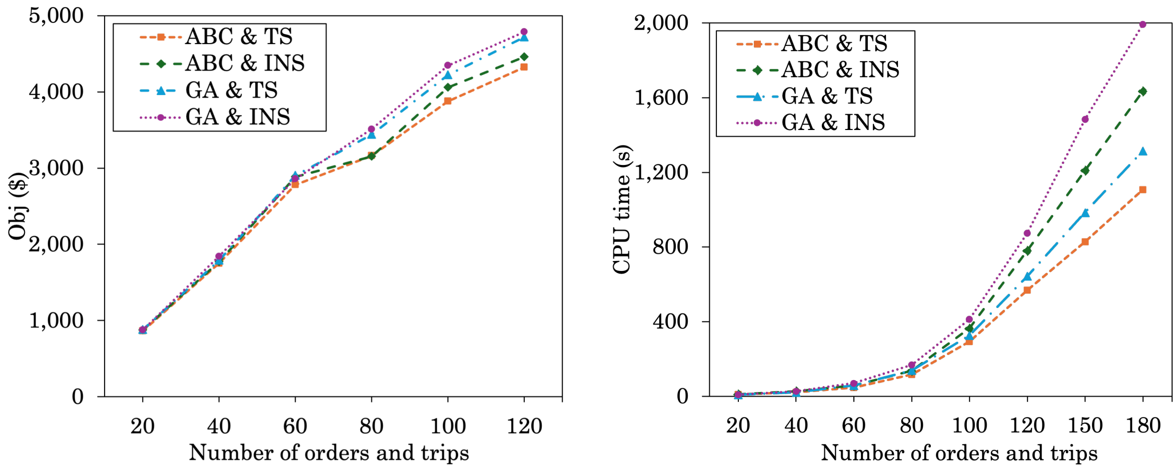

(a) Objective value

(b) CPU time

Figure 5.4. Variations of Obj and CPU time under different scales of instances

5.4.3 Case study

We then simulate a series of real-life cases in Chongqing, China to evaluate the benefit of hybrid delivery system with the new PT-based CM transportation service and derive managerial insights for the applications of the delivery services.

Chongqing, a megacity in southwestern China, has a well-developed public transit network that efficiently meets the transportation needs of its residents. LSPs have established urban CDCs near the city's airports, with many RDSs spread throughout the city. For our study, we selected a specific logistics company YTO Express's CDC and RDSs to source data for parcel delivery requests. We also obtained information on nearly 1,000 bus routes in the city via the Baidu Maps API, which forms the basis for our public transit-based CM transportation services.

Specifically, we designate the CDC as the origin for parcel deliveries and various RDSs as the destinations. The opening time window for the CDC is defined as [9:00, 20:00], and opening time windows for the RDSs are randomly generated within the off-peak hours of [9:30, 12:00] and [14:00, 16:00]. The load of parcel requests at each RDS is randomly selected from the range of [10 kg, 30 kg], and the duration allocated for servicing each parcel is established at five minutes. Subsequently, we prepare the bus scheduled trips. We choose bus trips with destinations near the CDC or RDSs. The carrying capacity of each bus trip is randomly selected from the range of [20 kg, 40 kg]. The duration for parcel service by bus and the necessary activities are both set at five minutes, while the available time duration for consecutive scheduled trips for each bus is defined as 20 minutes. The fixed cost of utilizing a dedicated vehicle is set at \$100, while the unit costs for dedicated vehicle transportation and bus transportation are set at \$3/km and \$1.2/km, respectively. The speed of both buses and dedicated vehicles is set at 30 km/h.

5.4.4 Impact analysis of PT-based CM transportation service

To evaluate the benefits of the hybrid delivery system (HDS), we compare several key metrics between HDS and traditional dedicated delivery services (DDS) using different cases with different number of parcel delivery requests and bus trips, as shown in Table 5.2. These metrics include the total cost incurred by the LSP (TC), the total profit generated by the PTO through serving additional parcel requests (TP), the average cost of serving each load of parcel by the LSP (AveCost), the total fleet size of dedicated vehicles utilized by the LSP (FS), the optimal price for CM transportation services (Price), and the acceptance rate for parcel delivery requests outsourced by the LSP (AcpRate). Furthermore, we present the percentage of the cost savings (CostSav%), the number of vehicles saved (VehSav%), and the average cost saved per unit parcel load (AveCost%) in the HDS model compared to the DDS model.

Table 5.2 demonstrates that PT-based CM transportation significantly cuts costs for the LSP and boosts profits for the PTO. First, PT vehicles are more cost-efficient than dedicated delivery vehicles for parcel deliveries, with the fact that the price of using them is relatively low (less than \$2). Second, by using PT-based CM transportation, LSPs can reduce their fleet size from an average of 18.3 vehicles to 11.6. This reduction lowers operating costs, especially the fixed costs associated with a larger fleet. Additionally, the average cost of using dedicated vehicles decreases from \$2.91/kg to \$2.52/kg, further reducing overall costs. Moreover, in the hybrid delivery model with PT-based CM transportation, handling 100 parcel delivery requests results in costs dropping from \$5,067 to \$4,579, while profits increase from \$765 to \$1,767 as the number of available bus trips rises from 50 to 200. More available bus trips allow a greater number of parcels to be served by the cost-effective PT-based CM transportation, increasing the

Table 5.2. Comparison of the dedicated delivery system (DDS) and hybrid delivery system (HDS)

Case	#ParReq	#BusTrp	DDS			HDS						CostSav%	VehSav%	AveCostSav%
			TC (\$)	AveCost (\$/kg)	FS	TC (\$)	TP (\$)	AveCost (\$/kg)	Price (\$)	FS	AcpRate (%)			
1	50	50	3,429	3.07	12	2,600	605	2.80	1.6	6	39.6%	24.2%	50.0%	8.7%
2	60	60	4,069	3.08	14	2,826	593	2.48	1.5	8	34.9%	30.5%	42.9%	19.4%
3	70	70	4,472	2.94	16	3,447	984	2.50	1.9	10	38.8%	22.9%	37.5%	15.1%
4	80	80	5,267	2.97	17	4,029	1,044	2.55	1.8	11	37.5%	23.5%	35.3%	14.1%
5	90	90	5,797	2.89	19	4,734	1,142	2.66	1.8	13	35.4%	18.3%	31.6%	7.8%
6	100	50	6,236	2.83	21	5,067	765	2.41	1.9	17	21.0%	18.7%	19.0%	15.0%
7	100	75	6,236	2.83	21	4,956	1,122	2.41	1.9	15	30.4%	20.5%	28.6%	15.1%
8	100	100	6,236	2.83	21	4,884	1,364	2.50	1.8	13	39.8%	21.7%	38.1%	11.9%
9	100	150	6,236	2.83	21	4,746	1,560	2.45	1.8	12	45.1%	23.9%	42.9%	13.6%
10	100	200	6,236	2.83	21	4,579	1,767	2.47	1.7	11	50.8%	26.6%	47.6%	12.7%
Average	–	–	5,417	2.91	18.3	4,187	1,095	2.52	1.77	11.6	37.3	23.1%	37.4%	13.3%

acceptance rate from 21.0% to 50.8%. Consequently, total cost savings expand and profits rise, with the decrease in the average cost per parcel and the required fleet size for the LSP.

To further investigate the factors influencing the effectiveness of the hybrid delivery system incorporating PT-based CM transportation service, we conducted a sensitivity analysis on several key factors.

Time duration between two consecutive scheduled trips

We first assessing how varying the time intervals between consecutive scheduled trips, from 15 to 50 minutes, influences the system's performance. The results are depicted in Figure 5.5.

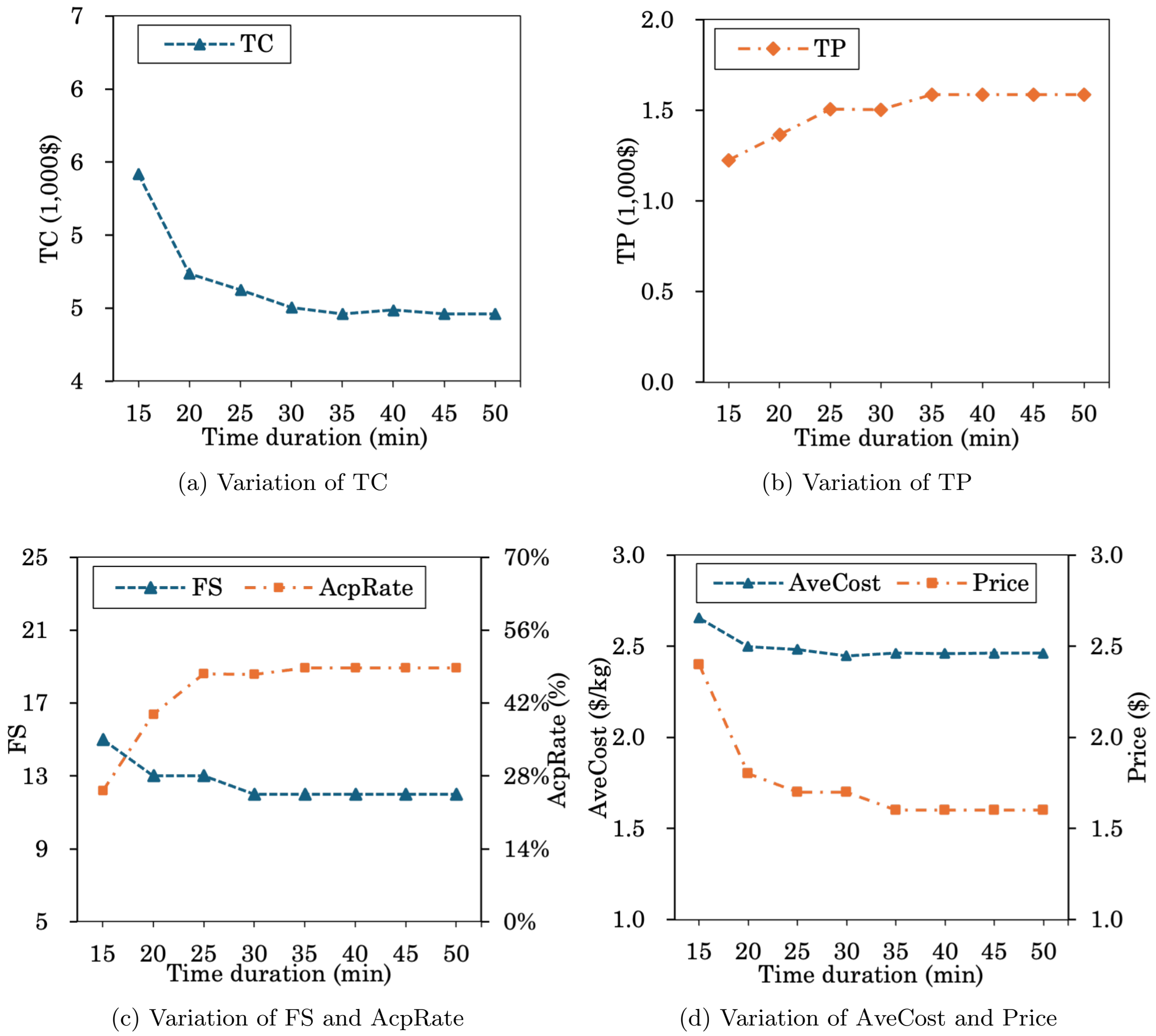

(a) Variation of TC

(b) Variation of TP

(c) Variation of FS and AcpRate

(d) Variation of AveCost and Price

Figure 5.5. Variations of TC, TP, AveCost, Price, FS, and AcpRate under time duration

Figure 5.5 illustrates that extending the interval between consecutive bus trips results in a gradual reduction in total costs, decreasing from \$5,701 to \$4,551, and stabilizing after 35 minutes, as depicted in Figure 5.5(a). Similarly, the total profit for the PTO also increases until it plateaus beyond 35 minutes, as shown in Figure 5.5(b). On the one hand, as time duration increases, an increasing number of parcel requests are accommodated by PT-based CM transportation services, as indicated by the rising acceptance rate in Figure 5.5(c). Given that the average cost of CM transportation is lower than that of dedicated delivery vehicles, the total cost diminishes as the interval extends. On the other hand, there is a reduction in the number of high-fixed-cost dedicated vehicles used, and the average cost of dedicated delivery decreases from \$2.65/kg to \$2.46/kg, as illustrated in Figure 5.5(d). For the PTO, a longer time duration between consecutive bus trips allows for greater utilization of buses for parcel services, potentially generating additional profits up to \$1,586. However, despite the ability to use buses for parcel delivery without disrupting the fixed timetable, the unfavorable cost-effectiveness limits the use of additional buses for delivery, as service costs increase with distance traveled.

Carrying capacity of each bus

We assess how varying the carrying capacity of buses, from 20 kg to 60 kg, influences the system's performance. The results are depicted in Figure 5.6.

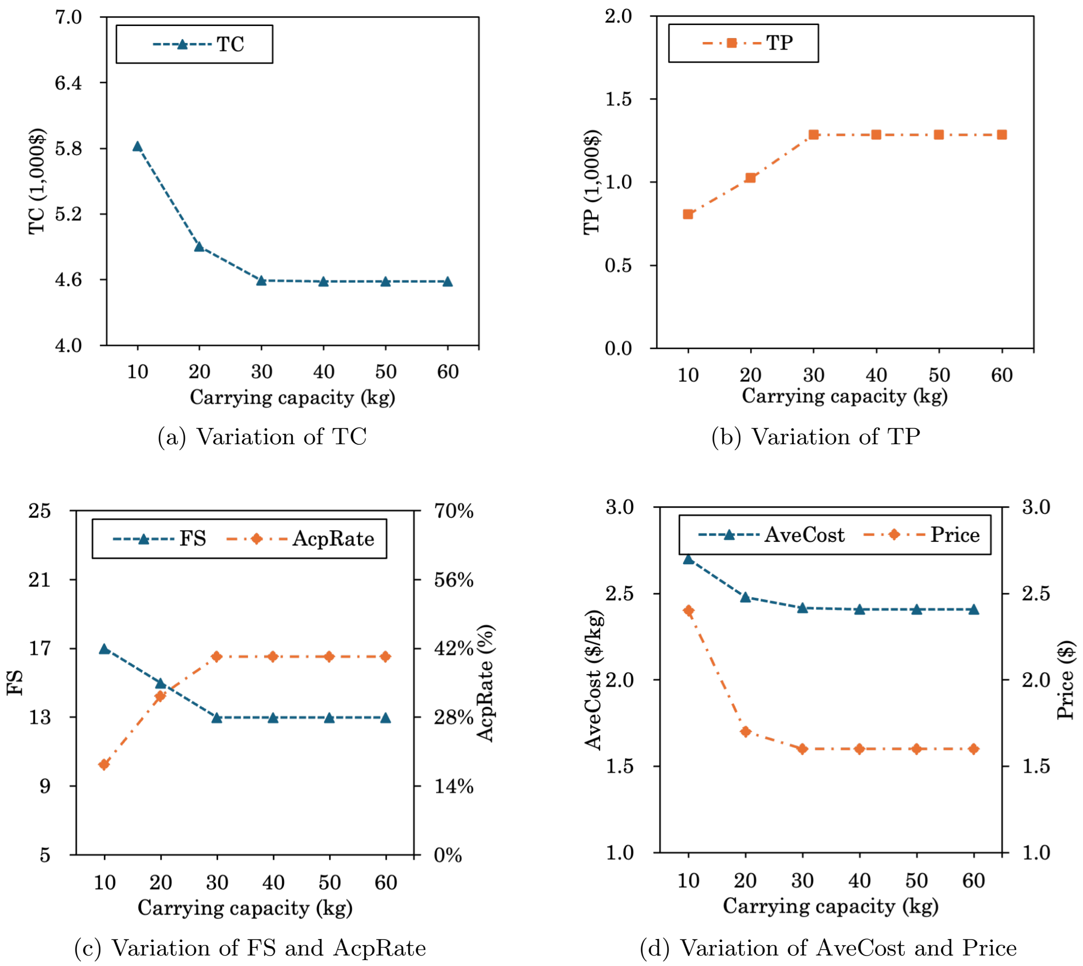

Figure 5.6. Variations of TC, TP, AveCost, Price, FS, and AcpRate under different bus capacities

It can be seen that as the carrying capacity of each bus increases, the total cost for the LSP gradually decreases and stabilizes beyond a capacity of 30 kg, as illustrated in Figure 5.6(a). Concurrently, the total profit for the PTO gradually increases, reaching a plateau beyond the same capacity threshold, as shown in Figure 5.6(b). This trend is attributed to the fact that increased carrying capacity allows each bus to accommodate more parcels, enhancing the efficiency of CM transportation services and reducing reliance on dedicated delivery vehicles, as indicated by the rising acceptance rate and decreasing fleet size in Figure 5.6(c). Additionally, the average cost associated with public transport-based CM transportation is lower than that of dedicated delivery services, resulting in cost reductions for the LSP, as depicted in Figure 5.6(d). For the PTO, higher bus carrying capacity facilitates additional parcel services, thereby generating increased profits. However, due to scheduling constraints, revenue from bus-based parcel services reaches a maximum and does not continue to rise. The sensitivity analysis suggests that the LSP should conduct a thorough market survey and engage in communication with the PTO to determine the available time and carrying capacity of buses to make mutually beneficial collaboration decisions.

5.5 Concluding Remarks

This chapter introduces a new PT-based CM transportation service and examines the CSP problem taking into account the Stackelberg gameplay between LSP and PTO during the formulation of their business cooperation. A bilevel path-based programming model is formulated for the CSP problem, consisting of a lower-level model [BTS] that maximizes the PTO's total profits from additional parcel deliveries, and an upper-level model [VRP-P] that minimizes the LSP's total cost, including outsourcing expenses paid to the PTO and costs associated with dedicated delivery vehicles. To solve the CSP problem, a tailored ITH method is proposed, which combines two TS algorithms with granular strategy and an ABC algorithm. The ITH method iteratively solves the lower-level BTS problem, the upper-level reduced VRP-P problem, and updates the service price in three stages. Numerical experiments conducted on randomly generated instances demonstrate the effectiveness of the proposed ITH method in finding good-quality solutions within reasonable computation times. Simulated case studies conducted in Chongqing, China demonstrate the mutual benefits of the LSP and PTO by introducing the CM transportation cooperation with a well-designed service price. Specifically, the LSP experiences reductions in total cost, fleet size of dedicated vehicles, and average cost per parcel delivered, while the PTO obtains profits by serving additional parcel delivery requests. Sensitivity analysis highlights the significant impact of carrying capacity and available time duration between consecutive scheduled trips on the availability of the PT-based CM transportation service.

5.6 Appendix: Notations

Set	
$\mathcal{V}$	Set of dedicated vehicles $v \in \mathcal{V}$
$\mathcal{H}$	Set of RDS and also the set of parcel requests, $h \in \mathcal{H}$
$\tilde{\mathcal{H}}(p)$	Set of RDSs whose parcel delivery requests are not fully satisfied under the given service price p
$\mathcal{B}$	Set of buses, $b \in \mathcal{B}$
$\mathcal{L}^b$	Set of scheduled trips served by bus $b \in \mathcal{B}$, $l \in \mathcal{L}^b = \{1, 2, \cdots, \|\mathcal{L}^b\|\}$, where $\|\mathcal{L}^b\|\}$ denotes the last trip that bus b serves
$\mathcal{L}$	Set of all scheduled bus trips, $\mathcal{L} := \bigcup_{b\in\mathcal{B}} \mathcal{L}^b$
$\mathcal{R}^h$	Set of all feasible trip chains serving RDS $r_h \in \mathcal{R}^h$
$\mathcal{R}$	Set of all feasible trip chains, $\mathcal{R} := \bigcup_{h\in\mathcal{H}} \mathcal{R}^h$
$\mathbf{\Omega}$	Set of all feasible dedicated vehicle routes, $\omega \in \mathbf{\Omega}$
Parameters	
Q_v	Maximum carrying capacity of the dedicated vehicle v
Q_l^b	Parcel carrying capacity of the bus b in the l-th trip, $b \in \mathcal{B}$, $l \in \mathcal{L}$
Q_{r_h}	Capacity of the bus trip chain r_h that can accommodate parcels
σ_h	Service duration of the parcel delivery request $h \in \mathcal{H}$
δ	Service time for loading or unloading parcels by the bus
σ	Service duration of the parcel delivery request $h \in \mathcal{H}$
q_h	Parcel load of the parcel delivery request $h \in \mathcal{H}$
$\tilde{q}_h(p)$	Remaining load of parcels of the request $h \in \mathcal{H}$ under price p
$[E_h, L_h]$	Opening time window of the RDS $h \in \mathcal{H}$
$[E_0, L_0]$	Opening time window of the CDC
$s_{b,l}^{\mathrm{o}}$	Origin terminal of the bus b's l-th trip
$s_{b,l}^{\mathrm{d}}$	Destination terminal of the bus b's l-th trip
$t_{b,l}^{\mathrm{o}}$	Departure time of bus b from the origin terminal
$t_{b,l}^{\mathrm{d}}$	Arrival time of bus b at the destination terminal
r_h	Bus trip chain that serves the RDS h, which includes the CDC 0, a series of bus scheduled trips $l \in \mathcal{L}$, and an RDS $h \in \mathcal{H}$
$\tau(i, j)$	Travel time by the bus from location i to j
C_{0,l_1}	Pickup cost incurred for the pickup operation by the bus
$C_{l_i,l_{i+1}}$	Cost of the relay operation between consecutive bus scheduled trips l_i and l_{i+1}
$C_{l_{n_r},h}$	Delivery cost incurred for delivery operation by the bus

c_{r_h}	Operating cost paid by PTO for scheduling bus trip chain r_h to serve the parcels
ω	Dedicated vehicle service route starting from CDC and ending at CDC
C^{f}	Fixed cost of using each dedicated vehicle
c_ω	Cost of a dedicated vehicle service route ω
$\phi(i,j)$	Travel time by the dedicated vehicle from location i to j
κ_{ij}	Transportation cost by the dedicated vehicle from location i to j
$\vartheta^l_{r_h}$	Incidence coefficient that equals 1 if bus scheduled trip $l \in \mathcal{L}$ is utilized in the bus trip chain $r_h \in \mathcal{R}^h$, and 0 otherwise
a^ω_h	Incidence coefficient that equals 1 if RDS $h \in \tilde{\mathcal{H}}(p)$ is served by route $\omega \in \mathbf{\Omega}$, and 0 otherwise
$\underline{p}$	Lower bound of the service price for delivering per parcel load
$\overline{p}$	Upper bound of the service price for delivering per parcel load
Variables	
p	Continuous variable to denote the service price provided by LSP for serving per load of parcel
x_{r_h}	Binary variable that equals 1 if bus trip chain $r_h \in \mathcal{R}^h$ is used for parcel deliveries, and 0 otherwise
y_ω	Binary variable that equals 1 if route ω is utilized for parcel delivery service, and 0 otherwise
z_{r_h}	Continuous variable that denotes the load of parcels served by the bus trip chain $r_h \in \mathcal{R}^h$
ξ_i	Time epoch that the dedicate vehicle start service at the location i

Chapter 6 Service Price Optimization for On-Demand Mobility Service-based Co-Modal Delivery Service

This chapter investigates an outsourcing service price (OSP) problem for the co-modal delivery service based on on-demand mobility services (COM) model considering the gameplay between parcel delivery service provider (PSP) and on-demand mobility service provider (OMP). We formulate the OSP problem in a bilevel framework based on the interaction of PSP and OMP. A lower-level co-modal delivery service problem with ridesharing (CSP-R) is formulated to determine the OMP's optimal decision, i.e., served parcel and passenger requests and corresponding service routes, for maximizing the OMP's total profit from the served requests under the outsourcing service price offered by PSP. An upper-level multi-depot pickup and delivery problem with pricing (MPDP-P) is formulated to determine the optimal outsourcing service price and self-operating service routes for minimizing the PSP's total cost, which consists of the outsourcing cost paid to the OMP and the cost of the self-operating service. A customized iterative hybrid (IH) algorithm based on the bilevel framework integrating two granular tabu search (GTS) algorithms and a genetic algorithm (GA) is developed to solve the problem. Particularly, we propose a profit-oriented and cost-oriented granularity to solve the lower-level CSP-R and upper-level reduced MPDP-P, respectively, to improve the computational efficiency of the tabu search algorithm. Numerical experiments on several randomly generated instances and a simulated case are conducted to test our proposed solution methods and the COM model.

The rest of this chapter is structured as follows. Assumptions, notations, and problem description are elaborated in Section 6.1. A bilevel arc-based programming model for the studied problems are developed in Section 6.2. To solve the problem, an IH algorithm is developed in Section 6.3. Numerical experiments on randomly generated instances and a simulated case in Hong Kong, China are conducted in Section 6.4. Conclusions of this chapter are summarized in Section 6.5. Notation used in this chapter is listed in Section 6.6 for readability.

6.1 Problem Statement

We consider a PSP who provides daily parcel delivery services using a fleet of self-operating vans in set $\mathcal{K}$ within an urban area, where several depots in set $\mathcal{H}$ are spatially distributed in the area for van parking. The PSP receives a bunch of parcel delivery requests. Each delivery request is associated with a pick-up location and corresponding time window and service duration for loading, a drop-off location and corresponding time window and service duration for unloading, and parcel load. Each van is initially parked at a designated depot. Subsequently, the van is dispatched to serve a series of parcel requests during the operational period. During the off-operational hours, the van returns to a depot; however, it does not dwell there while fulfilling the requests. In the same urban area, we consider an OMP who provides passenger transportation services using a fleet of on-demand mobility vehicles in set $\mathcal{V}$, where several stations in set $\mathcal{S}$ are scattered in the area for parking these vehicles. The OMP receives a set of passenger ride requests. Each ride request is associated with an origin, a destination, pick-up time window at the origin, drop-off time window at the destination, and number of passengers. Each on-demand mobility vehicle initially departs from a station at the beginning of the operational period, is then free-floating throughout the city to serve requests without returning to a station, and finally arrive at a station at the end of the operational period (i.e., off-operation hours).

Let $\boldsymbol{\Omega}^{f,o}$ and $\boldsymbol{\Omega}^{f,d}$ denote the sets of pick-up locations and drop-off locations of parcel delivery requests, respectively, and $\boldsymbol{\Omega}^{p,o}$ and $\boldsymbol{\Omega}^{p,d}$ denote the sets of origins and destinations of passenger ride requests, respectively. For ease of presentation, let m and n denote the number of parcel requests and passenger requests, respectively. We arrange the index of locations following the sequence of $\boldsymbol{\Omega}^{f,o} = \{1, 2, \cdots, m\}, \boldsymbol{\Omega}^{p,o} = \{m+1, m+2, \cdots, \sigma\}$, $\boldsymbol{\Omega}^{f,d} = \{\sigma+1, \sigma+2, \cdots, \sigma+m\}$, and $\boldsymbol{\Omega}^{p,d} = \{\sigma+m+1, \sigma+m+2, \cdots, 2\sigma\}$, where $\sigma = m+n$. We define $\boldsymbol{\Omega} := \boldsymbol{\Omega}^{f,o} \cup \boldsymbol{\Omega}^{p,o} \cup \boldsymbol{\Omega}^{f,d} \cup \boldsymbol{\Omega}^{p,d}$. The drop-off location/destination of the parcel/passenger with pick-up location/origin $i \in \boldsymbol{\Omega}^{f,o} \cup \boldsymbol{\Omega}^{p,o}$ can thus be represented by $i + \sigma$. For simplicity, we use the index of pick-up location/origin of a parcel/passenger request to represent corresponding parcel/passenger request. Kindly note that the pick-up and drop-off locations of different parcel/passenger requests may be geographically identical, even if they have different indices. Furthermore, let $[e_i, l_i]$ denote the pick-up time window of request $i \in \boldsymbol{\Omega}^{f,o} \cup \boldsymbol{\Omega}^{p,o}$, where e_i and l_i indicate the earliest and latest pick-up time, respectively. Correspondingly, the drop-off time window of parcel/passenger request $i \in \boldsymbol{\Omega}^{f,o} \cup \boldsymbol{\Omega}^{p,o}$ is denoted by $[e_{i+\sigma}, l_{i+\sigma}]$. The load of parcel request $i \in \boldsymbol{\Omega}^{f,o}$ and number of passengers of passenger request $i \in \boldsymbol{\Omega}^{p,o}$ are denoted by q_i^f and q_i^p, respectively. The service durations for loading and unloading parcels for parcel request $i \in \boldsymbol{\Omega}^{f,o}$ are denoted by d_i and $d_{i+\sigma}$, respectively.

To fulfill the parcel delivery requests with the minimal cost, the PSP will collaborate with OMP by outsourcing parcel delivery tasks to OMP with a certain amount of monetary payment per unit parcel load denoted by u, which is referred to as outsourcing service price. Kindly note that the outsourcing service price in this chapter is defined as a load-based price. This is motivated by the real practice of typical logistic companies such as SF Express, the largest integrated logistics service provider in China, whose same-city express service in Hong Kong is charged by parcel load (SF Express, 2024). However, it is worth mentioning that the proposed modelling and algorithm framework in this chapter is applicable for any other service charging mechanisms such as the delivery distance-based pricing. With the outsourced parcel requests as well as the service price, the OMP will decide which delivery requests to serve together with its passenger ride request by a shared transportation mode, named OMS-based CM delivery service, using its on-demand mobility vehicles. Specifically, to form the collaboration between PSP and OMP, the PSP will first offer the parcel delivery requests and outsourcing service price to OMP. The OMP will then simultaneously consider these outsourced parcel requests as well as its passenger requests and determine the optimal served parcel and passenger requests to maximize its total profits. The unserved parcel requests as well as the corresponding outsourcing cost will be fed back to the PSP, and the PSP will finally satisfy the unserved parcel requests by its self-operating delivery service. We can see that the interaction and inter-dependency between PSP and OMP will result in a Stackelberg game, where the PSP serves as the leader aiming to propose an optimal outsourcing service price considering the OMP's optimal decision, and the OMP serves as the follower aiming to make its optimal decision, i.e., the parcel requests to serve, under the offered price. By collaborating with OMP, PSP fulfills parcel requests either by the CM delivery service from OMP or its own self-operating delivery service.

For OMP, each vehicle $v \in \mathcal{V}$, initially parked in a station $s \in \mathcal{S}$ with a parking capacity Q_s, can return to any station $s \in \mathcal{S}$ after the service. The maximum service time of vehicle $v \in \mathcal{V}$ is denoted by $\hat{W}_v$. Each vehicle $v \in \mathcal{V}$ can simultaneously serve multiple passenger and parcel requests subject to the passenger and parcel carrying capacities denoted by Q_v^p and Q_v^f, respectively. To ensure service quality for passengers, we consider the maximum ride duration $\hat{T}_i$ of passenger request $i \in \mathbf{\Omega}^{p,o}$. A limit $\xi_{\max}$ is also imposed on the total number of stops permitted for accommodating additional passenger or parcel pick-ups and drop-offs between origin and destination of each passenger. Moreover, the OMP will pay passenger monetary compensation c per unit detour duration. Let η denote the fixed operating cost of using each vehicle, R_i denote the revenue obtained by serving passenger request $i \in \mathbf{\Omega}^{p,o}$ and P_i be the penalty incurred if the passenger request is denied service. The travel time and cost by the on-demand mobility vehicle from location i to j are denoted by $t_{i,j}$ and $c_{i,j}$, respectively. The objective of OMP is to determine the optimal parcel and passenger requests to serve and corresponding service routes under the offered outsourcing service price such that (i) the service time window, maximum ride duration, and the maximum number of stops (if applicable) for the requests are satisfied; (ii) the station parking capacity, and vehicle capacity and maximum service time are respected; and (iii) the total profit is maximized.

As for the PSP, the unserved parcel requests will be satisfied by the self-operating fleet of vans in set $\mathcal{K}$. Each van $k \in \mathcal{K}$, initially parked in a depot $h \in \mathcal{H}$ with parking capacity Q_h, can return to any depot $h \in \mathcal{H}$ after the service. The fixed operating cost, parcel carrying capacity and the maximum service duration of van $k \in \mathcal{K}$ are denoted by ψ, Q_k, and $\hat{W}_k$, respectively. Let $\varphi_{i,j}$ and $\kappa_{i,j}$ represent the travel time and cost by the van from location i to j, respectively. The objective of PSP is to determine the outsourcing service price between a lower bound $\underline{u}$ and an upper bound $\bar{u}$, and the self-operating service routes such that (i) the service time window of the delivery requests is satisfied; (ii) the depot parking capacity, and van capacity and maximum service time are respected; and (iii) the total cost, including the outsourcing cost and self-operating cost, is minimized.

The OSP problem investigated in this chapter is to determine the optimal outsourcing service price as well as the self-operating service routes for PSP and the CM delivery service routes for OMP, considering the interaction between PSP and OMP. We can see that the studied OSP problem involves two different stakeholders, i.e., PSP and OMP, with conflicting objectives. For example, the PSP aims to find a low outsourcing price to reduce its total cost, while OMP expects a high outsourcing price to increase revenue. The interaction of the two players will result in a Stackelberg game, which should be modelled as a bilevel programming model.

6.2 Bilevel Arc-based Optimization Model Formulation

In this section, we formulate a bilevel optimization model for the OSP problem composed of the upper-level multi-depot pickup and delivery problem with pricing (MPDP-P) for PSP and lower-level CM delivery service problem with ridesharing (CSP-R) for OMP. Since the PSP will determine the optimal outsourcing service price considering the OMP's optimal decision under the offered price, in the next subsections, we will first present the lower-level CSP-R and then the upper-level MPDP-P. The notations used throughout this chapter are summarized in Section 6.6.

6.2.1 Lower-level CSP-R model

Given the outsourcing service price u and outsourcing parcel requests $\mathbf{\Omega}^{f,o}$, as well as the passenger requests $\mathbf{\Omega}^{p,o}$, a profit maximization model will be formulated to determine the optimal served requests and service routes that can maximize the OMP's total profit from serving parcel and passenger requests. We define CSP-R on a complete directed graph $\mathcal{G}_1 = (\mathcal{N}_1, \mathcal{A}_1)$, where $\mathcal{N}_1 = \mathbf{\Omega} \cup \mathcal{S}, \mathcal{A}_1 = \big(\mathcal{S} \times \big(\mathbf{\Omega}^{p,o} \cup \mathbf{\Omega}^{f,o}\big)\big) \cup (\mathbf{\Omega} \times \mathbf{\Omega}) \cup \big(\big(\mathbf{\Omega}^{p,d} \cup \mathbf{\Omega}^{f,d}\big) \times \mathcal{S}\big)$. Each node $i \in \mathcal{N}_1$ in the network is associated with a parcel load q_i^f, a passenger number q_i^p, a service time window $[e_i, l_i]$, a service duration d_i, a revenue R_i, and a penalty P_i, and each arc$(i,j) \in \mathcal{A}_1$ is associated with a travel time $t_{i,j}$ and travel cost $c_{i,j}$ by the on-demand mobility vehicle from node i to $j, \forall i, j \in \mathcal{N}_1$ with the following information:

- Parcel load and passenger number: $q_i^f = q_i^p = 0, \forall i \in \mathcal{S}; q_i^f = 0, \forall i \in \mathbf{\Omega}^{p,o}$; $q_i^p = 0, \forall i \in \mathbf{\Omega}^{f,o}; q_i^f = -q_{i+\sigma}^f, \forall i \in \mathbf{\Omega}^{f,o} \cup \mathbf{\Omega}^{p,o}; q_i^p = -q_{i+\sigma}^p, \forall i \in \mathbf{\Omega}^{p,o} \cup \mathbf{\Omega}^{f,o}$;

- Service duration: $d_i = 0, \forall i \in \mathcal{S} \cup \mathbf{\Omega}^{p,o} \cup \mathbf{\Omega}^{p,d}$;

- Revenue and penalty: $R_i = 0, \forall i \in \mathcal{N}_1 \backslash \mathbf{\Omega}^{p,o}$;

- Penalty: $P_i = 0, \forall i \in \mathcal{N}_1 \backslash \mathbf{\Omega}^{p,o}$.

In addition, we further define the following variables:

- z_i : Binary decision variable that equals 1 if request $i \in \mathbf{\Omega}^{p,o} \cup \mathbf{\Omega}^{f,o}$ is served, and 0 otherwise;

- $x_{i,j}^v$: Binary decision variable that equals 1 if vehicle $v \in \mathcal{V}$ travel directly from node i to j, $\forall i, j \in \mathcal{N}_1$, and 0 otherwise;

- τ_i^v : Continuous variable denoting the time epoch when vehicle v starts service at node $i \in \mathcal{N}_1$;

- r_i^v : Continuous variable denoting the total ride time of passenger $i \in \mathbf{\Omega}^{p,o}$ in vehicle $v \in \mathcal{V}$;

- α_i^v : Continuous variable denoting the number of passengers in vehicle $v \in \mathcal{V}$ after the service at node $i \in \mathcal{N}_1$;

- β_i^v : Continuous variable denoting the load of parcels in vehicle $v \in \mathcal{V}$ after the service at node $i \in \mathcal{N}_1$;

- ξ_i^v : Integer variable denoting the order of node $i \in \mathcal{N}_1$ in vehicle v 's service sequence, and $\xi_i^v \in \{1, 2, \cdots, 2(m+n+1)\}$

With the above notations, the lower-level model for CSP-R can be formulated as follows:

[CSP-R]

$$\begin{aligned}
\max_{\{\mathbf{z},\mathbf{x},\boldsymbol{\tau},\mathbf{r},\boldsymbol{\alpha},\boldsymbol{\beta},\boldsymbol{\xi}\}} TP = & \sum_{i \in \mathbf{\Omega}^{p,o}} R_i z_i + \sum_{i \in \mathbf{\Omega}^{f,o}} u q_i^f z_i \\
& - \sum_{v \in \mathcal{V}} \sum_{i \in \mathcal{S}} \sum_{j \in \mathbf{\Omega}^{p,o} \cup \mathbf{\Omega}^{f,o}} \eta x_{i,j}^v - \sum_{v \in \mathcal{V}} \sum_{i \in \mathcal{N}_1} \sum_{j \in \mathcal{N}_1} c_{i,j} x_{i,j}^v \\
& - \sum_{i \in \mathbf{\Omega}^{p,o}} P_i (1 - z_i) - \sum_{v \in \mathcal{V}} \sum_{i \in \mathbf{\Omega}^{p,o}} c \left(r_i^v - t_{i,i+\sigma} \right) z_i
\end{aligned} \tag{6.1}$$

subject to

$$\sum_{s\in\mathcal{S}}\sum_{i\in\mathbf{\Omega}^{p,o}\cup\mathbf{\Omega}^{f,o}\cup\mathcal{S}} x^v_{s,i} = \sum_{s\in\mathcal{S}}\sum_{i\in\mathbf{\Omega}^{p,o}\cup\mathbf{\Omega}^{f,o}\cup\mathcal{S}} x^v_{j,s} = 1, \qquad \forall v\in\mathcal{V} \tag{6.2}$$

$$\sum_{j\in\mathcal{N}_1} x^v_{j,i} = \sum_{j\in\mathcal{N}_1} x^v_{i,j}, \qquad \forall i\in\mathbf{\Omega}, v\in\mathcal{V} \tag{6.3}$$

$$z_i = \sum_{v\in\mathcal{V}}\sum_{j\in\mathcal{N}_1} x^v_{i,j} \le 1, \qquad \forall i\in\mathbf{\Omega}^{p,o}\cup\mathbf{\Omega}^{f,o} \tag{6.4}$$

$$\sum_{j\in\mathcal{N}_1} x^v_{i,j} = \sum_{j\in\mathcal{N}_1} x^v_{i+\sigma,j}, \qquad \forall i\in\mathbf{\Omega}^{p,o}\cup\mathbf{\Omega}^{f,o}, v\in\mathcal{V} \tag{6.5}$$

$$(\tau^v_i + d_i + t_{i,j})\, x^v_{i,j} \le \tau^v_j, \qquad \forall i,j\in\mathcal{N}_1, v\in\mathcal{V} \tag{6.6}$$

$$\tau^v_i \le \tau^v_{i+\sigma}, \qquad \forall i\in\mathbf{\Omega}^{p,o}\cup\mathbf{\Omega}^{f,o}, v\in\mathcal{V} \tag{6.7}$$

$$e_i \le \tau^v_i \le l_i, \qquad \forall i\in\mathcal{N}_1, v\in\mathcal{V} \tag{6.8}$$

$$r^v_i = \tau^v_{i+\sigma} - \tau^v_i, \qquad \forall i\in\mathbf{\Omega}^{p,o}, v\in\mathcal{V} \tag{6.9}$$

$$t_{i,i+\sigma} \le r^v_i \le \hat{T}_i, \qquad \forall i\in\mathbf{\Omega}^{p,o}, v\in\mathcal{V} \tag{6.10}$$

$$\sum_{i\in\mathcal{N}_1}\sum_{j\in\mathcal{N}_1} (t_{i,j} + d_i)\, x^v_{i,j} \le \hat{W}_v, \qquad \forall v\in\mathcal{V} \tag{6.11}$$

$$\left(\alpha^v_i + q^p_j\right) x^v_{i,j} \le \alpha^v_j, \qquad \forall i,j\in\mathcal{N}_1, v\in\mathcal{V} \tag{6.12}$$

$$\left(\beta^v_i + q^f_j\right) x^v_{i,j} \le \beta^v_j, \qquad \forall i,j\in\mathcal{N}_1, v\in\mathcal{V} \tag{6.13}$$

$$\max\{0, q^p_i\} \le \alpha^v_i \le \min\{Q^p_v, Q^p_v + q^p_i\}, \qquad \forall i\in\mathcal{N}_1, v\in\mathcal{V} \tag{6.14}$$

$$\max\left\{0, q^f_i\right\} \le \beta^v_i \le \min\left\{Q^f_v, Q^f_v + q^f_i\right\}, \qquad \forall i\in\mathcal{N}_1, v\in\mathcal{V} \tag{6.15}$$

$$\sum_{v\in\mathcal{V}}\sum_{i\in\mathbf{\Omega}^{p,d}\cup\mathbf{\Omega}^{f,d}\cup\mathcal{S}} x^v_{s,i} \le Q_s, \qquad \forall s\in\mathcal{S} \tag{6.16}$$

$$\sum_{v\in\mathcal{V}}\sum_{j\in\mathbf{\Omega}^{p,d}\cup\mathbf{\Omega}^{f,d}\cup\mathcal{S}} x^v_{j,s} \le Q_s, \qquad \forall s\in\mathcal{S} \tag{6.17}$$

$$\xi^v_i + 1 - M\left(1 - x^v_{i,j}\right) \le \xi^v_j, \qquad \forall i,j\in\mathcal{N}_1, v\in\mathcal{V} \tag{6.18}$$

$$\xi^v_i + 1 + M\left(1 - x^v_{i,j}\right) \ge \xi^v_j, \qquad \forall i,j\in\mathcal{N}_1, v\in\mathcal{V} \tag{6.19}$$

$$\xi^v_{i+\sigma} - \xi^v_i - 1 \le \xi_{\max}, \qquad \forall i\in\mathbf{\Omega}^{p,o}, v\in\mathcal{V} \tag{6.20}$$

$$x^v_{i,j} \in \{0,1\}, \qquad \forall i,j\in\mathcal{N}_1, v\in\mathcal{V} \tag{6.21}$$

$$z_i \in \{0,1\}, \qquad \forall i \in \boldsymbol{\Omega}^{p,o} \cup \boldsymbol{\Omega}^{f,o} \tag{6.22}$$

$$\tau_i^v, r_i^v, \alpha_i^v, \beta_i^v \geq 0, \qquad \forall i \in \mathcal{N}_1, v \in \mathcal{V} \tag{6.23}$$

$$\xi_i^v \in \{1, 2, \cdots, 2(m+n)\}, \qquad \forall i \in \mathcal{N}_1, v \in \mathcal{V} \tag{6.24}$$

The objective function in Eq. (6.1) is to maximize the OMP's total profit, which is the difference between the revenues from requests and the total cost, including the fixed operating cost, transportation cost, penalty for the unmet passenger requests, and compensation cost for passengers. Constraints (6.2) and (6.3) are the flow balance constraints, where constraint (6.1) specifies that each vehicle departs from a station and finally travels back to any station, while constraint (6.3) expresses the flow balance constraint at any node except the origin and destination of vehicles. Constraint (6.4) ensures that each parcel delivery request or passenger ride request can be served at most once. Constraint (6.5) guarantees that the pick-up and drop-off operations for each parcel or passenger request should be served by the same vehicle. Constraint (6.6) updates the time epoch of starting service for each request along the route of a vehicle. Constraint (6.7) stipulates the sequence order of the pickup and delivery operation for each request. Constraint (6.8) enforces the service time window for serving requests. Constraint (6.9) calculates the actual ride duration of each served passenger. Constraint (6.10) enforces the maximum ride time that the passenger can tolerate. Constraint (6.11) limits the maximum service time of each vehicle. Constraints (6.12) and (6.13) update the number of on-board passengers and the load of in-vehicle parcels, respectively. The capacities for carrying passengers and parcels are limited by constraints (6.14) and (6.15). Constraints (6.16) and (6.17) enforce the capacity constraint of the parking station. Constraint (6.16) specifies that the total number of vehicles initially scheduled from the station should not surpass the maximum parking capacity, while constraint (6.17) ensures that the number of vehicles ultimately parked at the station does not exceed its capacity. Constraints (6.18) and (6.19) calculate the travel sequences of the requests, where M can be set as $2(m+n+1)$. Constraint (6.20) stipulates the maximum number of stops between the origin and destination of a passenger request. Constraints (6.21)–(6.24) define the domains of the variables.

6.2.2 Upper-level MPDP-P model

Given the optimal decision of OMP, we can obtain the unserved parcel requests under the outsourcing service price. A cost minimization model will be then formulated to determine the optimal outsourcing service price and self-operating service routes for serving those unserved parcel requests to minimize the PSP's total cost. Let $\boldsymbol{\Omega}_{rej}^{f,o^*}(u)$ and $\boldsymbol{\Omega}_{rej}^{f,d^*}(u)$ denote sets of pick-up locations and drop-off locations of unserved parcel requests, respectively. We define MPDP-P on a complete directed graph $\mathcal{G}_2 = (\mathcal{N}_2, \mathcal{A}_2)$, where $\mathcal{N}_2 = \mathbf{\Omega}_{rej}^{f,o^*}(u) \cup \mathbf{\Omega}_{rej}^{f,d^*}(u) \cup \mathcal{H}$, $\mathcal{A}_2 = \left(\mathcal{H} \times \mathbf{\Omega}_{rej}^{f,o^*}(u)\right) \cup \left(\left(\mathbf{\Omega}_{rej}^{f,o^*}(u) \cup \mathbf{\Omega}_{rej}^{f,d^*}(u)\right) \times \left(\mathbf{\Omega}_{rej}^{f,o^*}(u) \cup \mathbf{\Omega}_{rej}^{f,d^*}(u)\right) \cup \left(\mathbf{\Omega}_{rej}^{f,d^*}(u) \times \mathcal{H}\right)$. Each node $i \in \mathcal{N}_2$ in the network is associated with a parcel load q_i^f, a service time window $[e_i, l_i]$, a service duration d_i, and each arc $(i,j) \in \mathcal{A}_2$ is associated with a travel time $\varphi_{i,j}$ and travel cost $\kappa_{i,j}$ by the van from node i to $j, \forall i, j \in \mathcal{N}_2$ with the following information: parcel load $q_i^f = 0, \forall i \in \mathcal{H}$ and $q_i^f = -q_{i+\sigma}^f, \forall i \in \mathbf{\Omega}_{rej}^{f,o^*}(u)$, and service duration: $d_i = 0, \forall i \in \mathcal{H}$. In addition, we define the following variables:

- $y_{i,j}^k$: Binary decision variable that equals 1 if van $k \in \mathcal{K}$ travels directly from node i to $j, \forall i, j \in \mathcal{N}_2$, and 0 otherwise;
- τ_i^k : Continuous variable denoting the time epoch when van $k \in \mathcal{K}$ starts the service at node $i \in \mathcal{N}_2$;
- β_i^k : Continuous variable denoting the load of parcels in van $k \in \mathcal{K}$ after the service at node $i \in \mathcal{N}_2$.

With the above notations, the [MPDP-P] model can be formulated as follows:

[MPDP-P]

$$\min_{\{\mathbf{u},\mathbf{y},\boldsymbol{\tau},\boldsymbol{\beta}\}} TC = \sum_{k\in\mathcal{K}}\sum_{i\in\mathcal{H}}\sum_{j\in\mathbf{\Omega}_{rej}^{p,o*}(u)} \psi y_{i,j}^k + \sum_{k\in\mathcal{K}}\sum_{i\in\mathcal{N}_2}\sum_{j\in\mathcal{N}_2} \kappa_{i,j} y_{i,j}^k + \sum_{i\in\mathbf{\Omega}^{f,o}\setminus\mathbf{\Omega}_{rej}^{f,o*}(u)} u q_i^f \tag{6.25}$$

subject to

$$\sum_{h\in\mathcal{H}}\sum_{i\in\mathbf{\Omega}_{rej}^{f,o*}(u)\cup\mathcal{H}} y_{h,i}^k = \sum_{h\in\mathcal{H}}\sum_{j\in\mathbf{\Omega}_{rej}^{f,d*}(u)\cup\mathcal{H}} y_{j,h}^k = 1, \qquad \forall k \in \mathcal{K} \tag{6.26}$$

$$\sum_{j\in\mathcal{N}_2} y_{j,i}^k = \sum_{j\in\mathcal{N}_2} y_{i,j}^k, \qquad \forall i \in \mathbf{\Omega}_{rej}^{f,o^*}(u) \cup \mathbf{\Omega}_{rej}^{f,d^*}(u), k \in \mathcal{K} \tag{6.27}$$

$$\sum_{k\in\mathcal{K}}\sum_{j\in\mathcal{N}_2} y_{i,j}^k = 1, \qquad \forall i \in \mathbf{\Omega}_{rej}^{f,o^*}(u) \tag{6.28}$$

$$\sum_{j\in\mathcal{N}_2} y_{i,j}^k = \sum_{j\in N_2} y_{i+\sigma,j}^k, \qquad \forall i \in \mathbf{\Omega}_{rej}^{f,o^*}(u), k \in \mathcal{K} \tag{6.29}$$

$$\left(\tau_i^k + d_i + \varphi_{i,j}\right) y_{i,j}^k \le \tau_j^k, \qquad \forall i, j \in \mathcal{N}_2, k \in \mathcal{K} \tag{6.30}$$

$$\tau_i^k \le \tau_{i+\sigma}^k, \qquad \forall i \in \mathbf{\Omega}_{rej}^{f,o^*}(u), k \in \mathcal{K} \tag{6.31}$$

$$e_i \le \tau_i^k \le l_i, \qquad \forall i \in \mathcal{N}_2, k \in \mathcal{K} \tag{6.32}$$

$$\sum_{j\in\mathcal{N}_2}\sum_{i\in\mathcal{N}_2}(\varphi_{i,j}+d_i)\,y_{i,j}^k \le \hat{W}_k, \qquad \forall k\in\mathcal{K} \tag{6.33}$$

$$\left(\beta_i^k + q_j^f\right) y_{i,j}^k \le \beta_j^k, \qquad \forall i,j\in\mathcal{N}_2, k\in\mathcal{K} \tag{6.34}$$

$$\max\left\{0, q_i^f\right\} \le \beta_i^k \le \min\left\{Q_k, Q_k + q_i^f\right\}, \qquad \forall i\in\mathcal{N}_2, k\in\mathcal{K} \tag{6.35}$$

$$\sum_{k\in\mathcal{K}}\sum_{j\in\mathbf{\Omega}_{rej}^{f,o*}(u)\cup\mathcal{H}} y_{h,j}^k \le Q_h, \qquad \forall h\in\mathcal{H} \tag{6.36}$$

$$\sum_{k\in\mathcal{K}}\sum_{i\in\mathbf{\Omega}_{rej}^{f,d*}(u)\cup\mathcal{H}} y_{i,h}^k \le Q_h, \qquad \forall h\in\mathcal{H} \tag{6.37}$$

$$\underline{u} \le u \le \bar{u} \tag{6.38}$$

$$y_{i,j}^k \in \{0,1\}, \qquad \forall i,j\in\mathcal{N}_2, k\in\mathcal{K} \tag{6.39}$$

$$\tau_i^k, \beta_i^k \ge 0, \qquad \forall i\in\mathcal{N}_2, k\in\mathcal{K} \tag{6.40}$$

The objective function in Eq. (6.25) is to minimize the PSP's total cost, including the fixed operating cost of vans, the transportation cost, and the outsourcing cost paid to the OMP, which depends on the results from lower-level problem. Constraints (6.26) and (6.27) are the flow balance constraints, where constraint (6.26) specifies that each van departs from a depot and finally travels back to any depot after completing the delivery tasks, while constraint (6.27) ensures the flow balance at any intermediate node. Constraints (6.28) and (6.29) ensure that each parcel delivery request should be served exactly once by a single van. Kindly note that the vehicle may revisit the geographically same location for more than once by visiting the different indices of locations but with geographically same location. Constraint (6.30) updates the time epoch of starting service for each parcel request along the route of a van. Constraint (6.31) ensures a sequence order of the pickup and delivery operation for each parcel delivery request. Constraints (6.32) and (6.33) enforce the service time window for serving requests and the maximum service time for each van, respectively. Constraint (6.34) updates the load of the van. The capacity of the van is limited by constraint (6.35). Constraints (6.36) and (6.37) specify the depot capacity. Kindly note that each van can arrive at any depot (including any other depots and the depot it departs from) unless the parking capacity is not exceeded. Constraint (6.38) restricts the upper and lower bounds of the outsourcing service price specified by the PSP. Constraints (6.39)–(6.40) define the domains of the decision variables.

6.3 IH Solution Method

The OSP problem is a bilevel optimization problem with the lower-level CSP-R nested in the upper-level MPDP-P. The upper-level MPDP-P is an extension of the multi-depot vehicle routing problem, whereas the lower-level CSP-R is a variant of the dial-a-ride problem. Both problems have been proven to be NP-hard (Kirchler and Calvo, 2013; Renaud et al., 1996). The complexity of the OSP problem makes it unable to be solved by commercial solvers. We can see from the bilevel framework of the OSP problem that once the outsourcing service price is confirmed, the upper-level problem will reduce to an MPDP, which is to determine the self-operating service routes of PSP to fulfill the unserved parcel requests obtained by solving the lower-level CSP-R under the aforementioned price. Motivated by this, we propose a customized IH algorithm to obtain good-quality solutions for OSP problem by iteratively solving CSP-R, reduced MPDP-P, and updating the outsourcing service price. Specifically, we first propose a profit-oriented granular tabu search algorithm (TS-P) to solve the lower-level CSP-R to obtain the unserved parcel requests under an initialized price. We will then use a cost-oriented granular tabu search algorithm (TS-C) to solve the reduced MPDP-P under the aforementioned price. A genetic algorithm (GA) is employed to update the outsourcing service price based on the performance of previous prices. The above procedure will iterate until the maximum number of generations is reached. The service price and corresponding service routes of PSP and OMP will be finally obtained. The overall framework of the IH algorithm is illustrated in Figure 6.1.

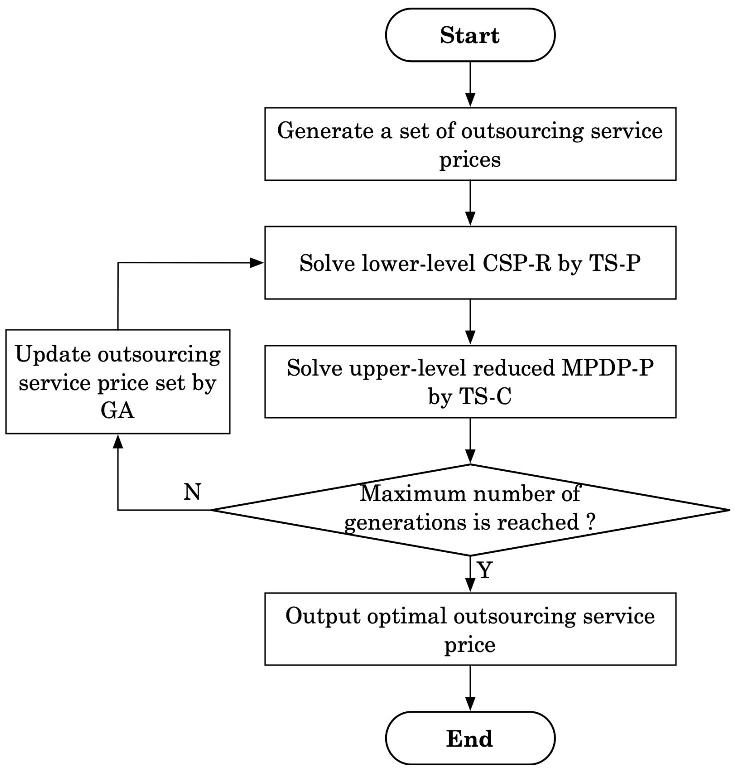

Figure 6.1. Overall framework of the IH algorithm

It can be seen that the IH algorithm combines two granular tabu search algorithms (GTSs) and a GA. The GTS has been proven effective in solving pickup and delivery problems, dial-a-ride problems, and related variants (Kirchler and Calvo, 2013; Goeke, 2019). GA is a population-based metaheuristic algorithm that can generate multiple new individuals, e.g., outsourcing service prices in the OSP problem, by simulating biological genetic operations and retaining excellent individuals by fitness values, e.g., the total cost of PSP in the OSP problem (Mirjalili, 2019). To enhance the likelihood of finding the optimal solution, we have considered two aspects for the GA and GTS: firstly, we have developed a customized binary-coded GA that aligns with the practical scenario, reducing computational complexity and eliminating the need to explore unnecessary price values. The GA enables rapid convergence towards good-quality outsourcing price with lower total cost of PSP by employing a series of genetic operations such as crossover, mutation with random perturbations, fitness value comparison, and selection with elite retention strategies. Additionally, we have proposed two customized GTSs, considering objective-oriented granularity strategies tailored to the characteristics of the upper- and lower-level problems. The strategy can improve computational efficiency at each iteration by reducing unnecessary exploration of low-quality neighborhood solutions. By combining GTSs and GA, we can identify the good-quality outsourcing service price that minimizes the total cost of PSP while considering the interaction between PSP and OMP. In the following subsections, we will describe the GA and the GTSs in detail.

6.3.1 Price initialization and updating by GA

In the proposed IH algorithm, a set of feasible outsourcing service prices falling in interval $[\underline{u}, \bar{u}]$ needs to be generated and updated. In practice, we know that services are often charged by a number with a certain level of precision, such as \$1.0 or \$1.5 per unit parcel load with a precision of 0.1. This is for the ease of price calculation in real cases. Therefore, we employ GA with a binary encoding approach to achieve the goal. The binary encoding approach allows us to represent the price using binary numbers, where the number of bits in the binary representation reflects the desired precision. Specifically, let binary number $[A_{1-1}A_{1-2}\cdots A_i \cdots A_1A_0]_2$ represent a price value, where l is the total bits of the binary number and $A_i = \{0, 1\}, \forall i = \{0, 1, \cdots l-1\}$. The larger the value of l, the higher the precision of the price represented by the binary number. For example, we can use a 10 bits binary number to represent a price in interval $[0, 10]$. Then integers from 0 to 1023 can be used to represent the prices in $[0, 10]$, and the precision is $10/1024 \approx 0.01$. This encoding method transforms the continuous price variable into a discrete value, aligning with the practical definition of prices. Meanwhile, the use of binary encoding reduces computational complexity and eliminates the need to explore unnecessary price values.

To implement the algorithm, we will randomly generate a set of l-bit binary numbers as the initial population, in which each binary number is named 'individual'. The population can be updated by a series of genetic operations, including selection, crossover, and mutation. To be more specific, we will first apply the roulette wheel selection strategy proposed by Holland (1992) to select the candidate individuals from the current population for further conducting the crossover and mutation. This selection strategy chooses individuals with good fitness values and high probability. For the OSP problem, the PSP's total cost is defined as the fitness value. Then, a single-point crossover operation and bit flip mutation operation are applied to the selected individuals to generate new individuals and form a new population. An illustrative example in Figure 6.2 shows the crossover and mutation operations. Finally, the updated prices coded in binary will be transformed to practical price values to be used as the input parameters for solving the CSP-R and reduced MPDP-P by the following equation:

$$u = \underline{u} + \frac{\bar{u} - \underline{u}}{2^l - 1} \sum_{i=1}^{l} A_{i-1} \times 2^{i-1} \tag{6.41}$$

For example, a binary number $[0100000000]_2$ can be transformed to the real price $0 + (10 - 0)/\left(2^{10} - 1\right) \times 2^8 \approx 2.50$ by Eq. (6.41).

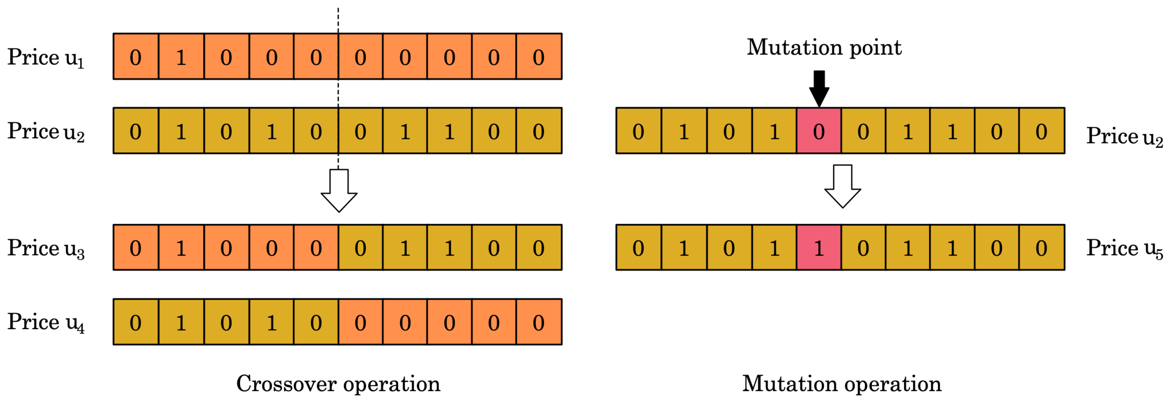

Figure 6.2. Illustration of the crossover and mutation operations

6.3.2 Profit-oriented GTS for lower-level CSP-R

Two customized GTSs are proposed to solve the lower-level CSP-R and upper-level reduced MPDP-P sequentially. The GTS is adapted from the classical tabu search (TS) algorithm, which is a well-known meta-heuristic applied to solve various combinatorial optimization problems. TS starts with an initial solution, which is also set as the current solution and the optimal solution at the very beginning. Then, a series of moves defined by a set of operators will be applied to the current solution to generate new solutions, referred to as neighborhood solutions. For instance, an operator can be simply defined as removing a request from the current route and inserting it into a different route. The different choices of requests, routes, and insertion locations correspond to different moves. The current solution will be updated to be the best neighbourhood solution, whereas the current optimal solution will be updated only if the objective value of the best neighborhood solution is better than the incumbent one. Note that when applying moves to the current solution, a memory structure named tabu list, will be employed to avoid cyclic iteration and escape from local optima (Glover, 1986). Specifically, each time a neighborhood solution is obtained, the corresponding move that generates this solution will be declared as tabu. Then, the inverse operation of this move will be forbidden for a certain number of iterations unless it can generate a better solution than the current optimal solution (Glover, 1986). The classical TS, where all possible moves will be explored when an operator is conducted, can be very time-consuming. To improve the computational efficiency, Toth and Vigo (2003) introduced an effective granularity strategy into the TS, named as GTS, which explores only the promising moves that are likely to generate good-quality solutions. The granularity strategy has shown significant efficiency in finding good-quality solutions in less computation time. We will propose a new granularity strategy based on the characteristics of the OSP problem and apply it to solve the upper- and lower-level problems.

For the upper- and lower-level optimization problems, we first generate initial solutions for CSP-R and reduced MPDP-P by a request-to-vehicle assignment method proposed by Cordeau and Laporte (2003). The method assigns every request i to a randomly selected vehicle route starting from a depot/station and ending at a depot/station, by inserting the corresponding node i and $i + \sigma$ sequentially in the selected routes. This technique ensures the fulfilment of the capacity constraint of parking station/depot and pick-up and drop-off operations of each request. All other constraints, such as time window constraint of requests and maximum ride duration constraint of passengers, however, may be violated by the generated initial solution. To eliminate the violation of constraints, we will impose the penalty on the solutions by defining the unit penalty coefficient for the violation of each constraint and including the penalty cost in the objective function value. We will then apply the aforementioned simple operator that relocates a request to a different route. It is notable that, unlike the upper-level reduced MPDP-P that aims to fulfill all the unserved requests with a minimized total cost, the lower-level CSP-R seeks to maximize the total profit while allowing requests rejection given the limited on-demand mobility vehicles. To enable the generation of new solutions with the operator that relocates a request from one route to another route, some dummy vehicle routes, originating and ending at a dummy station, will be constructed. The requests assigned to a dummy vehicle are those unserved ones by OMP, and thus no profit and cost will be generated by serving these requests.

Two customized granularity strategies, named profit-oriented granularity and cost-oriented granularity, are proposed to generate a reduced number of neighborhood solutions for the CSP-R and reduced MPDP-P, respectively. A feasibility check for the best neighborhood solution will be conducted, and the penalty coefficient for the violated constraint will be increased by a predefined value to further reduce its occurrence in future iterations. The optimal solution will be updated only if we find a feasible neighbourhood solution better than the incumbent one. In what follows, we will elaborate on the two granularity strategies that define the criteria for promising moves.

Since the lower-level CSP-R is to find the profit-maximized service routes, a profit-oriented granularity strategy is developed to explore promising moves that can generate solutions with high profits. As such, we define $P_{i,j}^{\Pi}$ as the profit of a vehicle serving requests i and j following the sequence Π starting at request $i, \forall i, j \in \mathbf{\Omega}^{p,o} \cup \mathbf{\Omega}^{f,o}$. Considering the pickup and drop-off operations of each request, there are three possible sequences, i.e., $\Pi_1 = (i, i+\sigma, j, j+\sigma), \Pi_2 = (i, j, i+\sigma, j+\sigma)$, and $\Pi_3 = (i, j, j+\sigma, i+\sigma)$, serving request i before j, as shown in Figure 6.3.

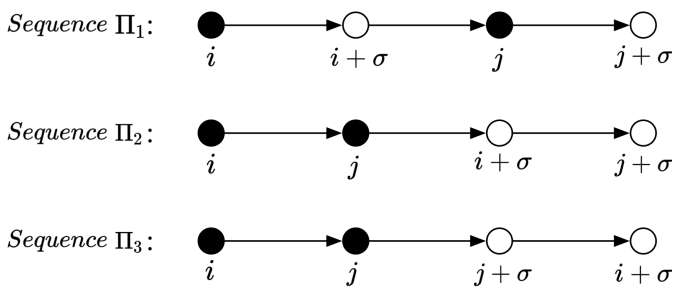

Figure 6.3. Possible sequences of the served request i and j starting at request i

Let $\bar{P}_{i,j}$ represent the average profit of a vehicle serving request i before j of the three sequences. A greater value of $\bar{P}_{i,j}$ indicates that it would be more profitable to utilize a vehicle to fulfill request j after request i. Therefore, the move that can make a vehicle serve request i before j with $\bar{P}_{i,j} \geq P_{\text{gran}}$, where P_{gran} is the profit granularity threshold, is defined as a promising move. For CSP-R, request i and j can be different types of requests, i.e., parcel request or passenger request. We thus calculate $P_{i,j}^{\Pi}$ according to the following four cases:

Case 1 (Requests i and j are both passenger ride requests):

$$P_{i,j}^{\Pi} = R_i + R_j - c_{\Pi} - c\left(r_i^v - t_{i,i+\sigma} + r_j^v - t_{j,j+\sigma}\right), \quad \forall \Pi \in \{\Pi_1, \Pi_2, \Pi_3\}, i, j \in \mathbf{\Omega}^{p,o} \tag{6.42}$$

Case 2 (Requests i and j are both parcel delivery requests):

$$P_{i,j}^{\Pi} = uq_i^f + uq_j^f - c_{\Pi}, \quad \forall \Pi \in \{\Pi_1, \Pi_2, \Pi_3\}, i, j \in \mathbf{\Omega}^{f,o} \tag{6.43}$$

Case 3 (Request i is passenger ride request, whereas request j is parcel delivery request):

$$P_{i,j}^{\Pi} = R_i + uq_j^f - c_{\Pi} - c\left(r_i^v - t_{i,i+\sigma}\right), \quad \forall \Pi \in \{\Pi_1, \Pi_2, \Pi_3\}, i \in \mathbf{\Omega}^{p,o}, j \in \mathbf{\Omega}^{f,o} \tag{6.44}$$

Case 4 (Request i is parcel delivery request, whereas request j is passenger ride request):

$$P_{i,j}^{\Pi} = R_j + uq_i^f - c_{\Pi} - c\left(r_j^v - t_{j,j+\sigma}\right), \quad \forall \Pi \in \{\Pi_1, \Pi_2, \Pi_3\}, i \in \mathbf{\Omega}^{f,o}, j \in \mathbf{\Omega}^{p,o} \tag{6.45}$$

where c_{Π} is the total transportation cost along the sequence Π. For example, for a sequence $\Pi_1 = (i, i+\sigma, j, j+\sigma)$, we have $c_{\Pi} = c_{i,i+\sigma} + c_{i+\sigma,j} + c_{j,j+\sigma}$.

Note that if the sequence Π violates any related constraint, i.e., time window constraint of the request, i.e., Eq. (6.8), ride duration constraint of passenger, i.e., Eq. (6.10), working time constraint of vehicle, i.e., Eq. (6.11), or vehicle load capacity constraint, i.e., Eqs. (6.14) and (6.15), we will set $P_{i,j}^{\Pi} = \infty$, which means request i and j can not be served by the same vehicle following the corresponding sequence. The average profit $\bar{P}_{i,j}$ is thus calculated by

$$\bar{P}_{i,j} = \frac{\sum_{\Pi \in \{\Pi_1, \Pi_2, \Pi_3\}} P_{i,j}^{\Pi} \zeta^{\Pi}}{\sum_{\Pi \in \{\Pi_1, \Pi_2, \Pi_3\}} \zeta^{\Pi}}, \quad \forall i, j \in \mathbf{\Omega}^{p,o} \cup \mathbf{\Omega}^{f,o} \tag{6.46}$$

where ζ^{Π} is an auxiliary variable, which equals 1 if $P_{i,j}^{\Pi} \neq \infty$, and 0 otherwise. If $\zeta^{\Pi_1} + \zeta^{\Pi_2} + \zeta^{\Pi_3} = 0$, we set $\bar{P}_{i,j} = 0$, which means the request i and j cannot be served by the same vehicle starting at serving request i. With the calculated $P_{i,j}^{\Pi}$ and a given profit granularity threshold P_{gran}, we can figure out the promising moves such that $P_{i,j}^{\Pi} \geq P_{\text{gran}}$. Then, we implement the moves upon the current solution to generate neighborhood solutions while complying with the move requirement, e.g., serve request i before j.

Figure 6.4 illustrates an example of generating neighborhood solutions considering profit-oriented granularity for the current solution that two paired pick-up and drop-off requests are served by two vehicles. In this figure, with the calculated profit-oriented granularity $\bar{P}_{i,j}$ and the pre-specified $P_{\text{gran}} = 4$, we can obtain the promising moves, i.e., the moves that can make the vehicle serves request 3 before request 2. Then, we apply moves on the current solution to generate neighborhood solutions. Two possible scenarios can be explored: i) move request 3 from the current route to the route that serves request 2, and ii) move request 2 from the current route to the route that serves request 3. The right-hand side of Figure 6.4 exemplifies two neighborhood solutions of the two scenarios.

Compared to the classical TS where all possibilities of chosen requests and insertion position are explored, the granularity strategy can get reduced neighborhood solutions by only exploring

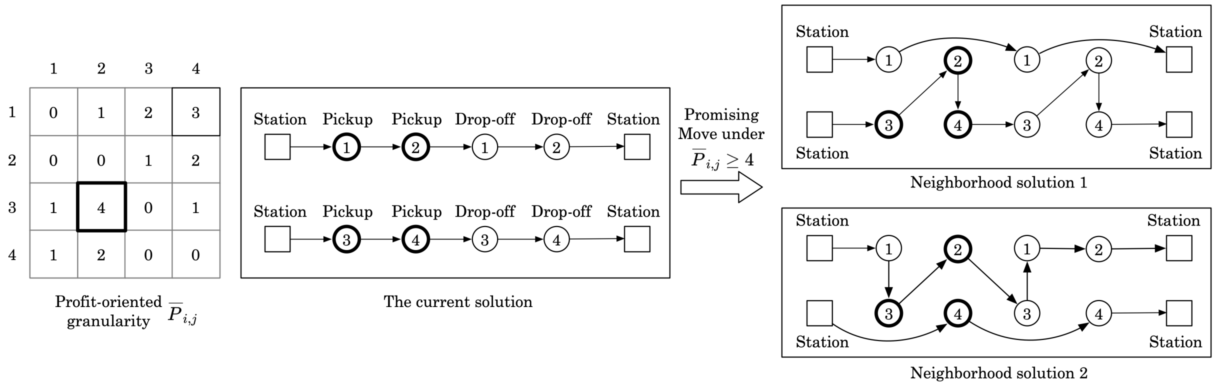

Figure 6.4. An illustrative example of generating neighborhood solutions considering profit-oriented granularity

the promising moves. Kindly note that a large P_{gran} means less moves are explored, resulting in less time-consuming but limited searching for neighborhood solutions. In our study, the profit granularity threshold P_{gran} is defined as dynamic with the implementation of iteration. The granularity threshold P_{gran} will be initially set as $P_{\text{gran}} = \max_{i,j \in \mathbf{\Omega}^{f,o} \cup \mathbf{\Omega}^{p,o}} \left\{ \bar{P}_{i,j} \right\}$ and then gradually decreased by $P_{\text{gran}} \leftarrow P_{\text{gran}} - \delta$ until the lower bound $\underline{P}_{\text{gran}}$ is reached, where the lower bound $\underline{P}_{\text{gran}}$ can be defined according to the $\bar{P}_{i,j}$, e.g., $\underline{P}_{\text{gran}} = \chi_p \max_{i,j \in \mathbf{\Omega}^{f,o} \cup \mathbf{\Omega}^{p,o}} \left\{ \bar{P}_{i,j} \right\}$, where χ_p denote a parameter controlling the move exploration.

The step-by-step procedure of TS-P for solving lower-level CSP-R is summarized as follows:

- **Step 0: (Initialization and data input)** Input the parcel delivery requests $\mathbf{\Omega}^{f,o}$, passenger ride requests $\mathbf{\Omega}^{p,o}$, and outsourcing service price u. Initialize current number of iteration $N_L \leftarrow 1$, maximum number of iterations $N_L^{\max}$, penalty coefficient ω, adaptive factor for penalty coefficient Δ, and the $TabuList$.
- **Step 1: (Generation and evaluation of the initial solution)**
  - **Step 1.1:** Generate an initial solution ϑ_0 with the requests $\mathbf{\Omega}^{f,o}$ and $\mathbf{\Omega}^{p,o}$, and calculate the OMP's total profit denoted by $f(\vartheta_0, u)$ under solution ϑ_0 and price u considering the penalty cost.
  - **Step 1.2:** Initialize current optimal solution by $\vartheta^* \leftarrow \vartheta_0$ and OMP's total profit under current optimal solution by $f_{\text{best}} \leftarrow f(\vartheta_0, u)$.
- **Step 2: (Neighborhood search)**
  - **Step 2.1:** Initialize current solution by $\vartheta \leftarrow \vartheta_0$. Initialize the set of neighborhood solutions $\mathcal{N}(\vartheta)$ as $\varnothing$.
  - **Step 2.2:** Explore promising $Moves$ with the profit-oriented granularity strategy.

- * **Step 2.2.1:** Calculate average profit $\bar{P}_{i,j}, \forall i,j \in \mathbf{\Omega}^{f,o} \cup \mathbf{\Omega}^{p,o}$.
  * **Step 2.2.2:** Initialize P_{gran} as $P_{\text{gran}} \leftarrow \max_{i,j \in \mathbf{\Omega}^{f,o} \cup \mathbf{\Omega}^{p,o}} \left\{ \bar{P}_{i,j} \right\}$ and obtain the lower bound of profit granularity threshold by $\underline{P}_{\text{gran}} \leftarrow \chi_p P_{\text{gran}}$.
  * **Step 2.2.3:** Obtain the promising $Moves$ such that $\bar{P}_{i,j} \geq P_{\text{gran}}$.
- **Step 2.3:** Generate neighborhood solutions by applying $Moves$ on current solution ϑ considering the tabu strategy, i.e., $\mathcal{N}(\vartheta) = \text{Neighbor}(\vartheta, Moves, TabuList, f_{best})$, where Neighbor$(\cdot)$ is the neighborhood search procedure. Specifically, we apply $Moves$ on current solution ϑ to generate its neighborhood solutions. For each generated neighborhood solution ϑ', we will further check whether the move that generates the neighborhood solution ϑ' is forbidden by TabuList: if not, the solution ϑ' will be included in $\mathcal{N}(\vartheta)$; otherwise we will check whether $f(\vartheta', u) > f_{\text{best}}$: if yes, the solution ϑ' will be included in $\mathcal{N}(\vartheta)$.
- **Step 2.4:** If $\mathcal{N}(\vartheta) \neq \varnothing$, go to **Step 2.4.1**; otherwise go to **Step 2.5**.
  * **Step 2.4.1:** Find the best solution among all neighborhood solutions, i.e., $\hat{\vartheta} = \underset{g' \in \mathcal{N}(\vartheta)}{\arg\max} f(\vartheta', u)$.
  * **Step 2.4.2:** Conduct feasibility check on solution $\hat{\vartheta}$. If violation occurs, we modify the corresponding penalty coefficient by $\omega \leftarrow \omega + \Delta$; otherwise update current optimal solution by $\vartheta^* \leftarrow \hat{\vartheta}, f$ best $\leftarrow f(\hat{\vartheta}, u)$ if $f(\hat{\vartheta}, u) > f_{\text{best}}$.
  * **Step 2.4.3:** Let $\vartheta \leftarrow \hat{\vartheta}$, and update $TabuList$ with the move that generates solution $\hat{\vartheta}$ and go to **Step 3**.
- **Step 2.5:** If $P_{\text{gran}} > \underline{P}_{\text{gran}}$, let $P_{\text{gran}} \leftarrow P_{\text{gran}} - \delta$ and go to **Step 2.2.3**; otherwise go to **Step 4**.

- **Step 3: (Stopping condition)** If $N_L \leq N_L^{\max}$, let $N_L \leftarrow N_L + 1$ and go to **Step 2.3**, otherwise go to **Step 4**.
- **Step 4: (Output)** Output current optimal solution ϑ^* and OMP's total profit f_{best}.

Kindly note that the optimal solution ϑ^* should not cause any violation on corresponding constraints, which can be guaranteed by a feasibility check in Step 2.4.2. The total profit of the optimal solution ϑ^* is thus $\text{TP}(\vartheta^*, u)$. Meanwhile, by exploring the optimal solution ϑ^*, the unserved parcel delivery requests under the offered price u will be grouped in set $\mathbf{\Omega}_{rej}^{f,o^*}(u)$, which will be then input for the optimization of the upper-level reduced MPDP-P.

6.3.3 Cost-oriented GTS for upper-level MPDP-P

Since the upper-level reduced MPDP-P is to find a cost-minimized service route to meet all unserved parcel delivery requests, a cost-oriented granularity strategy is developed to explore the promising moves that can generate solutions with low costs. As such, we define $C_{i,j}^{\Pi}$ as the cost of a vehicle serving request i and j following the sequence Π starting at request $i, \forall i, j \in \mathbf{\Omega}_{rej}^{f,o^*}(u)$. Similarly, there exist three possible sequences, i.e., Π_1, Π_2, and Π_3, that serve request i before j. Let $\bar{C}_{i,j}$ denote the average cost of a vehicle serving request i before j of the three sequences. A smaller value of $\bar{C}_{i,j}$ indicates that it would be more cost-effective to use a vehicle to fulfill request j after request i. Therefore, the move that can make a vehicle serve request i before j with $\bar{C}_{i,j} \leq C_{\text{gran}}$, where C_{gran} is the cost granularity threshold, is defined as a promising move. For reduced MPDP-P, $C_{i,j}^{\Pi}$ can be calculated by

$$C_{i,j}^{\Pi} = \kappa_{\Pi}, \quad \forall \Pi \in \{\Pi_1, \Pi_2, \Pi_3\}, i, j \in \mathbf{\Omega}_{rej}^{f,o^*}(u) \tag{6.47}$$

where κ_{Π} is the total transportation cost of the van along the sequence Π. For example, for a sequence $\Pi_1 = (i, i+\sigma, j, j+\sigma), \kappa_{\Pi} = \kappa_{i,i+\sigma} + \kappa_{i+\sigma,j} + \kappa_{j,j+\sigma}$. Similarly, if the sequence Π violates any related constraint, i.e., time window constraint of the request, i.e., Eq. (6.33), working time constraint of van, i.e., Eq. (6.34), or van load capacity constraint, i.e., Eq. (6.36), we set $C_{i,j}^{\Pi} = \infty, \forall \Pi \in \{\Pi_1, \Pi_2, \Pi_3\}, i, j \in \mathbf{\Omega}_{rej}^{f,o^*}(u)$, which means request i and j can not be served by a same vehicle following the corresponding sequence. The average cost $\bar{C}_{i,j}$ is thus calculated by

$$\bar{C}_{i,j} = \frac{\sum_{\Pi \in \{\Pi_1,\Pi_2,\Pi_3\}} C_{i,j}^{\Pi} l^{\Pi}}{\sum_{\Pi \in \{\Pi_1,\Pi_2,\Pi_3\}} t^{\Pi}}, \quad \forall i, j \in \mathbf{\Omega}_{rej}^{f,o^*}(u) \tag{6.48}$$

where t^{Π} is an auxiliary variable that $l^{\Pi} = 1$ if $C_{i,j}^{\Pi} \neq \infty$, and $t^{\Pi} = 0$ otherwise. If $t^{\Pi_1} + t^{\Pi_2} + t^{\Pi_3} = 0$, we set $\bar{C}_{i,j} = \infty$, which means the requests i and j cannot be served by the same van by starting at serving request i. With the calculated $\bar{C}_{i,j}$ and a given cost granularity threshold C_{gran} , we can figure out the promising moves such that $\bar{C}_{i,j} \leq C_{\text{gran}}$. Then, we implement the moves upon the current solution to generate neighborhood solutions while complying with the move requirement, e.g., serve request i before j. Similar to the dynamic setting of P_{gran} , the cost granularity threshold C_{gran} will be initially set as $C_{\text{gran}} = \min_{i,j \in \mathbf{\Omega}_{rej}^{f,o*}(u)} \{\bar{C}_{i,j}\}$ and gradually increased by $C_{\text{gran}} \leftarrow C_{\text{gran}} + \delta$ until the upper bound $\bar{C}_{\text{gran}}$ is reached, where the upper bound $\bar{C}_{\text{gran}}$ can be defined according to the $\bar{C}_{i,j}$, e.g., $\bar{C}_{\text{gran}} = \chi_c \min_{i,j \in \mathbf{\Omega}_{rej}^{f,o*}(u)} \{\bar{C}_{i,j}\}$, where χ_c denote a parameter controlling the move exploration.

The step-by-step procedure of TS-C for solving upper-level reduced MPDP-P is summarized as follows:

- **Step 0: (Initialization and data input)** Input the unserved parcel delivery requests $\mathbf{\Omega}_{rej}^{f,o^*}(u)$ under corresponding outsourcing service price u. Initialize current number of iteration as $N_U \leftarrow 1$, maximum number of iterations $N_U^{\max}$, penalty coefficient ω, adaptive factor for penalty coefficient Δ, and $TabuList$.

- **Step 1: (Generation and evaluation of the initial solution)**

  - **Step 1.1:** Generate an initial routing solution θ_0 with the requests $\mathbf{\Omega}_{rej}^{f,o^*}(u)$, and calculate the PSP's total cost denoted by $g(\theta_0, u)$ under solution θ_0 considering the penalty cost.

  - **Step 1.2:** Initialize current optimal solution by $\theta^* \leftarrow \theta_0$ and PSP's total cost under current optimal solution by $g_{\text{best}} \leftarrow g(\theta_0, u)$.

- **Step 2: (Neighborhood search)**

  - **Step 2.1:** Initialize the current solution $\theta \leftarrow \theta_0$. Initialize the set of neighborhood solutions $\mathcal{N}(\theta)$ as $\varnothing$.

  - **Step 2.2:** Explore promising $Moves$ with the cost-oriented granularity strategy.

    * **Step 2.2.1:** Calculate average cost $\bar{C}_{i,j}, \forall i, j \in \mathbf{\Omega}_{rej}^{f,o^*}(u)$.

    * **Step 2.2.2:** Initialize cost granularity threshold by $C_{\text{gran}} \leftarrow \min_{i,j \in \mathbf{\Omega}_{rej}^{f,o^*}(u)} \{\bar{C}_{i,j}\}$ and obtain upper bound of cost granularity threshold by $\bar{C}_{\text{gran}} \leftarrow \chi_c \cdot C_{\text{gran}}$.

    * **Step 2.2.3:** Obtain the promising $Moves$ such that $\bar{C}_{i,j} \leq C_{\text{gran}}$.

  - **Step 2.3:** Generate neighborhood solutions by applying $Moves$ on current solution θ considering the tabu strategy, i.e., $\mathcal{N}(\theta) = \text{Neighbor}(\theta, Moves, TabuList, g_{\text{best}})$, where $\text{Neighbor}(\cdot)$ is the neighborhood search procedure. Specifically, we apply $Moves$ on current routing solution θ to generate its neighborhood solutions. For each generated neighborhood solution θ', we will first check whether the move that generates the neighborhood solution θ' is forbidden by TabuList: if not, the solution θ' will be included in $\mathcal{N}(\theta)$; otherwise, we will check whether $g(\theta', u) < g_{\text{best}}$: if yes, the solution θ' will be included in $\mathcal{N}(\theta)$.

  - **Step 2.4:** If $\mathcal{N}(\theta) \neq \varnothing$, go to **Step 2.4.1**, otherwise go to **Step 2.5**.

    * **Step 2.4.1:** Find the best solution among all neighborhood solutions, i.e., $\hat{\theta} = \arg\min_{\theta \in \in \mathcal{N}(\theta)} g(\theta', u)$.

    * **Step 2.4.2:** Conduct feasibility check on solution θ. If violation occurs, we modify the corresponding penalty coefficient by $\omega \leftarrow \omega + \Delta$; otherwise update the optimal solution by $\theta^* \leftarrow \hat{\theta}$, $g_{\text{best}} \leftarrow g(\hat{\theta}, u)$ if $g(\hat{\theta}, u) < g_{\text{best}}$.

    - * **Step 2.4.3:** Let $\theta \leftarrow \hat{\theta}$, and update TabuList with the move that generates solution $\hat{\theta}$ and go to **Step 3**.
  - **Step 2.5:** If $C_{\text{gran}} < \bar{C}_{\text{gran}}$, let $C_{\text{gran}} \leftarrow C_{\text{gran}} + \delta$ and go to **Step 2.2.3**; otherwise go to **Step 4**.

- **Step 3: (Stopping condition)** If $N_U \leq N_U^{\max}$, let $N_U \leftarrow N_U + 1$ and go to **Step 2.3**; otherwise go **Step 4**.
- **Step 4: (Output)** Output current optimal solution θ^* and the PSP's total cost g_{best}.

Kindly note that the final optimal solution θ^* should not cause any violation on corresponding constraints, which can be guaranteed by a feasibility check on θ^* in Step 2.4.2. The total cost of the optimal routing solution θ^* is thus $TC(\theta^*, u)$.

6.4 Numerical Experiments

In this section, random instances are generated to test the performance of our proposed IH algorithm in solving the studied OSP problem. The efficiency of the proposed objective-oriented granularity strategies for neighborhood search, is verified by comparing them with the traditional strategy. A real-life case study in Hong Kong is conducted to evaluate the proposed COM model and explore the impact of some key factors on the performance of the COM business model. The algorithms are coded in MATLAB 2021a on a personal computer with MacOS Big Sur 11.6, Apple M1 3.2GHz CPU.

6.4.1 Test instance generation and parameter setting

We will generate some illustrative instances to test the efficiency of our proposed solution methods. The instances are adapted from the Solomon datasets. Each instance within the datasets contains a single depot and multiple delivery requests, incorporating details related to delivery location, load of the request, service time window, and service duration. To ensure the applicability of these instances to our specific problem context-wherein each package or passenger request is associated with corresponding pick-up and drop-off requests, we introduce certain modifications. For illustrative purposes and without loss of generality, we will select data from the C121 case and implement further adaptations. Specifically, we first select m and n requests from dataset to serve as the parcel and passenger pick-up requests, respectively. An equal number of requests with distinct locations are chosen from the same set to act as corresponding drop-off requests. To uphold the validity of requests, we introduce modifications to several parameters, including the service time window, load, passenger number, and service duration. All requests within the set operate within a time window spanning from 0 to 1351 , regarded as the operation period. For the parcel pick-up requests, we maintain the original service time window and a service duration of 90. Each parcel pick-up request is allocated a positive integer load of parcels, randomly generated within the range [1,5]. For the passenger pick-up requests, we retain the original service time window, assigning each request a positive integer number of passengers, randomly generated within the range [1,4], and a service duration of zero. For the drop-off requests, the earliest service time is calculated as the sum of the earliest pick-up time and the travel time from the pick-up to the drop-off location. Similarly, the latest service time is determined by adding the maximum delivery or ride time to the latest pick-up time. The load of parcels and the number of passengers for drop-off requests are set as the negative values of their corresponding pick-up requests. The service duration for parcel drop-off requests is set at 90, whereas it is zero for passenger drop-off requests. In addition to these parameters, five locations are randomly selected to serve as depots for parking vans. A total of 20 vans are randomly allocated to these depots, ensuring that each depot houses no more than five vans. Five other locations are also randomly selected to serve as stations for parking on-demand mobility vehicles. A total of 20 vehicles are randomly distributed across these stations, with each station accommodating no more than five vehicles. The model's detailed parameter setting is illustrated in Table 6.1.

Table 6.1. Parameter setting for the randomly generated instances

	Parameters	value	Parameters	value	Parameters	value
Upper-level	$K_{i,j}$	\$10/unit	ψ	\$50/veh	$\hat{W}_k$	800
	Q_k	15	Q_h	5	q_i^f	{1,2,3,4,5}
	e_i	[0,1351]	l_i	[0,1351]	m	{40,50,60,70}
	$e_{i+\sigma}$	$e_i + \phi_{i+\sigma}$	$l_{i+\sigma}$	$e_{i+\sigma} + 300$		
Lower-level	$c_{i,j}$	\$3/unit	c	\$2	R_i	\$10/unit
	Q_v^p	4	Q_v^f	10	Q_s	5
	$\hat{W}_v$	800	e_i	[0,1351]	l_i	$e_i + \hat{T}_i$
	q_j^p	{1,2,3,4}	$e_{i+\sigma}$	$e_i + t_{i,i+\sigma}$	$l_{i+\sigma}$	$e_{i+\sigma} + \hat{T}_i$
	$\xi_{\max}$	4	$\underline{u}$	0	$\overline{u}$	\$10
	$\hat{T}_i$	200	n	{40,50,60}	P_i	\$10

The upper- and lower-level problems are both assigned a maximum iteration of 200. We utilize a total of 20 generations, each comprising 10 individual outsourcing service prices, to update these prices. Based on experimental testing, the penalty coefficients for violated constraints are established as follows: the penalty coefficients for the violated time window constraint of the request $\omega_{\text{tw}} = 100$, the working time constraint of the van and on-demand mobility vehicle $\omega_{\text{wtk}} = \omega_{\text{wtv}} = 20$, the van load capacity constraint $\omega_{\text{cap\_k}} = 30$, the ride duration constraint of the passenger $\omega_{\text{rd}} = 20$, and the vehicle load capacity constraint $\omega^{\text{f}}_{\text{cap\_v}} = 15$ and $\omega_{\text{cap\_p}} = 10$.

6.4.2 Performance of IH method on test instances

Different combinations of parcel and passenger requests are utilized to evaluate the performance of our proposed IH algorithm with objective-oriented granularity strategy for solving the OSP problem. A comparison is conducted between the results obtained from the method with classical TS method, which considers all possible moves (TS algorithm), and our proposed IH algorithm with objective-oriented granularity strategy, which focuses on promising moves under the objective-oriented granularity strategy (IH algorithm). The detailed results are shown in Table 6.2. We compare the final obtained outsourcing service price (u^*), and overall computation time (CPU) for different instances with varying total numbers of passenger ride requests (n) and parcel delivery requests (m). In addition, we compare the PSP's total cost and the OMP's total profit under the obtained outsourcing service price by the classical TS method and our developed TS method with granularity strategy, as depicted in Figure 6.5.

Table 6.2. Results obtained by TS and IH methods under different instances

Instance	n	m	IH Method		TS algorithm	
			u^*(\$)	CPU (min)	u^*(\$)	CPU (min)
1	40	40	6.4	14.2	6.4	24.1
2		50	6.3	16.3	6.3	41.5
3		60	6.3	19.3	6.3	57.7
4		70	6.7	24.2	6.7	82.1
5	50	40	6.4	17.1	6.4	29.3
6		50	6.6	21.4	6.6	45.9
7		60	6.2	28.9	6.2	76.4
8		70	6.6	33.2	6.6	97.1
9	60	40	6.9	21.2	6.9	34.1
10		50	6.6	29.5	6.6	55.2
11		60	6.5	36.7	6.5	89.4
12		70	6.3	47.5	6.3	113.5
Average	-	-	-	**25.8**	-	62.2

The results presented in Table 6.2 demonstrate that, given the same number of iterations for all instances, our proposed method achieves an equivalent outsourcing service price in a shorter computational time (25.8 minutes vs. 62.2 minutes on average) compared to TS algorithm. In our numerical experiments, the TS algorithm requires a substantial amount of time to exhaustively explore all possible moves. In contrast, our approach employs a granularity strategy that focuses on exploring promising moves, leading to the discovery of high-quality solutions in less time. This time-efficient solution offers significant decision-making support for PSP.

Furthermore, Figure 6.5 indicates that the total cost and total profit achieved by the GTS method are superior to those achieved by the classical TS method, i.e., lower TC for PSP and

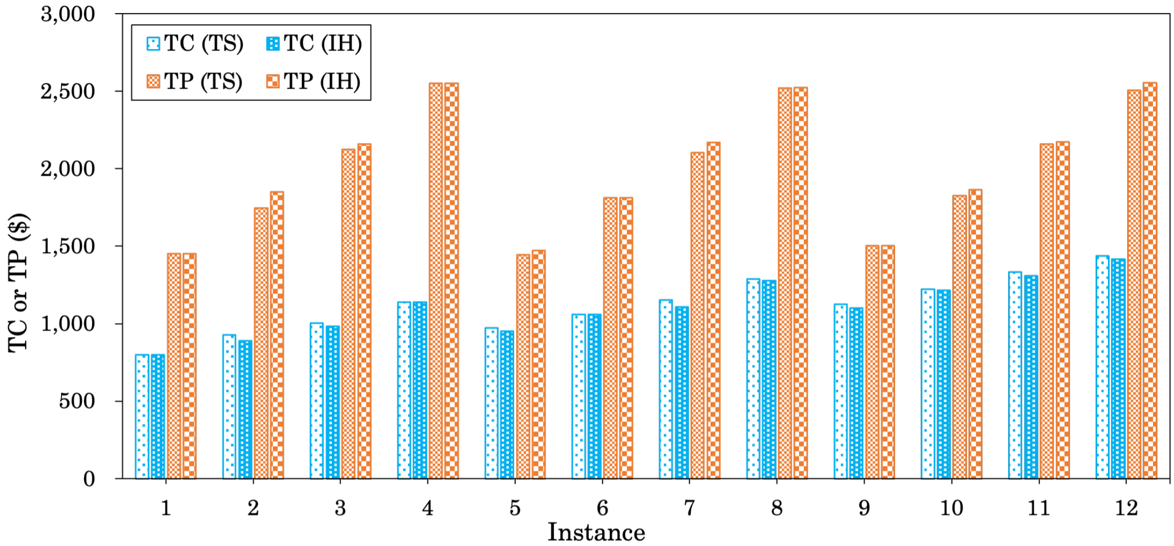

Figure 6.5. Comparison of TC and TP by classical TS and GTS in different instances

higher TP for OMP. This underscores the efficacy of the GTS method in identifying optimal service routes, while reducing computation time due to the incorporation of the customized objective-oriented granularity strategy. Therefore, the IH algorithm, which incorporates costoriented and profit-oriented granularity, exhibits reliability in terms of computation time and optimization effectiveness. Consequently, we apply the IH algorithm to a real-life case study to gain valuable managerial insights for the operations and management of the COM model.

6.4.3 Case study

We then examine a real-life case study conducted in Hong Kong to demonstrate the applicability and effectiveness of the proposed COM business model. We first capture some geographical data of supermarkets and daily necessities stores in Hong Kong, such as Wellcome, ParknShop, Watsons as the pick-up locations of the parcel delivery requests, and some residential areas as the drop-off locations of the parcel delivery requests (See Figure 6.6a). As for the passenger ride request data, we include business districts, schools, and residential areas to generate origin and destination pairs for these requests (See Figure 6.6b). The specific requirements associated with these requests, such as time windows, the number of parcels for each parcel request, and the number of passengers for each passenger request, are randomly assigned in accordance with the parameters outlined in Table 6.3. A PSP possesses a fleet of 20 vans that are available for providing parcel delivery services to fulfill parcel delivery requests. Initially, these vans are randomly distributed across five depots, which are selected from various parking areas in Hong Kong. On the other hand, the OMP operates a total of 20 ondemand mobility vehicles capable of serving both parcel and passenger requests. Similar to the vans, these vehicles are randomly distributed among five stations. Subsequently, the PSP aims to satisfy all parcel delivery requests by collaborating with the OMP within the framework of the COM model.

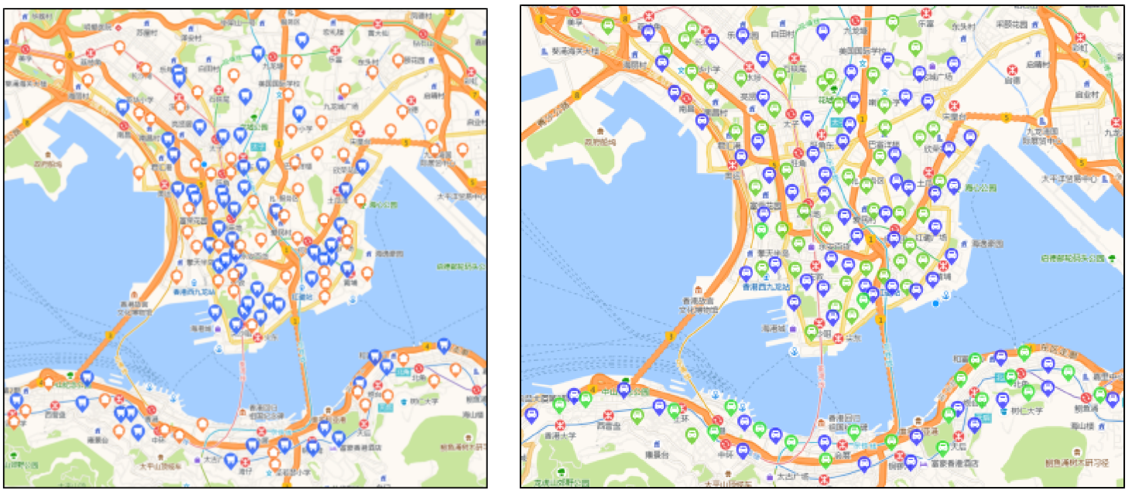

(a) Distribution of parcel delivery requests

(b) Distribution of passenger ride requests

Figure 6.6. Distribution of parcel and passenger requests

Table 6.3. Parameter setting for the case study

	Parameters	value	Parameters	value	Parameters	value
Upper-level	$K_{i,j}$	\$10/unit	ψ	\$50/veh	$\hat{W}_k$	4h
	Q_k	15	Q_h	5	q_i^f	1
	e_i	[12:00,14:00]	l_i	14:00	m	70
	$e_{i+\sigma}$	$e_i + \phi_{i+\sigma}$	$l_{i+\sigma}$	$e_{i+\sigma} + 2hrs$		
Lower-level	$c_{i,j}$	\$3/unit	c	\$2	R_i	\$10/unit
	Q_v^p	4	Q_v^f	10	Q_s	5
	$\hat{W}_v$	4h	e_i	[12:00,14:00]	l_i	$e_i + \hat{T}_i$
	q_j^p	{1,2,3,4}	$e_{i+\sigma}$	$e_i + t_{i,i+\sigma}$	$l_{i+\sigma}$	$e_{i+\sigma} + \hat{T}_i$
	$\xi_{\max}$	2	$\underline{u}$	0	$\overline{u}$	\$10
	$\hat{T}_i$	1h	n	{40,50,60}	P_i	\$10

6.4.4 Impact analysis of OMS-based CM delivery service

To test the efficacy of the proposed COM model, we compare some key indicators under the COM model and the traditional non-co-modal delivery model in a case with 70 parcel delivery requests and 70 passenger ride requests. In the non-co-modal delivery model, the PSP aims to fulfill all parcel delivery requests using its fleet while minimizing costs. Simultaneously, the OMP solely concentrates on maximizing its total profits by serving passenger ride requests. We compare various metrics under the two different models, including the PSP's total cost (TC), outsourcing cost paid by the PSP (OC), total profit earned by the OMP (TP), obtained outsourcing service price (u^*), passenger service rate of the OMP (PSR), and parcel service rate by the OMP (FSR). Additionally, we examine the percentages of cost saving for the PSP

(Saving) and the percentages of increased profit for the OMP (Increased) achieved by the COM model compared to the non-co-modal delivery mode. Detailed result is shown in Table 6.4.

Table 6.4. Comparison of Non-co-modal and co-modal delivery models

Model	TC($)	Saving(%)	OC($)	TP($)	Increased(%)	u^*($)	PSR(%)	FSR(%)
Non-co-modal	2013.4	-	0.0	2532.1	-	0.0	90%	0.00%
CM delivery	1671.1	17.0%	541.0	2932.2	15.8%	6.5	86%	43%

In Table 6.4, in the case of non-co-modal delivery model, the PSP and OMP serve the parcel delivery requests and passenger ride requests independently. For the PSP, due to the fixed cost of employing dedicated delivery staffs and using delivery vans, the total cost paid by the PSP is relatively large. For the OMP, in the absence of COM mode, the OMP can only serve passenger ride requests and cannot make full use of their idle transportation capacity, thus obtaining limited profit. However, when the PSP collaborates with the OMP under the COM model, the PSP can reduce up to 17.0% of the total cost by outsourcing partial parcel delivery requests (43%) to the OMP. This collaboration allows the PSP to alleviate the financial burden associated with fully self-operating services. This reduction in cost can be attributed to the lower average unit cost of outsourcing services compared to self-operating services. Furthermore, outsourcing to the OMP incurs no additional fixed costs for labor and vehicle usage. These findings highlight the superiority of our proposed COM model over traditional delivery models, such as those focused on fulfilling customer delivery requests through selfoperating logistics (e.g., the study by Qu and Bard (2013)). From the perspective of the OMP, accepting additional parcel delivery requests from the PSP leads to a growth in total profit of up to 15.8%, while the impact on passenger services is relatively modest, with only a 4% reduction in passenger requests being accommodated. This result aligns with the findings of Li et al. (2014), which suggest that serving additional parcel requests can yield higher profits for the OMP.

To gain a deeper understanding of the factors influencing the collaboration between PSP and OMP within the COM model, we perform a sensitivity analysis on several key factors that may impact the decision-making of the partners. We aim to extract valuable managerial insights and provide decision support to the PSP and other stakeholders interested in implementing the COM model to enhance their service capacity and improve service quality. Our analysis focuses on key indicators such as the PSP's total cost (TC), the OMP's total profit (TP), and the parcel request service acceptance rate by the OMP (FSR).

Ride duration tolerances of passenger

As we mentioned before, the COM model operates under the assumption that passengers are willing to share a ride with parcels and other passengers, provided it falls within their maximum ride time tolerance. The maximum tolerance for passengers' ride time may significantly impact the feasibility of accepting parcel requests by the OMP, as the OMP must prioritize passenger transportation services. Consequently, we compare the results obtained under various ride duration tolerances ranging from 60 to 120 minutes for passengers, as shown in Figure 6.7.

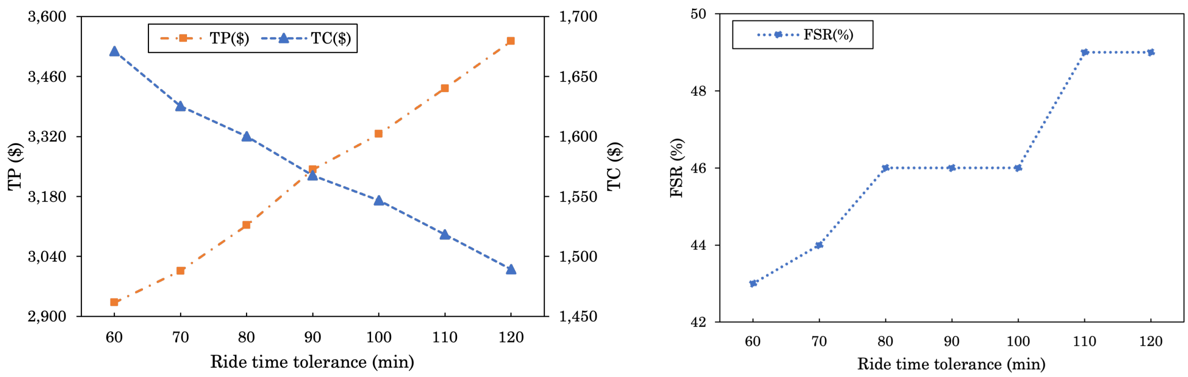

(a) Variations of the TP and TC

(b) Variations of FSR

Figure 6.7. Results under different ride duration tolerances of passenger

Figure 6.7 clearly demonstrates that as the maximum tolerance for passengers' ride time increases, there is a notable increase in the service rate of parcel requests by the OMP, as illustrated in Figure 6.7(b). This can be attributed to the broader ride duration tolerance, which allows the OMP to effectively utilize the spare space in their vehicles and accommodate a greater number of parcel requests. Consequently, the OMP's total profit exhibits an upward trend, as shown in Figure 6.7(a). Simultaneously, the PSP benefits from a significant reduction in total costs, primarily due to the outsourcing of a portion of the parcel delivery requests. Moreover, the sensitivity analysis concerning passenger detour tolerance suggests that as this tolerance increases, the PSP can lower the outsourcing service price to reduce the total cost while maintaining a high service rate by OMP. This is possible because vehicles have the potential to accommodate more parcel requests with the spare capacity provided by the increased detour tolerance, even if the outsourcing service price is not particularly significant.

Parcel load of delivery request

Given that the primary business of the OMP is passenger transportation, the capacity to serve additional parcels is limited without causing significant disruptions to passenger service. Additionally, the load associated with each parcel request may influence the OMP's decision regarding serving those requests. To examine the impact of the load of the parcel delivery request on the COM model, we examine the variations of TP, TC, and FSR under different loads of the parcel, as illustrated in Figure 6.8. We randomly generate a positive number within different load thresholds, such as [1,2], to represent the load of each parcel request.

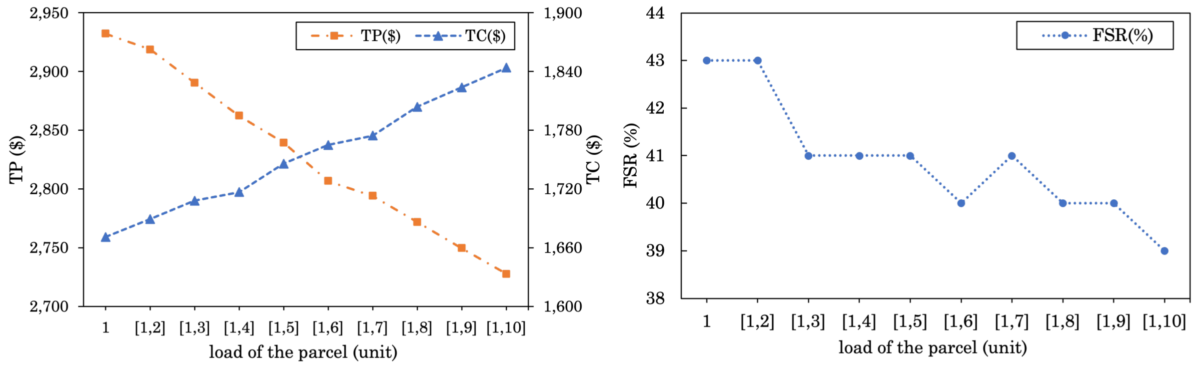

(a) Variations of the TP and TC

(b) Variations of FSR

Figure 6.8. Results under different loads of each parcel delivery request

Figure 6.8 indicates that as the load of each parcel request increases, the service rate of the OMP for parcel requests decreases, as shown in Figure 6.8(b). This can be attributed to the fact that when a single parcel request occupies a significant capacity of the vehicle's available capacity, the vehicle cannot accommodate additional parcel requests during its itinerary. Furthermore, as the load of each parcel delivery request increases, the PSP's total cost rises, while the OMP's total profit decreases, as illustrated in Figure 6.8(a). This finding suggests that the PSP can effectively outsource parcel delivery requests with small loads to the OMP, allowing them to concentrate on handling parcel requests with larger loads. By doing so, the PSP can maximize cost savings while optimizing its operational efficiency. The result suggests that when the load of the outsourced parcels is large, the PSP may need to increase the outsourcing service price to enhance the parcel service rate by OMP. This is because setting a higher profit per unit parcel can incentivize the vehicles to serve parcels with large loads, given the limited spare loading capacity, while covering the cost of detour and subsidizing passengers.

Penalty for unmet passenger request

Due to the service-oriented nature of passenger transportation, penalties are imposed for unfulfilled passenger requests. Consequently, these penalties may influence the decision-making process of the OMP regarding parcel delivery requests. To investigate the impact of penalties on the COM model, we analyze the variations in TP, TC, and FSR under different penalty settings, as presented in Figure 6.9. We can see that when a high penalty is imposed for unfulfilled passenger requests, the FSR decreases. A higher penalty discourages the OMP from serving parcel delivery requests by prioritizing passenger requests due to their associated high costs. Consequently, the TP decreases while the TC increases simultaneously. Conversely, when a low penalty is imposed, the FSR increases. Additionally, TP exhibits a slight increase, while TC experiences a slight decrease. Notably, the growth of TP plateaus even as the penalty decreases. This may be attributed to the fact that although the OMP can stimulate profit growth by rejecting passengers and focusing on parcel delivery requests, the loss of profit from passenger service and the limited profit from parcel delivery hinder further profit increment.

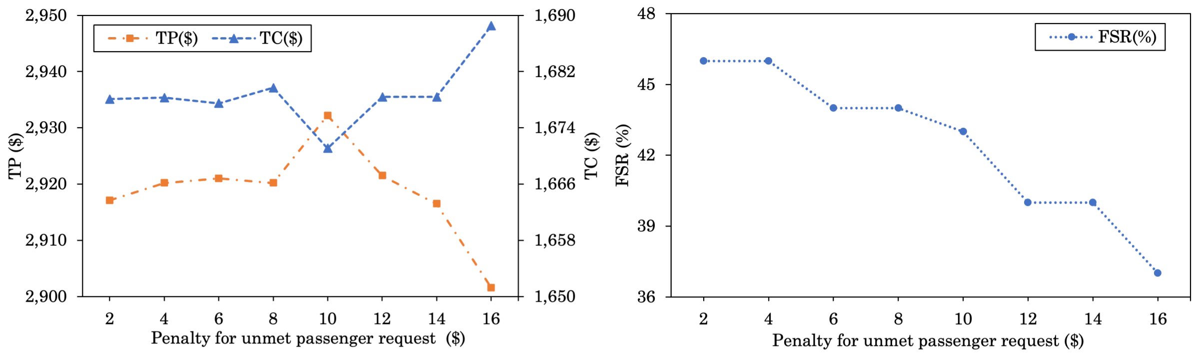

(a) Variations of the TP and TC

(b) Variations of FSR

Figure 6.9. Results under different penalties for unmet passenger request

6.5 Concluding Remarks

This chapter investigates the OSP problem for the COM service, taking into account the Stackelberg gameplay between PSP and OMP when formulating the business collaboration. Based on the gameplay between PSP and OMP, a bilevel optimization model is formulated for the OSP problem, where the upper-level model [MPDP-P] aims to minimize the PSP's total cost consisting of the outsourcing cost and the self-operating cost, while the lower-level model [CSP-R] is intended to maximize the total profits earned by serving the accepted passenger ride requests and parcel delivery requests. An IH algorithm combining two GTS algorithms, i.e., the TS-P and the TS-C, and the genetic algorithm is developed to solve this problem. The numerical experiments, including several randomly generated instances and a real-life case study, are finally conducted to test our models and solution methods. The results show that our proposed model and solution methods can provide the co-modal delivery service participants with a reliable outsourcing service price that enables them to obtain mutual benefit from this collaborative mode. On the one hand, the PSP gets up to 17.0% cost-savings by outsourcing partial parcel requests to the OMP. On the other hand, the OMP obtained improved up to 15.8% total profit by serving additional parcel requests with the spare capacity of the passenger transportation vehicles during the itinerary of serving passengers. Sensitivity analysis indicates that the ride duration tolerance of passengers, carrying capacity of parcel load, and penalty cost of unmet passenger requests affect the OMS-based CM delivery service, providing managerial insights for stakeholders.

6.6 Appendix: Notations

Set	
$\mathcal{S}$	Set of stations for parking vehicles, $s \in S$
$\mathcal{S}^o$	Set of origin stations of on-demand mobility vehicles, $s \in \mathcal{S}^o$
$\mathcal{S}^d$	Set of destination stations of on-demand mobility vehicles, $s \in \mathcal{S}^d$
$\mathcal{H}$	Set of depots for parking vans, $h \in \mathcal{H}$
$\mathcal{H}^o$	Set of origin depots of vans, $h \in \mathcal{H}^o$
$\mathcal{H}^d$	Set of destination depots of vans, $h \in \mathcal{H}^d$
$\mathcal{V}$	Set of vehicles $v \in \mathcal{V}$
$\mathcal{K}$	Set of vans $k \in \mathcal{K}$
$\mathbf{\Omega}^{f,o}$	Set of pick-up nodes of parcel delivery requests, $\mathbf{\Omega}^{f,o} = \{1, 2, \cdots, m\}$
$\mathbf{\Omega}^{p,o}$	Set of origins of passenger ride requests, $\mathbf{\Omega}^{p,o} = \{m+1, m+2, \cdots, \sigma\}$
$\mathbf{\Omega}^{f,d}$	Set of drop-off nodes of parcel delivery requests, $\mathbf{\Omega}^{f,d} = \{\sigma+1, \sigma+2, \cdots, \sigma+m\}$
$\mathbf{\Omega}^{p,d}$	Set of destinations of passenger ride requests, $\mathbf{\Omega}^{p,d} = \{\sigma+m+1, \sigma+m+2, \cdots, 2\sigma\}$
$\mathbf{\Omega}^{f,o^*}_{rej}(u)$	Set of pick-up nodes of unserved parcel delivery requests by OMP under price u
$\mathbf{\Omega}^{f,d^*}_{rej}(u)$	Set of drop-off nodes of unserved parcel delivery requests by OMP under price u
Parameters	
m	Number of parcel delivery requests
n	Number of passenger ride requests
σ	Total number of requests, $\sigma = m + n$
R_i	Revenue for serving each passenger request by on-demand mobility service
P_i	Penalty incurred if the passenger request is denied service
d_i	Service duration for serving parcel or passenger request
Q^p_v	Maximum capacity of vehicle v for loading passengers
Q^f_v	Maximum capacity of vehicle v loading parcels
Q^f_k	Maximum capacity of van k loading parcels
$\xi_{\max}$	Maximum number of allowed stops between a passenger request
Q_s	Capacity of the station s for parking vehicles
Q_h	Capacity of the depot h for parking vans
η	Fixed operating cost for using each on-demand mobility vehicle
ψ	Fixed operating cost for using each van
$c_{i,j}$	Travel cost by the on-demand mobility vehicle from node i to j
$\kappa_{i,j}$	Travel cost by the van from location i to j
c	Compensation paid to passengers for each unit detour duration

$[e_i, l_i]$	Time window at node i
$\hat{T}_i$	Maximum tolerance of ride time for passenger request i
$\hat{W}_v$	Maximum service time of vehicle v
$\hat{W}_k$	Maximum service time of van k
$t_{i,j}$	Travel time from node i to j by vehicle
$\varphi_{i,j}$	Travel time from node i to j by van
$\underline{u}$	Lower bound of the price for delivering each parcel
$\bar{u}$	Upper bound of the price for delivering each parcel
M	A large number
Variables	
r_i^v	Continuous variable to denote the passenger's total ride time in vehicle $v \in \mathcal{V}$ of passenger request $i \in \mathbf{\Omega}^{p,o}$
τ_i^v	Continuous variable to denote the time epoch when vehicle v starts service at node $i \in \mathcal{N}_1$
τ_i^k	Continuous variable to denote the time epoch when van k starts service at node $i \in \mathcal{N}_2$
α^v	Continuous variable to denote the number of passengers in vehicle $V \in \mathcal{V}$ after the service at node $i \in \mathcal{N}_1$
β^v	Continuous variable to denote the load of parcels in vehicle $v \in \mathcal{V}$ after service at node $i \in \mathcal{N}_1$
β_i^k	Continuous variable to denote the load of parcels in van $k \in \mathcal{K}$ after service at node
ξ_i^v	Integer variable to denote the order of node $i \in \mathcal{N}_1$ in vehicle v 's service sequence, $\xi_i^v \in \{1, 2, \cdots, 2(m+n+1)\}$
z_i	Binary variable that equals 1 if request $i \in \mathbf{\Omega}^{p,o} \cup \mathbf{\Omega}^{f,o}$ is served, and 0 otherwise
$x_{i,j}^v$	Binary variable that equals 1 if vehicle $v \in \mathcal{V}$ travel directly from node i to j, $i, j \in \mathcal{N}_1$, and 0 otherwise
$y_{i,j}^k$	Binary decision variable that equals 1 if van $k \in \mathcal{K}$ travel directly from node i to j, $i, j \in \mathcal{N}_2$, and 0 otherwise
u	Continuous variable to denote the outsourcing service price provided by PSP for serving per unit parcel

Chapter 7 Conclusions and Recommendations

7.1 Overview and Research Contributions

This thesis has addressed four research problems concerning pricing optimization and a series of strategical and operational decision-making optimizations for urban delivery service providers using three types of IPG transportation services: (1) crowd-shipping service utilizing ordinary travelers for door-to-door O2O orders, (2) co-modal transportation service leveraging public transit systems for parcel backbone transportation, and (3) co-modal delivery service with on-demand mobility services for multiple parcel pickup and delivery demands.

Chapter 3 addresses pricing optimization for the OT-based CS service. To bridge the research gap regarding the joint compensation and service routing optimization for a hybrid delivery system with dedicated delivery service and OT-based CS service, Chapter 3 investigates a C&R problem to jointly determine the uniform or differentiated compensation rates and service routes for crowd-couriers and dedicated vehicles to fulfill all O2O orders at minimal cost. An MINLP model is formulated for the C&R-U problem, and linearization techniques are employed to transform it to an MILP model. Additionally, a customized H-ILS-VNS algorithm is developed to solve larger-scale cases by iteratively addressing the R-C&R-U problem via a VNS-TS algorithm with the compensation rate updated by ILS. The C&R-D problem is formulated as an MILP model by exploring the problem features, and the adjusted VNS-TS is utilized to solve its larger-scale cases. Numerical experiments on a series of instances with varying numbers of O2O orders and crowd-couriers are conducted to assess the performance of the proposed models and solution methods. Additionally, numerical experiments and sensitivity analysis are also performed to evaluate the benefits of the OT-based CS service and the impact of ETP and carrying capacity of crowd-courier on the operations management of the collaborative delivery system.

Chapter 4 extends the exploration of pricing optimization of OT-based CS service by Chapter 3, examining a CACR problem for a collaborative delivery system with collaborative delivery strategy for shared customers. The studied problem aims to optimize the collaboration strategy, allocate O2O orders among the retailers efficiently, set appropriate compensation rates, and determine optimal service routes for both dedicated vehicles and crowd-couriers. A bi-objective optimization model with the objectives of minimizing operational costs and carbon emissions is formulated for the CACR problem. To solve the complicated problem, we develops a DIO method, which aims to find Pareto-optimal solutions for the master CACR problem by iteratively solves a series of decomposed bi-objective sub-problems with updated candidate compensation rate and collaboration strategy. For solving the bi-objective sub-problems, a 'cluster-first, route-second' approach is employed, where a STC method is first proposed to allocate O2O orders among retailers based on spatiotemporal proximity and an enhanced CW-NSGA-II is developed to determine efficient routing solutions for both dedicated vehicles and crowd-couriers. To validate our proposed solution method and the collaborative delivery system, we conduct numerical experiments using adapted benchmark instances and a simulated case in Chongqing, China.

Chapter 5 addresses pricing optimization for the PT-based CM transportation service. To close the research gap concerning pricing optimization and the coordination and scheduling of PT vehicles, Chapter 5 delves into a CSP, aiming to determine the optimal service price and PT vehicle schedules for the PT-based CM transportation service, alongside the optimal routing of dedicated vehicles for a conventional delivery service. A bilevel programming framework is employed to model the CSP problem, capturing the dynamic interactions between LSP and PTO. In this framework, the lower-level BTS model is established to ascertain the optimal operating schedules for PTO's transit vehicles under the given service price. Concurrently, the upper-level VRP-P model is formulated to determine the optimal service price and routing plans for the LSP's dedicated delivery vehicles. A tailored ITH method incorporating two GTS algorithms and an ABC algorithm is developed to solve the intricate bilevel optimization problem, by iteratively solving the lower-level BTS problem, the reduced upper-level VRP-P problem, and updating the service price. Numerical experiments on a series of randomly generated instances and a group of real-life cases are conducted to evaluate the performance of the proposed ITH method and benefits of incorporating PT-based CM transportation services. Furthermore, sensitivity analyses are carried out to examine the key factors affecting the new business model and derive managerial implications for stakeholders.

Chapter 6 addresses pricing optimization for the OMS-based CM delivery service. To bridge the research gap about the neglect of the consideration of strategic interplay between the PSP and OMP participated in the OMS-based CM delivery service, Chapter 6 studies an OSP problem to find the optimal outsourcing service price and efficient service routes that enable the PSP to fulfill all parcel delivery requests cost-effectively while maximizing the OMP's profits from both passenger and parcel services. A bilevel arc-based programming model is developed to effectively calibrate the leader-follower dynamics inherent in the game between PSP and OMP. In this framework, the lower-level CSP-R model is developed to determine the OMP's optimal decisions under the PSP's proposed outsourcing price, whereas the upper-level MPDP-P model is built to identify the optimal outsourcing service price and the PSP's self-operating service routes. To solve this complex bilevel problem, a customized Iterative Hybrid (IH) algorithm is developed, incorporating two granular tabu search algorithms and a genetic algorithm. This algorithm is uniquely tailored to the problem structure, adopting a profit-oriented granularity approach for the lower-level CSP-R and a cost-oriented granularity for the upper-level reduced MPDP-P, enhancing the computational efficiency of the tabu search components. Numerical experiments are conducted on a series of randomly generated instances and a real-world case to evaluate the performance and practicality of the proposed models and solution strategies. Additionally, sensitivity analysis explores how various factors, such as the ride duration tolerance of passengers, affect the OMS-based CM delivery service, providing essential managerial insights for stakeholders.

7.2 Recommendations for Future Studies

There are various aspects in which prospective research for the three forms of IPG transportation services can be undertaken.

(1) Recommendations for future studies on OT-based CS

Current research on OT-based CS service has primarily focused on examining the importance of jointly optimizing compensation and service routes within hybrid delivery systems that integrate dedicated vehicles and crowd-sourced couriers, with an emphasis on static scenarios. Future studies can extend this focus to dynamic and stochastic environments. This would help refine dynamic compensation structures and task allocation by considering real-time O2O orders and the variability in crowd-courier availability. Additionally, future research could explore the elasticity of CS service supply, allowing for more adaptable strategies in compensation and routing design based on varying compensation levels. While existing studies optimize operations across a collaborative system involving multiple retailers under a unified brand, future research could investigate optimization strategies for individual retailers with different brands and operational costs. Another important area for future research is the equitable allocation of costs and carbon emissions among retailers, especially when system-wide optimization results in disparate impacts on individual participants.

(2) Recommendations for Future Studies on PT-based CM transportation

Future studies on PT-based co-modal transportation can address uncertainties related to the carrying capacities and travel times of buses within a stochastic service model. Research could also explore differentiated pricing strategies that determine optimal pricing for co-modal transportation services, considering the variability in bus schedules and capacities. Additionally, future analyses could examine more complex scenarios, such as many-to-many or one-to-many-to-one pickup and delivery requests, to gain deeper insights into the operational performance of

PT-based co-modal transportation services under varied conditions.

(3) Recommendations for Future Studies on OMS-based CM delivery

Research on OMS-based co-modal delivery currently focuses on developing pricing strategies that support collaboration between PSP and OMP, aiming to establish cost-effective outsourcing prices for sustainable operations amidst fluctuating parcel and passenger demands. Future research should incorporate the stochastic nature of these demands to refine dynamic pricing models and tailor outsourcing prices to specific temporal scenarios. Additionally, while current studies model individual vehicles and requests, future research could adopt a more holistic approach that considers aggregate vehicle flows and spatial distributions, addressing broader-scale challenges. Future studies should also model a more nuanced passenger demand function that reflects behavioral variations, offering a more precise understanding of passenger tolerance towards crowdsourced services. Lastly, considering diverse pickup and delivery configurations, such as paired and hybrid scenarios, could provide a more comprehensive understanding of logistical efficiencies in co-modal delivery.

(4) Other recommendations for future studies

In this study, we examine three distinct singular IPG transportation models for the integrated transportation of people and goods. Future research could explore the synergistic delivery involving multiple IPG transportation models. For example, the transportation process could be divided into tiers: initial transportation could be conducted using FRPT vehicles, such as buses and metro systems, followed by last-mile delivery executed by ordinary travelers or on-demand mobility vehicles. Furthermore, due to the lack of real-life data in this study, we have relied on simulated data. Future research should focus on establishing collaborations with enterprises to obtain actual operational data from public transportation systems and shared mobility services. Access to real-world data would greatly enhance the depth and applicability of research, allowing for a more thorough examination and effectiveness analysis of various IPG transportation models. Additionally, it is recommended that future studies integrate advanced data analytics and machine learning techniques to better predict logistics outcomes and optimize the integration of different IPG transportation models. Engaging with policymakers could also help tailor these models to comply with regulatory frameworks and address any socioeconomic implications, thereby facilitating smoother implementation and scaling of integrated IPG transportation services.

References

Alnaggar, A., Gzara, F., Bookbinder, J.H., 2021. Crowdsourced delivery: A review of platforms and academic literature. *Omega* 98, 102139.

Amiri, M., Farvaresh, H., 2023. Carrier collaboration with the simultaneous presence of transferable and non-transferable utilities. *European Journal of Operational Research* 304, 596–617.

Archetti, C., Savelsbergh, M., Speranza, M.G., 2016. The vehicle routing problem with occasional drivers. *European Journal of Operational Research* 254, 472–480.

Arslan, A.M., Agatz, N., Kroon, L., Zuidwijk, R., 2019. Crowdsourced delivery—a dynamic pickup and delivery problem with ad hoc drivers. *Transportation Science* 53, 222–235.

Behiri, W., Belmokhtar-Berraf, S., Chu, C., 2018. Urban freight transport using passenger rail network: Scientific issues and quantitative analysis. *Transportation Research Part E: Logistics and Transportation Review* 115, 227–245.

Beirigo, B.A., Schulte, F., Negenborn, R.R., 2018. Integrating people and freight transportation using shared autonomous vehicles with compartments. *IFAC-PapersOnLine* 51, 392–397.

Belhaiza, S., Hansen, P., Laporte, G., 2014. A hybrid variable neighborhood tabu search heuristic for the vehicle routing problem with multiple time windows. *Computers & Operations Research* 52, 269–281.

Bonn, 2013. DHL crowd sources deliveries in Stockholm with MyWays. URL: https://www.pressebox.com/inactive/deutsche-post-ag-2/DHL-crowd-sources-deliveries-in-Stockholm-with-MyWays/boxid/622127. (Accessed on: June 20, 2024).

Castillo, V.E., Bell, J.E., Rose, W.J., Rodrigues, A.M., 2018. Crowdsourcing last mile delivery: strategic implications and future research directions. *Journal of Business Logistics* 39, 7–25.

Chen, C., Pan, S., Wang, Z., Zhong, R.Y., 2017. Using taxis to collect citywide E-commerce reverse flows: a crowdsourcing solution. *International Journal of Production Research* 55, 1833–1844.

Chen, C., Zhang, D., Ma, X., Guo, B., Wang, L., Wang, Y., Sha, E., 2016. Crowddeliver: Planning city-wide package delivery paths leveraging the crowd of taxis. *IEEE Transactions on Intelligent Transportation Systems* 18, 1478–1496.

Cheng, G., Guo, D., Shi, J., Qin, Y., 2018. When packages ride a bus: Towards efficient city-wide package distribution, in: 2018 IEEE 24th international conference on parallel and distributed systems (ICPADS), IEEE. pp. 259–266.

Cheng, R., Jiang, Y., Nielsen, O.A., 2023. Integrated people-and-goods transportation systems: from a literature review to a general framework for future research. *Transport Reviews* 43, 997–1020.

Cordeau, J.F., Laporte, G., 2003. A tabu search heuristic for the static multi-vehicle dial-a-ride problem. *Transportation Research Part B: Methodological* 37, 579–594.

Croes, G.A., 1958. A method for solving traveling-salesman problems. *Operations Research* 6, 791–812.

Deb, K., Pratap, A., Agarwal, S., Meyarivan, T., 2002. A fast and elitist multiobjective genetic algorithm: NSGA-II. *IEEE Transactions on Evolutionary Computation* 6, 182–197.

Delle Donne, D., Alfandari, L., Archetti, C., Ljubić, I., 2023. Freight-on-Transit for urban last-mile deliveries: A strategic planning approach. *Transportation Research Part B: Methodological* 169, 53–81.

Dondo, R., Cerdá, J., 2007. A cluster-based optimization approach for the multi-depot heterogeneous fleet vehicle routing problem with time windows. *European Journal of Operational Research* 176, 1478–1507.

Elbert, R., Rentschler, J., 2022. Freight on urban public transportation: A systematic literature review. *Research in Transportation Business & Management* 45, 100679.

Fernández, E., Roca-Riu, M., Speranza, M.G., 2018. The shared customer collaboration vehicle routing problem. *European Journal of Operational Research* 265, 1078–1093.

Fleszar, K., Osman, I.H., Hindi, K.S., 2009. A variable neighbourhood search algorithm for the open vehicle routing problem. *European Journal of Operational Research* 195, 803–809.

Garcia-Najera, A., Bullinaria, J.A., 2011. An improved multi-objective evolutionary algorithm for the vehicle routing problem with time windows. *Computers & Operations Research* 38, 287–300.

Ghaderi, H., Zhang, L., Tsai, P.W., Woo, J., 2022. Crowdsourced last-mile delivery with parcel lockers. *International Journal of Production Economics* 251, 108549.

Ghilas, V., Cordeau, J.F., Demir, E., Woensel, T.V., 2018. Branch-and-price for the pickup and delivery problem with time windows and scheduled lines. *Transportation Science* 52, 1191–1210.

Ghilas, V., Demir, E., Van Woensel, T., 2013. Integrating passenger and freight transportation: Model formulation and insights. .

Ghilas, V., Demir, E., Van Woensel, T., 2016a. A scenario-based planning for the pickup and delivery problem with time windows, scheduled lines and stochastic demands. *Transportation Research Part B: Methodological* 91, 34–51.

Ghilas, V., Demir, E., Van Woensel, T., 2016b. An adaptive large neighborhood search heuristic for the pickup and delivery problem with time windows and scheduled lines. *Computers & Operations Research* 72, 12–30.

Glover, F., 1986. Future paths for integer programming and links to artificial intelligence. *Computers & Operations Research* 13, 533–549.

Goeke, D., 2019. Granular tabu search for the pickup and delivery problem with time windows and electric vehicles. *European Journal of Operational Research* 278, 821–836.

Guajardo, M., Rönnqvist, M., Flisberg, P., Frisk, M., 2018. Collaborative transportation with overlapping coalitions. *European Journal of Operational Research* 271, 238–249.

Han, Y., 2021. Advantages of self-logistics and the third-party logistics-taking Jingdong electronic shopping mall as an example, in: E3S Web of Conferences, EDP Sciences. p. 03008.

He, P., 2023. Chinese supermarket chain Yonghui superstores preannounces 2022 earnings. URL: https://equalocean.com/news/2023020119423. Accessed on: June 20, 2024.

Holland, J.H., 1992. Adaptation in natural and artificial systems: An introductory analysis with applications to biology, control, and artificial intelligence. MIT Press.

Homberger, J., Gehring, H., 2005. A two-phase hybrid metaheuristic for the vehicle routing problem with time windows. *European Journal of Operational Research* 162, 220–238.

Hou, S., Gao, J., Wang, C., 2022. Optimization framework for crowd-sourced delivery services with the consideration of shippers' acceptance uncertainties. *IEEE Transactions on Intelligent Transportation Systems* 24, 684–693.

Ji, Y., Zheng, Y., Zhao, J., Shen, Y., Du, Y., 2020. A Multimodal Passenger-and-Package Sharing Network for Urban Logistics. *Journal of Advanced Transportation* 2020, 6039032.

Karaboga, D., Basturk, B., 2008. On the performance of artificial bee colony (ABC) algorithm. *Applied Soft Computing* 8, 687–697.

de Kemmeter, F., 2021. Zurich's cargo tram. URL: https://mediarail.wordpress.com/new-cargo-tram-test-in-karlsruhe/. (Accessed on: June 20, 2024).

Kindervater, G.A., Savelsbergh, M.W., 1997. Vehicle routing: Handling edge exchanges. *Local Search in Combinatorial Optimization* , 337–360.

Kirchler, D., Calvo, R.W., 2013. A granular tabu search algorithm for the dial-a-ride problem. *Transportation Research Part B: Methodological* 56, 120–135.

Kızıl, K.U., Yıldız, B., 2023. Public transport-based crowd-shipping with backup transfers. *Transportation Science* 57, 174–196.

Kumar, B.A., Prasath, G.H., Vanajakshi, L., 2019. Dynamic bus scheduling based on real-time demand and travel time. *International Journal of Civil Engineering* 17, 1481–1489.

Le, T.V., Ukkusuri, S.V., Xue, J., Van Woensel, T., 2021. Designing pricing and compensation schemes by integrating matching and routing models for crowd-shipping systems. *Transportation Research Part E: Logistics and Transportation Review* 149, 102209.

Li, B., Krushinsky, D., Reijers, H.A., Van Woensel, T., 2014. The share-a-ride problem: People and parcels sharing taxis. *European Journal of Operational Research* 238, 31–40.

Li, B., Krushinsky, D., Van Woensel, T., Reijers, H.A., 2016a. An adaptive large neighborhood search heuristic for the share-a-ride problem. *Computers & Operations Research* 66, 170–180.

Li, B., Krushinsky, D., Van Woensel, T., Reijers, H.A., 2016b. The share-a-ride problem with stochastic travel times and stochastic delivery locations. *Transportation Research Part C: Emerging Technologies* 67, 95–108.

Li, Z., Shalaby, A., Roorda, M.J., Mao, B., 2021. Urban rail service design for collaborative passenger and freight transport. *Transportation Research Part E: Logistics and Transportation Review* 147, 102205.

Lourenço, H.R., Martin, O.C., Stützle, T., 2019. Iterated local search: Framework and applications. *Handbook of Metaheuristics* , 129–168.

Lu, C.C., Diabat, A., Li, Y.T., Yang, Y.M., 2022. Combined passenger and parcel transportation using a mixed fleet of electric and gasoline vehicles. *Transportation Research Part E: Logistics and Transportation Review* 157, 102546.

Macrina, G., Di Puglia Pugliese, L., Guerriero, F., Laganà, D., 2017. The vehicle routing problem with occasional drivers and time windows, in: Optimization and Decision Science: Methodologies and Applications: ODS, Sorrento, Italy, September 4-7, 2017 47, Springer. pp. 577–587.

Macrina, G., Pugliese, L.D.P., Guerriero, F., Laporte, G., 2020. Crowd-shipping with time windows and transshipment nodes. *Computers & Operations Research* 113, 104806.

Mancini, S., Gansterer, M., Hartl, R.F., 2021. The collaborative consistent vehicle routing problem with workload balance. *European Journal of Operational Research* 293, 955–965.

Masson, R., Trentini, A., Lehuédé, F., Malhéné, N., Péton, O., Tlahig, H., 2017. Optimization of a city logistics transportation system with mixed passengers and goods. *EURO Journal on Transportation and Logistics* 6, 81–109.

Mirjalili, S., 2019. Evolutionary algorithms and neural networks. *Studies in Computational Intelligence* 780, 43–53.

Mladenović, N., Hansen, P., 1997. Variable neighborhood search. *Computers & Operations Research* 24, 1097–1100.

Molina, J.C., Salmeron, J.L., Eguia, I., Racero, J., 2020. The heterogeneous vehicle routing problem with time windows and a limited number of resources. *Engineering Applications of Artificial Intelligence* 94, 103745.

Paul, J., Agatz, N., Spliet, R., De Koster, R., 2019. Shared capacity routing problem- An omni-channel retail study. *European Journal of Operational Research* 273, 731–739.

Peng, S., Park, W.Y., Eltoukhy, A.E., Xu, M., 2024. Outsourcing service price for crowd-shipping based on on-demand mobility services. *Transportation Research Part E: Logistics and Transportation Review* 183, 103451.

Placek, M., 2023. Size of the global last mile delivery market from 2020 to 2027. URL: https://www.statista.com/statistics/1286612/last-mile-delivery-market-size-worldwide/. (Accessed on: June 20, 2024.

Punel, A., Stathopoulos, A., 2017. Modeling the acceptability of crowdsourced goods deliveries: Role of context and experience effects. *Transportation Research Part E: Logistics and Transportation Review* 105, 18–38.

Qu, Y., Bard, J.F., 2013. The heterogeneous pickup and delivery problem with configurable vehicle capacity. *Transportation Research Part C: Emerging Technologies* 32, 1–20.

Ren, T., Jiang, Z., Cai, X., Yu, Y., Xing, L., Zhuang, Y., Li, Z., 2021. A dynamic routing optimization problem considering joint delivery of passengers and parcels. *Neural Computing and Applications* 33, 10323–10334.

Renaud, J., Laporte, G., Boctor, F.F., 1996. A tabu search heuristic for the multi-depot vehicle routing problem. *Computers & Operations Research* 23, 229–235.

Sampaio, A., Savelsbergh, M., Veelenturf, L.P., Van Woensel, T., 2020. Delivery systems with crowd-sourced drivers: A pickup and delivery problem with transfers. *Networks* 76, 232–255.

Savelsbergh, M.W., 1992. The vehicle routing problem with time windows: Minimizing route duration. *ORSA Journal on Computing* 4, 146–154.

SF Express, 2024. Hong Kong SF Speedy Express and International Standard Express Service Rate. URL: https://htm.sf-express.com/hk/tc/download/HK-Express-Service-Rate-sender-paid.pdf. (Accessed on: June 20, 2024).

Solomon, M.M., 1987. Algorithms for the vehicle routing and scheduling problems with time window constraints. *Operations Research* 35, 254–265.

Springer, J., 2017. Walmart expands Uber delivery test to more cities. URL: https://www.supermarketnews.com/online-retail/walmart-expands-uber-delivery-test-more-cities. (Accessed on: June 20, 2024).

Statista, 2024a. China: number of privately-owned motor vehicles 2009-2022. URL: https://www.statista.com/statistics/278475/privately-owned-vehicles-in-china/. (Accessed on: June 20, 2024).

Statista, 2024b. Retail e-commerce sales worldwide from 2014 to 2027. URL: https://www.statista.com/statistics/379046/worldwide-retail-e-commerce-sales/. (Accessed on: June 20, 2024).

Taillard, É., Badeau, P., Gendreau, M., Guertin, F., Potvin, J.Y., 1997. A tabu search heuristic for the vehicle routing problem with soft time windows. *Transportation Science* 31, 170–186.

Tao, J., Dai, H., Jiang, H., Chen, W., 2021. Dispatch optimisation in O2O on-demand service with crowd-sourced and in-house drivers. *International Journal of Production Research* 59, 6054–6068.

Toth, P., Vigo, D., 2003. The granular tabu search and its application to the vehicle-routing problem. *Informs Journal on Computing* 15, 333–346.

Vincent, F.Y., Jodiawan, P., Redi, A.P., 2022. Crowd-shipping problem with time windows, transshipment nodes, and delivery options. *Transportation Research Part E: Logistics and Transportation Review* 157, 102545.

Wahba, P., 2016. Walmart teams up with Uber and Lyft for grocery delivery test. URL: https://fortune.com/2016/06/03/walmart-lyft-uber/. (Accessed on: June 20, 2024).

Wang, Y., Peng, S., Xu, M., 2021. Emergency logistics network design based on space–time resource configuration. *Knowledge-Based Systems* 223, 107041.

Xiao, Y., Zhao, Q., Kaku, I., Xu, Y., 2012. Development of a fuel consumption optimization model for the capacitated vehicle routing problem. *Computers & Operations Research* 39, 1419–1431.

Yu, V.F., Purwanti, S.S., Redi, A.P., Lu, C.C., Suprayogi, S., Jewpanya, P., 2018. Simulated annealing heuristic for the general share-a-ride problem. *Engineering Optimization* 50, 1178–1197.

Yu, W., Bai, H., Chen, J., Yan, X., 2019. Analysis of space-time variation of passenger flow and commuting characteristics of residents using smart card data of Nanjing metro. *Sustainability* 11, 4989.

Zhan, X., Szeto, W., Wang, Y., 2023. The ride-hailing sharing problem with parcel transportation. *Transportation Research Part E: Logistics and Transportation Review* 172, 103073.

Zhao, L., Li, H., Li, M., Sun, Y., Hu, Q., Mao, S., Li, J., Xue, J., 2018. Location selection of intra-city distribution hubs in the metro-integrated logistics system. *Tunnelling and Underground Space Technology* 80, 246–256.

Zhao, X., Lin, W., Cen, S., Zhu, H., Duan, M., Li, W., Zhu, S., 2021. The online-to-offline (O2O) food delivery industry and its recent development in China. *European Journal of Clinical Nutrition* 75, 232–237.

Zitzler, E., Deb, K., Thiele, L., 2000. Comparison of multiobjective evolutionary algorithms: Empirical results. *Evolutionary Computation* 8, 173–195.

Zitzler, E., Thiele, L., 1998. Multiobjective optimization using evolutionary algorithms—a comparative case study, in: International Conference on Parallel Problem Solving from Nature, Springer. pp. 292–301.